VARIATIONAL METHODS
in
DISORDER PROBLEMS

Testing Approximation Techniques with and without Replicas on a Zero-Dimensional Disorder Model

Diploma Thesis by
Markus Düttmann

Department of Physics
Freie Universität Berlin
Arnimallee 14
14195 Berlin, Germany

Referee: Prof. Dr. Dr. h.c. Hagen Kleinert

January 6, 2009

Contents

Chapter 1

Introduction

1.1 Motivation

Physicists strive to discover the hidden order of nature. Finding and solving deterministic models while taking into account all properties of a physical system, however, is not always possible. As a matter of fact, most physical systems exhibit a certain randomness. Thus, the theory of disordered systems has become increasingly important over the past few decades. It describes unknown properties of a specific model with the help of random functions and has been applied to a wide range of physical, chemical, and biological problems. In real metals, for example, the lattice symmetry is broken by defects such as impurities and imperfections [1, 2]. Furthermore, Bose-Einstein condensates can be experimentally realized in traps. Taking into account disorder makes theoretical models for these experiments more realistic. Wire traps in atom chips hold a natural disorder due to the surface roughness. On the contrary, laser speckles can provide a highly disordered but stationary coherent light field in optical lattices and, therefore, both the strength of the disorder and its correlation length can be changed in a controlled manner [3, 4, 5]. Other examples are the transport in random media and diffusion-controlled reactions. They can be modeled by random walks in random trapping environments [6, 7]. In analogy to this, random potentials find areas of application even far from its physical origins. The dynamics of stock markets, for instance, have been modeled as a tracer in a Gaussian random field [8]. In the context of disorder theory, the Sherrington-Kirkpatrick (SK) model describing spin glasses, i.e., disordered magnets, is especially important as it has been studied capaciously [9]. One imagines half of the bonds between two spins randomly chosen as ferromagnetic and the other half as antiferromagnetic. The SK model describes this situation via an Ising model in which the spins are coupled by random infinite-range interactions. These interactions are assumed to be independent and normally distributed [9, 10, 11]. Because the spin variables are frozen at low temperatures, one speaks of quenched disorder. A standard method to deal with it is a mathematical trick called the replica method. Instead of treating the actual problem, one looks at n copies of the system [11, 12]. The central idea of the replica trick is to analytically continue the replicated system to $n \to 0$. Although it has proven to be successful many times, this procedure is still quite controversial from a mathematical point of view. Furthermore, it should be noted that the replica analyticity can break down in certain models [13].

Just as most physical systems exhibit a certain randomness, most problems cannot be solved exactly. Therefore, innumerable approximation methods have been developed throughout the course of physical history. An extremely powerful tool is perturbation theory. To further include non-perturbative contributions, variational perturbation theory (VPT) is applied. As the name

suggests, it combines standard perturbative methods with a variational principle [12, 14]. It plays a central role in the analysis of the SK model.

An improvement of the SK model was proposed by Giorgio Parisi in 1980 [10, 15, 16]. The so-called replica-symmetric solution describing the SK model up to that point was shown to break down beneath a critical temperature in certain cases [17]. The problem is caused by metastable states. If just one equilibrium state exits, the solution has to be invariant under permutation of the different replicas. Thus, at high temperatures or in the case of weak correlation, the replica-symmetric ansatz is intrinsically correct. In these cases local minima do not play a decisive role. Otherwise, different replicas can be arranged in different, locally stable equilibria [18]. Therefore, Parisi introduced the scheme of replica-symmetry breaking. It was shown to give a stable solution for the SK model for all temperatures. His method turned out to be a major breakthrough in disorder theory.

As a guinea pig for these variational approximation methods, we investigate in this thesis the simple model of a harmonic oscillator in a disorder environment.

1.2 Toy Model

One of the most famous problems in physics is the one-dimensional harmonic oscillator. A particle of mass m experiences a restoring force proportional to its displacement x. The corresponding potential is given as

$$V(x) = \frac{1}{2}\,\kappa\, x^2 \ , \tag{1.1}$$

where the constant κ denotes the spring constant in Hooke's law. In the following, we investigate this problem within a disorder environment that is described by a random external potential $U(x)$. It is taken to be a homogeneous and real-valued function. Furthermore, it should represent a normally distributed random variable satisfying

$$\overline{U(x)} = 0, \quad \overline{U(x)U(x')} = R(x - x') \ , \tag{1.2}$$

where the overbar denotes the average over all realizations of $U(x)$. In this thesis, we will focus on a Gaussian correlation

$$R(x - x') = \frac{1}{\sqrt{2\pi}\lambda} \exp\left\{-\frac{(x - x')^2}{2\lambda^2}\right\} \ , \tag{1.3}$$

where the parameter λ denotes the correlation length. A δ-correlation can be described by formally taking the limit $\lambda \to 0$.

For this system the Hamilton function writes

$$H_{\mathrm{ho}}(x, p) = \frac{p^2}{2m} + \frac{1}{2}\,\kappa\, x^2 + \varepsilon\, U(x) \tag{1.4}$$

for real x and p. The parameter ε denotes the correlation strength. In the canonical ensemble, all thermodynamic properties of the system can be obtained via the free energy F. In order to calculate it, we define the classical partition function

$$Z_{\mathrm{ho}} = \int_{-\infty}^{\infty} \frac{dp}{2\pi\hbar} \int_{-\infty}^{\infty} dx\, \exp\left[-\beta H_{\mathrm{ho}}(x, p)\right] \tag{1.5}$$

with the reciprocal temperature $\beta = 1/k_B T$. For simplicity, the Boltzmann constant k_B will be set to 1 in the following considerations. It is now evident that the kinetic part of the Hamilton function (1.4) just contributes the constant prefactor $\sqrt{m/2\pi\hbar^2\beta}$ to the partition function, which represents the inverse of the thermal de-Broglie wavelength, and, accordingly, leads to a constant summand in the free energy $F_{\mathrm{ho}} = -\log(Z_{\mathrm{ho}})/\beta$. As this constant will not be of any importance in the discussion to follow, we will concentrate on the toy model Hamilton function

$$H(x) = \frac{1}{2}\kappa x^2 + \varepsilon U(x) \ , \tag{1.6}$$

where we omit the kinetic part. In this context the partition function reads

$$Z = \int_{-\infty}^{\infty} dx \, \exp[-\beta \, H(x)] \ . \tag{1.7}$$

Now, the free energy can be stated as $-\log(Z)/\beta$ for a fixed realization of the potential $U(x)$. Hence, in the toy system considered, the system's free energy is given as the free energy for fixed potential averaged over all its realizations:

$$F = -\frac{1}{\beta} \overline{\log \, Z} \, . \tag{1.8}$$

It is to note that the averaging process does not commutate with the logarithm and, therefore, it is not possible to calculate the free energy directly, not even for the extremely simple toy model.

The Hamilton function (1.6) depends on the two parameters κ and ε. The physics of the system, however, just depends on the ratio of these two parameters. This can be seen by a simple rescaling of the reciprocal temperature

$$\tilde{\beta} \to \varepsilon \, \beta \ , \tag{1.9}$$

which yields the Hamilton function

$$\tilde{H}(x) = \frac{1}{2}\frac{\kappa}{\varepsilon} x^2 + U(x) \ . \tag{1.10}$$

In the discussion to follow we will stick formally to (1.6). The advantage of this is quite clear: one just needs to throw a glance at a term to see in which order of the weak coupling expansion it originates. However, we will not discuss the parameters independently but concentrate on the case of fixed ε.

The toy model has already been studied in detail in Ref. [19] and, thus, we have some benchmark with which we can compare our results. Although the classical harmonic oscillator seems to be a very simple model, it is important on the interface to quantum mechanics. Its natural generalization is a quantum particle in a random environment [20]. An experimental realization of this model is the ion transport in disordered solid electrolytes. The design of the experiment, however, imposes periodic boundary conditions [21]. Also, the behavior of polymer chains in random media is strongly connected to this field of study [22]. Furthermore, a similar model in higher dimensions has been used in a different area to derive the phase diagram of vortices for certain high $\mathrm{T_c}$ superconductors such as YBCO [23, 24, 25, 26].

1.3 Brownian Motion

Instead of departing from classical thermodynamic equilibrium statistics, the toy model can also be approached from a different point of view. The starting point is a continuous-time stochastic processes - the Brownian motion. In 1827 it was rediscovered by the Scottish botanist Robert Brown. He observed the movement of particles suspended in a liquid studying the fertilization process of a certain species of flower [27, 28]. He did not discover this fluctuating movement, though. As a matter of fact, he mentions some of his precursors in his own publications. Nonetheless, *Brownian movement* or *Brownian motion* is named in honor of this famous scientist.

A physical description of Brownian motion was later proposed by Einstein in his *annus mirabilis*, in which he published the four famous papers about the photoelectric effect, which won him his Nobel Prize in 1921, the theory of special relativity, the equivalence of mass and energy, and, most important in this context, his physical treatment of the Brownian motion [29]. A crucial role in the development of this theory played his doctoral thesis stating among other things the diffusion formula. It was submitted to the University of Zurich in the same year and published in the journal *Annalen der Physik* just one year later [30]. Due to its practical applications, it became his most widespread paper that time. It is the least known yet the most quoted of his infamous works of 1905. Einstein explained the random movement of little particles in a liquid or gas via the kinetic theory of heat. It should be mentioned that, independently, Smoluchowski found a solution for the problem of moving Brownian particles [31]. Furthermore, it is interesting to know that from a completely different background and starting point a young French mathematics student also solved the problem predating the two physicists. Einstein and Smoluchowski did not know that Louis Bachelier published his PhD thesis on random walks as early as 1900. It is generally considered the beginning of mathematical finance [32]. A quite different approach to Brownian motion was proposed by Langevin in 1909, yielding the same results. Comparing with Einstein and Smoluchowski, he called it *'une démonstration infiniment plus simple'* [33]. In the following, we will stay close to his reasoning in order to understand the physical idea behind Brownian motion.

If a small particle is put, e.g., in a liquid, it starts to move. This resulting motion is quite unpredictable. Even with identical starting points, one cannot anticipate the exact position of the particle at any given time. This is caused by collisions with the thermally moving molecules of the liquid as visualized in Fig. 1.1 [34]. It is to note that Brownian motion may be described by a random walk. A random walk is the trajectory that results from taking successive random steps of width ε in a discrete time grid of width dt. Brownian motion can be shown to emerge in the limit $\varepsilon \to 0$ and $dt \to 0$, i.e., infinitely small steps in the continuous-time limit [35]. One imagines the random walker to take smaller, but more steps in a fixed time interval. Thus, Brownian motion can be simulated as a random walk with small step size.

In classical physics, the whole problem could, in principle, be solved by a set of differential equations taking into account every molecule actively or passively involved in the collisions. But this cannot be done in praxis because the number particles and, therefore, the set of equations is of the magnitude of Avogadro's constant. The idea introduced by Langevin is to decompose the forces acting on the particle into a deterministic one $F_d(t)$, a friction force damping the motion, and a stochastic force $F_s(t)$ summarizing the effect of thermally activated collisions. By Stokes' law the damping force is well-known. For a slowly moving sphere of radius r it is

$$F_d(t) = -\alpha v(t) \tag{1.11}$$

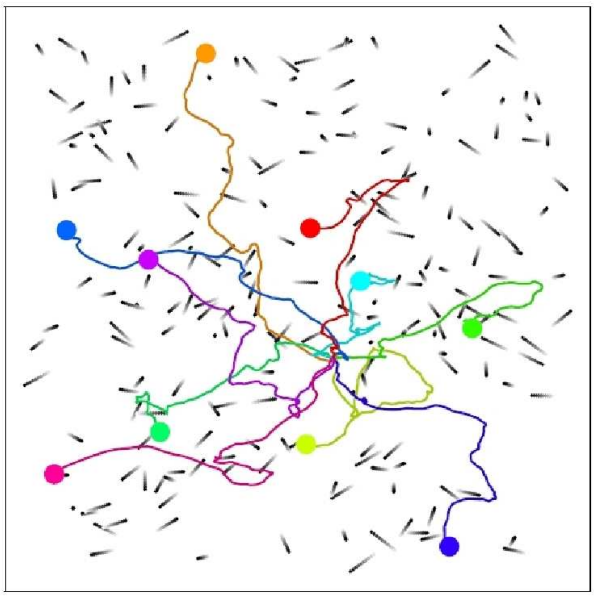

Figure 1.1: Visualization of Brownian motion.

with the coefficient α depending linearly on r and the viscosity of the liquid η:

$$\alpha = 6\pi r\eta \ . \tag{1.12}$$

The equation of motion for the particle then writes

$$m\frac{d}{dt}v(t) = F_d(t) + F_s(t) = -\alpha v(t) + F_s(t) \ . \tag{1.13}$$

It is easily seen that without the fluctuating force the velocity would exponentially go to zero. We will introduce the new quantities damping constant and Langevin force:

$$\gamma = \frac{\alpha}{m} \ , \qquad \Gamma(t) = \frac{F_s(t)}{m} \ . \tag{1.14}$$

Accordingly, one gets the new equation of motion

$$\frac{d}{dt}v(t) = -\gamma v(t) + \Gamma(t) \ . \tag{1.15}$$

In statistical physics an equation of this form is called a Langevin equation. To describe the stochastic force, one assumes as a natural condition spatial homogeneity: collisions from all directions have equal probabilities. Mathematically speaking this means

$$\langle \Gamma(t) \rangle = 0 \ . \tag{1.16}$$

Furthermore, we impose that the duration of a collision is much smaller than the relaxation time due to damping. Thus, the Langevin force is described as delta-correlated

$$\langle \Gamma(t)\Gamma(t') \rangle = D\delta(t - t') \ . \tag{1.17}$$

In mathematics, a process with these attributes is called a Wiener process. As already mentioned above, in thermodynamics the diffusion constant D is derived to be to

$$D = \frac{2\gamma k_B T}{m} \ . \tag{1.18}$$

It is a special result of the fluctuation-dissipation theorem often called Einstein-Smoluchowski or just Einstein equation [35, 36]. By calculating the moments of $\langle v(t)^n \rangle$, it is possible to calculate the stationary probability distribution of the Brownian motion. Nonetheless, we will pursue a different way on the trails of the two great physicists Adriaan Fokker and Max Planck.

1.4 Fokker-Planck Equation

A couple of years after the first physical description of Brownian movement, the Dutch physicist and musician Adriaan Fokker and the legendary Max Planck used differential equations to describe the time evolution of a proability distribution $P(x,t) = \langle \delta(x - x(t)) \rangle$, where $x(t)$ is determined by solving the underlying Langevin equation [37, 38]. The first use was, in fact, the statistical description of Brownian motion. The so-called Fokker-Planck equation writes

$$\frac{\partial}{\partial t} P(x,t) = -\frac{\partial}{\partial x} \left[K(x) P(x,t) \right] + \frac{1}{2} \frac{\partial^2}{\partial x^2} [D(x) P(x,t)] \ . \tag{1.19}$$

The functions $K(x)$ and $D(x)$ are called the drift and the diffusion coefficient, respectively. This equation is sometimes called Kolmogorov forward equation as it was obtained by Andrey Nikolaevich Kolmogorov in 1931 [39]. It is said that he was not familiar with the work of Fokker and Planck and he himself called the expression Fokker-Planck equation as he found out about it. However, the so-called Kolmogorov backward equation, the adjoint of the forward equation, which describes the evolution backwards in time, was not known up to that time. Eq. (1.19) can be generalized to a system depending on N variables $\mathbf{x} = (x_1, ..., x_N)$ in a straightforward manner [36]. The equation reads in this case

$$\frac{\partial}{\partial t} P(\mathbf{x},t) = -\sum_i \frac{\partial}{\partial x_i} \left[K_i(\mathbf{x}) P(\mathbf{x},t) \right] + \frac{1}{2} \sum_{i,j} \frac{\partial^2}{\partial x_i \partial x_j} [D_{ij}(\mathbf{x}) P(\mathbf{x},t)] \ , \tag{1.20}$$

with the drift vector $K_i(\mathbf{x})$ and the diffusion tensor $D_{ij}(\mathbf{x})$ which depend on the N variables x_i. An example for a Fokker-Planck equation with more than one stochastic variable will be discussed in one of the following sections. But first we return to the one variable case.

Starting from the Langevin equation of the system, drift and diffusion coefficient of the corresponding Fokker-Planck equation can be obtained directly [35]. In the case (1.15) the stochastic variable is the velocity $v(t)$ and, accordingly, we get

$$K(v) = -\gamma v \qquad , \qquad D(v) = D \ . \tag{1.21}$$

Thus, the Fokker-Planck equation for Brownian motion reads

$$\frac{\partial}{\partial t} P(v,t) = \gamma \frac{\partial}{\partial v} \left[v P(v,t) \right] + \frac{D}{2} \frac{\partial^2}{\partial v^2} P(v,t) \ . \tag{1.22}$$

The solution of the partial differential equation can be found, for example, by using heuristic arguments. A clever ansatz simplifies the equation considerably. For the calculations in full

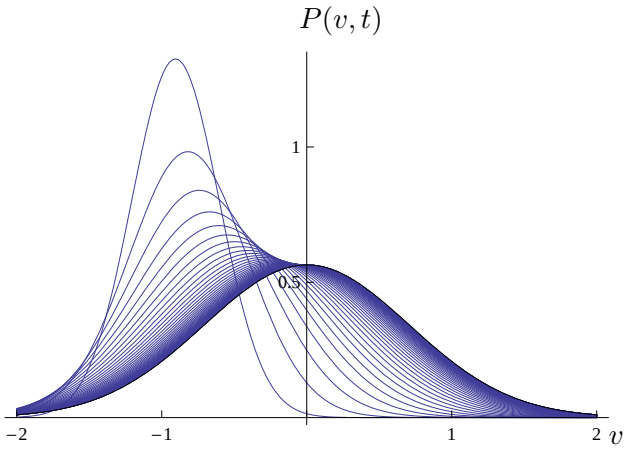

Figure 1.2: Time dependent probability density of Brownian motion $P(v,t)$ calculated from (A.25) for fixed times t starting at $t = 0.1$ increasing with time steps $\Delta t = 0.1$. The starting values are $x_0 = -1$ and $t_0 = 0$ and we have chosen the damping constant $\gamma = 1$ as well as the diffusion constant $D = 1$. We see that the center of $P(v,t)$ shifts towards 0 and the probability distribution tends exponentially fast to the stationary Gaussian one (1.23) plotted with a black line.

length see App. A, where the solution for the Brownian motion case is found to be (A.25). The time dependent solution evolves exponentially fast into a stationary one, as can be seen in Fig. 1.2. In the following, we will only be interested in the stationary solution, which is also known as the Maxwell distribution (A.16):

$$P(v) = \sqrt{\frac{m}{2\pi k_B T}} \exp\left(-\frac{m}{2k_B T} v^2\right) \ . \tag{1.23}$$

1.4.1 Nonlinear Drift Coefficient

As seen in (A.9), the stationary solution depends of the drift and diffusion coefficients. Assuming constant diffusion, the general result is derived in App. A to be

$$P_{\mathrm{st}}(x) = \frac{N}{D} \exp\left[-\frac{2}{D} V_{\mathrm{FP}}(x)\right] \ , \tag{1.24}$$

with the definition of the Fokker-Planck potential

$$V_{\mathrm{FP}}(x) = -\left[\int^x K(\xi) d\xi\right] \ . \tag{1.25}$$

Now the case of nonlinear drift coefficients can be examined. A simple example is the anharmonic drift

$$K(x) = -\gamma x - g x^3 \ . \tag{1.26}$$

The stationary solution of this problem can be calculated and with variational methods even the time dependent solution can be approximated rather well [34, 40, 41].

1.4.2 Kramers and Smoluchowski Equation

A simple example for a problem with two stochastic variables is the Brownian motion with additional external force. The corresponding Langevin equation is

$$\begin{aligned} \dot{x}(t) &= v(t) \ , \\ \frac{d}{dt}v(t) &= -\gamma v(t) + F(x) + \Gamma(t) \ , \\ \langle \Gamma(t)\Gamma(t')\rangle &= D\,\delta(t-t') \ . \end{aligned} \tag{1.27}$$

We assume that the additional force can be described by an external potential: $F(x) = -V'_{\text{ext}}(x)$. The Kramers equation is the equation of motion for the probability distribution of the space variable x and the velocity variable v. It is a special form of the Fokker-Planck equation (1.20) and writes

$$\frac{\partial}{\partial t}P(x,v,t) = -\frac{\partial}{\partial x}\left[v\,P(x,v,t)\right] + \frac{\partial}{\partial v}\Big\{\left[\gamma v + V'_{\text{ext}}(x)\right]P(x,v,t)\Big\} + \frac{1}{2}D\frac{\partial^2}{\partial v^2}P(x,v,t) \ . \tag{1.28}$$

Even more specialized, the case of a large friction constant γ is going to be investigated. In this case the second derivative with respect to time may be neglected [36]. We therefore have the equation of motion

$$m\gamma\dot{x} = -V'_{\text{ext}}(x) + m\Gamma(t) \ . \tag{1.29}$$

Thus, we are left with a system depending on just one variable x. We can also see that (1.29) has the form of the Langevin equation

$$\dot{x} = K(x) + \widetilde{\Gamma}(t) \tag{1.30}$$

with $\langle\widetilde{\Gamma}(t)\widetilde{\Gamma}(t')\rangle = \widetilde{D}\,\delta(t-t')$. With the Einstein-Smoluchowski relation (1.18), we see that

$$\widetilde{D} = \frac{D}{\gamma^2} = \frac{2k_BT}{m\gamma} \ . \tag{1.31}$$

Furthermore, the drift coefficient is given as

$$K(x) = -\frac{1}{m\gamma}V'_{\text{ext}}(x) \ . \tag{1.32}$$

The Fokker-Planck equation with this type of drift coefficient is often called Smoluchowski equation.

1.4.3 Overdamped Brownian Motion in Random Potentials

In this work the aim will be to investigate stationary solutions of the Smoluchowski equation in a special case: the external force will be determined by a Gaussian distributed random potential $U(x)$. It is assumed to be a homogeneous and real-valued function with the properties (1.2) and (1.3). To ensure fast enough decay, we will add a restoring force ensuring the confinement of the Brownian particle. Thus, the external force writes

$$F(x) = -\kappa x - \varepsilon\,U'(x) \ . \tag{1.33}$$

With the drift coefficient of the Smoluchowski equation (1.32), we get the Fokker-Planck potential

$$V_{\mathrm{FP}} = \frac{1}{2}\frac{\kappa}{m\gamma}x^2 + \frac{\varepsilon}{m\gamma}U(x) \ . \tag{1.34}$$

Accordingly, the stationary probability distribution writes with (1.24)

$$P_{\mathrm{st}}(x) = N[U] \exp\left\{-\beta\left[\frac{1}{2}\kappa x^2 + \varepsilon\, U(x)\right]\right\} \ , \tag{1.35}$$

with a normalization factor $N[U]$, which depends on the random function $U(x)$. This problem can be described by the Hamilton function (1.6). Therefore, the problem of finding the stationary solution of the Smoluchowski equation with the external force (1.33) can be solved in close analogy to the problem of finding the thermodynamic properties of a harmonic oscillator in a disorder environment. This view is quite appealing to physicists as the harmonic oscillator is probably the best studied problem in physics.

1.5 Outline

The main goal of this thesis is to find good approximations for the harmonic oscillator in a disorder environment or, equivalently, the stationary solution of Brownian motion in a confined disorder potential. To this end, methods with and without replicas will be employed. But which are the properties of Gaussian distributed random fields? And what does averaging over the ensemble of all random functions mean? In **Chapter 2** these questions are discussed and the idea of functional averaging is introduced. Furthermore, we familiarize ourselves with an algorithm to generate continuous random potentials with a given correlation function in order to evaluate the quality of the approximations to be found. We show that this algorithm works with good accuracy.

Subsequently, we use non-replica based methods. We start out **Chapter 3** by applying standard perturbation theory for weak correlation strength. Problems will appear for small temperatures and, thus, the approximations turn out not to converge in this parameter regime. As an attempt to improve the approximation, we make use of the square root substitution in order to introduce a variational parameter to perform a resummation of the perturbation series. The results remain unconvincing. However, we gain a remarkable agreement with numerical results by heuristically applying a variational method involving the temperature as a variational parameter.

In the following, we make use of the replica trick to restate the single-particle disorder problem as a non-random many-body system. Proceeding conceptually as in the SK model, we adopt a variational method to also include non-perturbative terms in the discussion of the thermodynamic properties. The Jensen-Peierls inequality provides us with a safe upper bound for the free energy. In **Chapter 4** a simple solution, the replica-symmetric ansatz (RSA), is discussed. It can, however, become unstable for small temperatures depending on the parameters of the system.

Chapter 5 deals with the so-called replica-symmetry breaking (RSB) scheme. In detail, we explain the Parisi algebra and its formalism will be commented. Furthermore, the improvements of the finite-step symmetry breaking approach is calculated.

In the last part of this thesis, we compare all approximation methods. **Chapter 6** contains a summary of all results and a brief outlook.

Chapter 2

Random Fields

In this chapter, we will introduce the idea of Gaussian distributed random fields. It will be shown how to treat both the distribution and the correlation function mathematically. In order to test analytic results of disorder problems, it is convenient to generate random potentials numerically. In this context, the main problem is to assign specific characterizations to the random fields. In the following, an algorithm is presented to generate normally distributed random functions with given correlation function. As a special ansatz the so-called Randomization Method is investigated by the examples of Gaussian and Cauchy-type correlations. For the more interested reader, further accuracy considerations are made in App. B.

2.1 Gaussian Random Fields

In classical statistics, the correlation function is by definition (1.2) a real valued and even function

$$R(x)^* = R(x) \ , \qquad R(x) = R(-x) \ . \tag{2.1}$$

For later purposes, we define the spectral density as the Fourier transform of the correlation function

$$S(k) = \frac{1}{2\pi} \int_{-\infty}^{\infty} dx \, e^{-ikx} R(x) \ . \tag{2.2}$$

As a consequence of (2.1), the spectral density has to be real valued and even:

$$S(k)^* = S(k) \ , \qquad S(k) = S(-k) \ . \tag{2.3}$$

In the following, general aspects of Gaussian random fields are mentioned [42]. The probability distribution $P\,[U]$ is a functional of the random potentials $U(x)$. We denote the averaging process by

$$\overline{\bullet} = \int \mathcal{D}U \bullet P[U]. \tag{2.4}$$

The functional integral corresponds to an infinite product of ordinary integrals

$$\int \mathcal{D}U = \prod_x \int_{-\infty}^{\infty} dU(x) \tag{2.5}$$

with an integration measure which obeys the normalization condition

$$\int \mathcal{D}U P[U] = 1. \tag{2.6}$$

Because the functions are normally distributed, one can specify the probability distribution according to

$$P[U] = \exp\left\{-\frac{1}{2}\int_{-\infty}^{\infty} dx \int_{-\infty}^{\infty} dx'\, R^{-1}(x-x')U(x)U(x')\right\}, \tag{2.7}$$

where the integral kernel $R^{-1}(x-x')$ is the functional inverse of the correlation function:

$$\int_{-\infty}^{\infty} dy\, R^{-1}(x-y)R(y-x') = \delta(x-x'). \tag{2.8}$$

In order to calculate all moments of $P[U]$, it remains to compute the generating functional

$$I[j] = \overline{\exp\left\{i\int_{-\infty}^{\infty} dx\, j(x)U(x)\right\}}. \tag{2.9}$$

Little arithmetics gives

$$I[j] = \exp\left\{-\frac{1}{2}\int_{-\infty}^{\infty} dx \int_{-\infty}^{\infty} dx'\, j(x)j(x')R(x-x')\right\}. \tag{2.10}$$

In Ref. [14] the expectation value (2.9) is calculated for the discrete case which is then generalized to the case of continuous variables by interchanging sum and integral, yielding (2.10). Now the moments can be calculated as successive derivatives of the generating functional

$$\overline{U(x_1)U(x_2)...U(x_n)} = \frac{1}{i^n}\frac{\delta^n I[j]}{\delta j(x_1)\delta j(x_2)...\delta j(x_n)}\bigg|_{j(x)=0}. \tag{2.11}$$

As a consequence of this special form of the generating functional, uneven moments must vanish and even moments can be calculated using Wick's Theorem. The 4-point correlation function, for instance, can be calculated to

$$\begin{aligned}\overline{U(x_1)U(x_2)U(x_3)U(x_4)} = \quad & R(x_1-x_2)R(x_3-x_4) + R(x_1-x_3)R(x_2-x_4) \\ & + R(x_1-x_4)R(x_2-x_3)\ ,\end{aligned} \tag{2.12}$$

which also follows directly from (2.10) and (2.11).

2.2 Generating Random Potentials

Motivated by Fourier series, a simple ansatz for the random functions is made. The potential is written as a finite superposition of $\sin(k\,x)$ and $\cos(k\,x)$ terms with properly picked amplitudes A_n and B_n and wave numbers k_n [43]:

$$U(x) = \frac{1}{\sqrt{N}}\sum_{n=0}^{N-1}\left[A_n\,\cos(k_n\,x) + B_n\,\sin(k_n\,x)\right]\ . \tag{2.13}$$

We assume A_n and B_n to be mutually independent Gaussian random variables with zero mean and variance α^2

$$\begin{aligned} \langle A_n\, B_m \rangle &= 0, \\ \langle A_n\, A_m \rangle &= \langle B_n\, B_m \rangle = \alpha^2 \delta_{mn}\ . \end{aligned} \tag{2.14}$$

Furthermore, the wave numbers k_n are independent random variables, as well, picked from the probability distribution

$$p(k) = \frac{S(k)}{\int_{-\infty}^{\infty} S(k')\, dk'.}. \tag{2.15}$$

Note that choosing wave numbers $k_n = 2\pi n/L$ would produce a periodic function with period L. In the limit of very large L one would generate potentials that resemble random Gaussian correlated functions sufficiently. Computer simulations would be extremely costly, though. But the ansatz (2.13) will be shown to give a good approximation to normally distributed random potentials, if the parameter α is chosen according to

$$\alpha^2 = R(0) = \int_{-\infty}^{\infty} S(k)\, dk. \tag{2.16}$$

To justify the correct correlation and distribution function of the random process, one examines the generating functional. Inserting the decomposition (2.13) into (2.9) yields

$$I[j] = \left\langle \prod_{n=0}^{N-1} \exp\left\{ \frac{i}{\sqrt{N}} \int_{-\infty}^{\infty} dx\, j(x) [A_n\, \cos(k_n\, x) + B_n\, \sin(k_n\, x)] \right\} \right\rangle, \tag{2.17}$$

where the average over all random functions is rewritten in terms of ensemble averages over both the amplitudes A_n and B_n and the wave numbers k_n:

$$\langle \bullet \rangle = \frac{1}{\alpha^2} \frac{1}{2\pi\, \alpha^2} \prod_{n=0}^{N-1} \int_{-\infty}^{\infty} dk_n\, S(k_n) \int_{-\infty}^{\infty} dA_n\, e^{-A_n^2/2\alpha^2} \int_{-\infty}^{\infty} dB_n\, e^{-B_n^2/2\alpha^2}\, \bullet \quad . \tag{2.18}$$

The calculation of (2.17) can be done in a straightforward manner, just using the trigonometric addition theorem and completing the square. We get as the result

$$I[j] = \prod_{n=0}^{N-1} \int_{-\infty}^{\infty} dk_n\, \frac{S(k_n)}{\alpha^2}\, \exp\left\{ -\frac{\alpha^2}{2N} \int_{-\infty}^{\infty} \int_{-\infty}^{\infty} dx\, dx'\, j(x)\, j(x')\, \cos[k_n(x - x')] \right\}\ . \tag{2.19}$$

In view of the limit $N \to \infty$, we expand the exponential function and obtain

$$I[j] = \prod_{n=0}^{N-1} \int_{-\infty}^{\infty} dk_n \frac{S(k_n)}{\alpha^2} \left\{ 1 - \frac{\alpha^2}{2N} \int_{-\infty}^{\infty} \int_{-\infty}^{\infty} dx\, dx'\, j(x)\, j(x')\, \cos[k_n(x - x')] + O(1/N^2) \right\}. \tag{2.20}$$

After using the Euler formula, one finds for an even spectral density

$$I[j] = \prod_{n=0}^{N-1} \left\{ 1 - \frac{1}{2N} \int_{-\infty}^{\infty} \int_{-\infty}^{\infty} dx\, dx'\, j(x)\, j(x') \int_{-\infty}^{\infty} dk_n e^{ik_n(x-x')} S(k_n) + O(1/N^2) \right\}, \tag{2.21}$$

where (2.16) has been used. The k_n-integration is the inverse Fourier transform of (2.2) giving the correlation function $R(x-x')$.

For writing (2.21) more transparently, some general mathematical considerations will be done in order to carry out the product over all n. To this end, we write

$$\prod_{n=0}^{N-1}\left[1+\frac{x}{N}+O(1/N^2)\right]=\prod_{n=0}^{N-1}\exp\left\{\log\left[1+\frac{x}{N}+O(1/N^2)\right]\right\}\ . \tag{2.22}$$

This form is more comfortable, since the product can now be executed easily. As well, it is advantageous to write the logarithm in the exponent in form of its Taylor series

$$\prod_{n=0}^{N-1}\left[1+\frac{x}{N}+O(1/N^2)\right]=\exp\left\{N\sum_{k=1}^{\infty}\frac{(-1)^{1+k}}{k}\left(\frac{x}{N}+O(1/N^2)\right)^k\right\} \tag{2.23}$$

Factoring out N inside the brackets in the exponent, we obtain

$$\begin{aligned}\prod_{n=0}^{N-1}\left[1+\frac{x}{N}+O(1/N^2)\right] &= \exp\left\{\sum_{k=1}^{\infty}\frac{(-1)^{1+k}}{k}\frac{1}{N^{k-1}}\left(x+O(1/N)\right)^k\right\}\\ &= \exp\left\{x+O(1/N)\right\}\ .\end{aligned} \tag{2.24}$$

After evaluating the exponential series, just a simple expression is left:

$$\prod_{n=0}^{N-1}\left[1+\frac{x}{N}+O(1/N^2)\right]=e^x+O(1/N)\ . \tag{2.25}$$

Considering this, the generating functional (2.21) can be rewritten as

$$I[j]=\exp\left\{-\frac{1}{2}\int_{-\infty}^{\infty}dx\int_{-\infty}^{\infty}dx'\,j(x)\,j(x')\,R(x-x')\right\}+O(1/N). \tag{2.26}$$

This discussion shows that the Randomization Method produces Gaussian correlated random potentials in the limit of $N\to\infty$. Even for smaller N it gives a good approximation with the error being of the order $1/N$. Also, one notices that the choice of the variance α^2 in (2.16) is quite reasonable as it cancels out of the exponent in the step from (2.20) to (2.21). Thus, it assures the right form of the generating functional.
Of course, there are more intricate ways of constructing random functions with a given correlation and distribution function. To get an overview see Ref. [44], where optimizations of the Randomization Method and another approach with better fractal properties, the so-called Fourier Wavelet Method, are introduced.

2.2.1 Gaussian Correlation

In the following, two sorts of correlation functions will be investigated. First, we concentrate on a Gaussian correlated random field as an example for short range correlations. They are represented by the correlation function

$$R(x)=\frac{\varepsilon^2}{\sqrt{2\pi}\lambda}\exp\left\{-\frac{x^2}{2\lambda^2}\right\}\ , \tag{2.27}$$

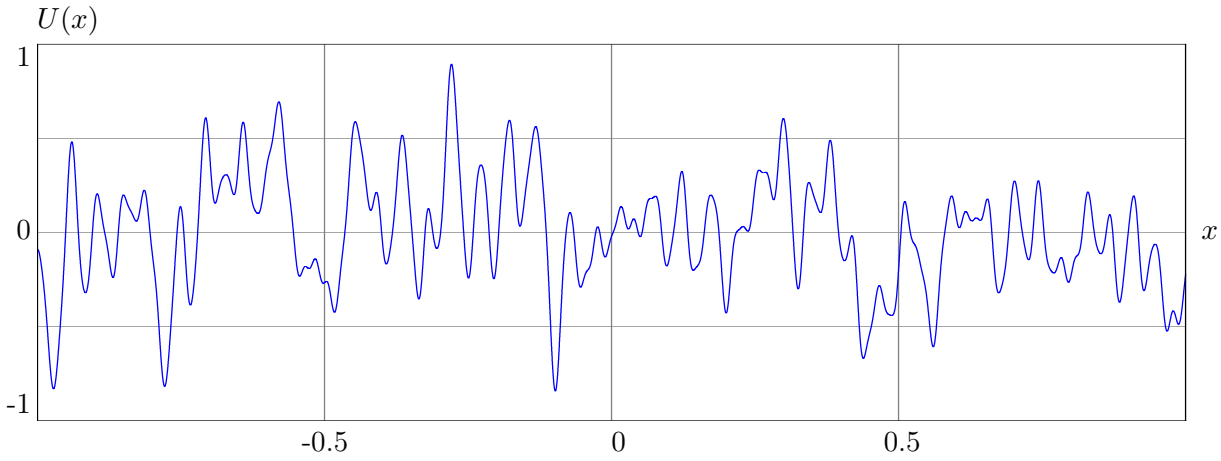

Figure 2.1: Sample potential for Gaussian correlation with $N = 100$, $\varepsilon = 1$, and $\lambda = 1$.

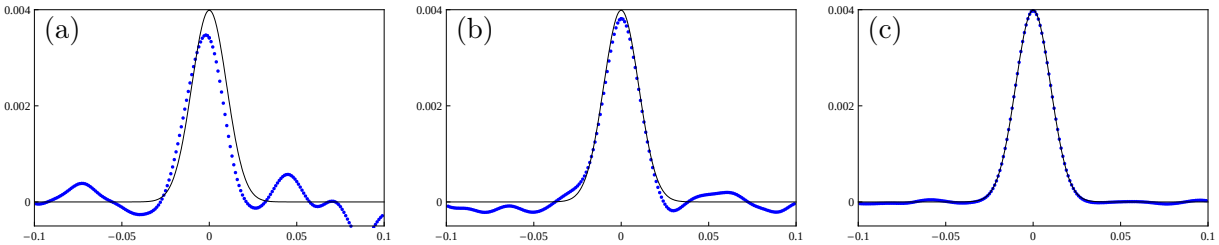

Figure 2.2: Correlation $\overline{U(x)U(0)}$ with $N = 100$ averaged over (a) 100, (b) 1 000, and (c) 10 000 sample potentials compared to $R(x)$ from (2.27) (black line).

where ε^2 is a measure of the strength of the correlation. In this case it is very simple to calculate its Fourier transform (2.2) via completing the square. One finds the spectral density

$$S(k) = \frac{\varepsilon^2}{2\pi} \exp\left\{-\frac{\lambda^2 k^2}{2}\right\}. \tag{2.28}$$

Integrating $S(k)$ over all k gives the first parameter of the Randomization Method according to (2.16):

$$\alpha^2 = \frac{\varepsilon^2}{\sqrt{2\pi}\,\lambda}. \tag{2.29}$$

The probability distribution of the wave numbers k, thus, is simply a normal distribution with variance $1/\lambda^2$:

$$p(k) = \frac{\lambda}{\sqrt{2\pi}} \exp\left\{-\frac{\lambda^2 k^2}{2}\right\}. \tag{2.30}$$

We show in Fig. 2.1 a typical example of a random potential generated by (2.13) for $\varepsilon = 1$ and $\lambda = 1$. The same values of α and λ are used to show in Fig. 2.2 the correlation function $U(x)U(0)$ (blue dots) sampled for $N = 100$ and averaged over 100, 1 000 and 10 000 pseudo-randomly generated functions, respectively. The results are compared to the expected correlator $R(x)$ plotted as a solid black line. The larger the value of N, the better the correlation is described by Gaussian curve.

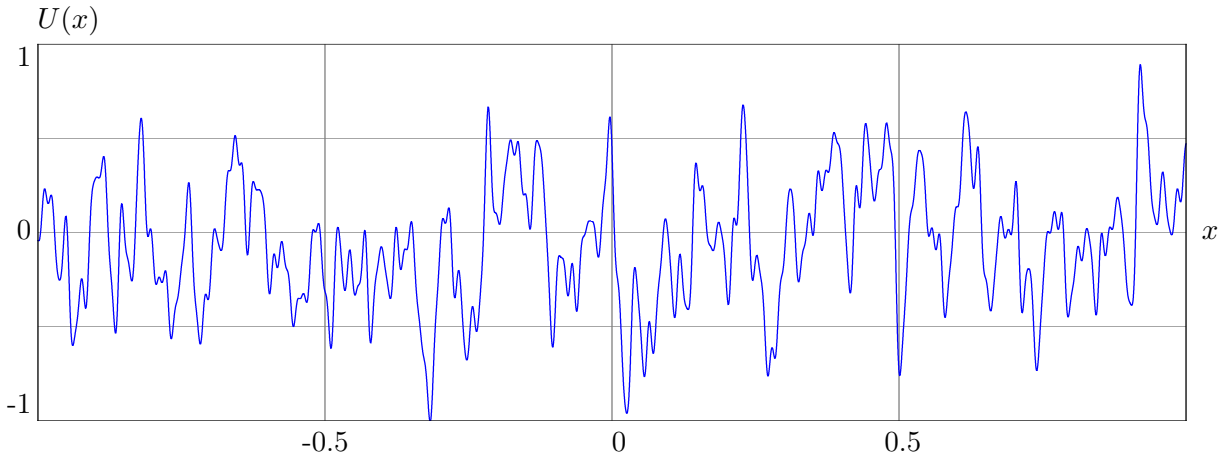

Figure 2.3: Sample potential for Cauchy-type correlation with $N = 100$, $\varepsilon = 1$, and $\lambda = 1$.

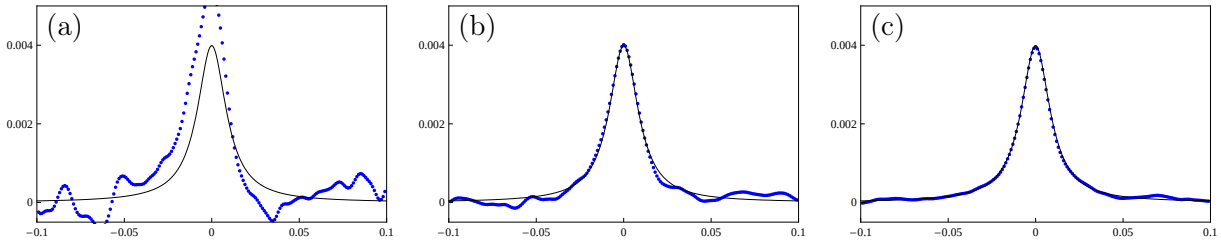

Figure 2.4: Correlation $\overline{U(x)U(0)}$ with $N = 100$ averaged over (a) 100, (b) 1 000 and (c) 10 000 sample potentials compared to $R(x)$ from (2.31) (black line).

2.2.2 Cauchy-Type Correlation

To model longer ranged correlations, a Cauchy-distribution is taken to be the correlation function, which is described by

$$R(x) = \varepsilon^2 \frac{\lambda}{\pi} \frac{1}{\lambda^2 + x^2} \,. \tag{2.31}$$

Again ε^2 is a measure of the strength of the correlation. The spectral density is calculated to be

$$S(k) = \frac{\varepsilon^2}{2\pi} \, e^{-\lambda |k|} \tag{2.32}$$

and its integration yields

$$\alpha^2 = \frac{\varepsilon^2}{\lambda \pi} \,. \tag{2.33}$$

Therefore, we get an exponential distribution for the probability density of the wave number k

$$p(k) = \frac{\lambda}{2} e^{-\lambda |k|} \,. \tag{2.34}$$

Fig. 2.3 shows a sample potential with Cauchy-type correlation but otherwise the same values for N, λ and α as used in the previous paragraph. Compared with the case of a Gauss correlator,

one notices faster and stronger fluctuations around zero. Again averaging over pseudo-randomly generated sample potentials, the correlation converges to the expected Cauchy-function for large N. Fig. 2.4 shows the numerically averaged correlation $U(x)U(0)$ over 100, 1 000 and 10 000 sample potentials.

Chapter 3

Harmonic Oscillator in Random Potential

In this chapter, we will focus on a harmonic oscillator in a random environment. This quite simple problem has vast applications, for example, in chemistry or biology [6, 7]. The aim is to find the disorder-averaged thermodynamic properties of this system. Unfortunately, it is problematic to calculate the free energy due to the averaging process. To overcome this, appropriate varitational techniques will be applied. They are based on standard perturbation theory. The quality of the obtained approximations will be judged by comparing them with Monte Carlo simulations. In the previous chapter, the algorithm to generate random functions was shown to work with controllable accuracy. Thus, we expect the simulations to be quite accurate. An example for such a source code can be found in App. B.

3.1 Perturbation Approach

The most straightforward approximation method is perturbation theory. Our starting point will be the Hamilton function without disorder

$$H_0 = \frac{1}{2}\kappa\, x^2 \tag{3.1}$$

and the additional random potential will be treated as a small perturbation of the system. The thermodynamic properties of the harmonic oscillator are well-known. The partition function Z_0 is calculated to be

$$Z_0 = \int_{-\infty}^{\infty} dx\, \exp\left(-\frac{1}{2}\beta\kappa x^2\right) = \sqrt{\frac{2\pi}{\beta\kappa}} \tag{3.2}$$

and, thus, the free energy (1.8) reads

$$F_0 = \frac{1}{2\beta}\log\left(\frac{\kappa\beta}{2\pi}\right)\ . \tag{3.3}$$

Furthermore, one defines the expectation value

$$\langle\, \bullet \,\rangle_{H_0} = \frac{1}{Z_0}\int_{-\infty}^{\infty} dx\, \exp[-\beta\, H_0(x)]\ \bullet\ . \tag{3.4}$$

With the help of these definitions, one can rewrite the partition function with disorder in terms of the expectation value (3.4):

$$Z = Z_0 \left\langle \exp\left[-\beta\,\varepsilon\,U(x)\right] \right\rangle_{H_0} \ . \tag{3.5}$$

In the following, we will expand the partition function in terms of ε.

3.1.1 Cumulant Expansion

Knowing the Taylor series of the exponential functions, we can expand the potential energy part of the partition function:

$$\begin{aligned}\left\langle \exp\left[-\beta\,\varepsilon\,U(x)\right] \right\rangle_{H_0} = \quad & 1 - \beta\,\varepsilon\,\langle U(x)\rangle_{H_0} + \frac{\beta^2\,\varepsilon^2}{2!}\langle U(x)^2\rangle_{H_0} \\ & -\frac{\beta^3\,\varepsilon^3}{3!}\langle U(x)^3\rangle_{H_0} + \ldots \ .\end{aligned} \tag{3.6}$$

The perturbative procedure (3.6) is called moment expansion. However, since the quantity of interest will be the free energy, we concentrate on the so-called cumulant expansion and determine the expansion of the logarithm [45]

$$\begin{aligned}\left\langle \exp\left[-\beta\,\varepsilon\,U(x)\right] \right\rangle_{H_0} = \quad & \exp\Big\{ -\beta\,\varepsilon\,\langle U(x)\rangle^c_{H_0} + \frac{\beta^2\,\varepsilon^2}{2!}\langle U(x)^2\rangle^c_{H_0} \\ & -\frac{\beta^3\,\varepsilon^3}{3!}\langle U(x)^3\rangle^c_{H_0} + \ldots\Big\} \ .\end{aligned} \tag{3.7}$$

Evaluating the series of the exponential function explicitly in the cumulant expansion (3.7) and equating the coefficients of the generated polynomial of ε yields the aspired expressions for the cumulants. In first-order cumulant and moment expansion are equal:

$$\langle U(x)\rangle^c_{H_0} = \langle U(x)\rangle_{H_0}. \tag{3.8}$$

The second cumulant corresponds to the variance

$$\langle U(x)^2\rangle^c_{H_0} = \langle U(x)^2\rangle_{H_0} - \langle U(x)\rangle^2_{H_0} \, . \tag{3.9}$$

In a similar way, the third cumulant yields

$$\langle U(x)^3\rangle^c_{H_0} = \langle U(x)^3\rangle_{H_0} - 3\langle U(x)^2\rangle_{H_0}\langle U(x)\rangle_{H_0} + 2\langle U(x)\rangle^3_{H_0} \ . \tag{3.10}$$

As it will be needed later on, the fourth cumulant reads accordingly

$$\begin{aligned}\langle U(x)^4\rangle^c_{H_0} = \quad & \langle U(x)^4)\rangle_{H_0} - 3\langle U(x)^3\rangle_{H_0}\langle U(x)\rangle_{H_0} - 3\langle U(x)^2\rangle^2_{H_0} \\ & +12\langle U(x)^2\rangle_{H_0}\langle U(x)\rangle^2_{H_0} - 6\langle U(x)\rangle^4_{H_0} \ .\end{aligned} \tag{3.11}$$

A systematic method to calculate the n-th cumulant in terms of the moments is mentioned in Ref. [36].
In terms of the cumulant expansion the free energy for a fixed representative of the ensemble of random potentials can now be computed as

$$F_{\text{rand}} = F_0 - \frac{1}{\beta}\sum_{k=1}^{\infty}\frac{(-\varepsilon\,\beta)^k}{k!}\Big\langle U(x)^k\Big\rangle^c_{H_0} \ . \tag{3.12}$$

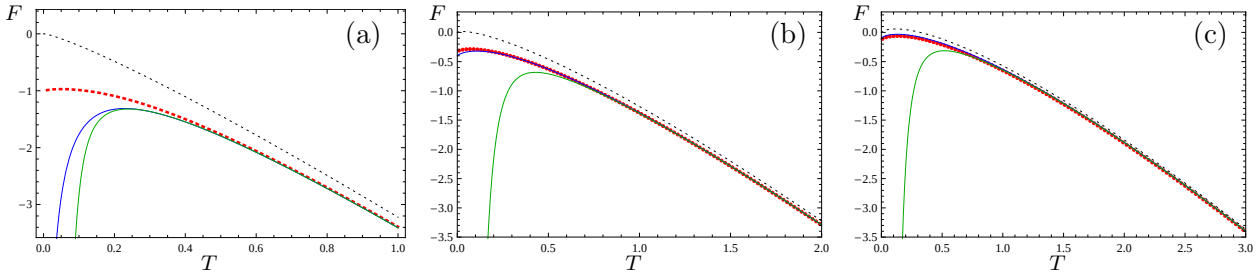

Figure 3.1: Zeroth (dotted, black), first (solid, blue), and second (solid, green) order expansion of the free energy with parameters $\varepsilon = 1$, $\lambda = 1$, and (a) $\kappa = 0.01$, (b) $\kappa = 0.5$, (c) $\kappa = 2$, respectively, compared to computer simulations (dashed, red).

The averaging process (2.4) yields the free energy F of the system. Because the random potentials are normally distributed, odd cumulants of $U(x)$ vanish. To approximate the free energy, we will truncate the series after N terms. Hence, up to N^{th} order we get

$$F_N = F_0 + \sum_{k=1}^{N} F^{(2k)} \quad , \tag{3.13}$$

with the coefficients

$$F^{(k)} = \frac{(-\beta)^{k-1}\varepsilon^k}{k!} \overline{\left\langle U(x)^k \right\rangle_{H_0}^{c}} \, . \tag{3.14}$$

The cumulant expansion is a weak coupling perturbation series for small correlation strength ε. At this point, we remind of the rescaled Hamilton function (1.10). The physics of the system just depends on the ratio of κ/ε. In the following, we discuss the three cases of $\kappa >> \varepsilon$, $\kappa \approx \varepsilon$, and $\varepsilon >> \kappa$ separately. We therefore will fix $\varepsilon = 1$ in all plots and discuss the cases for changing κ.

3.1.2 First- and Second-Order Free Energy

The first non-vanishing correction to F_0 arises from the second cumulant (3.9). Applying (1.2), one gets as the first non-vanishing order approximation

$$F^{(2)} = -\frac{\beta\,\varepsilon^2}{2}\left[\overline{\langle U(x)^2\rangle_{H_0}} - \overline{\langle U(x)\rangle_{H_0}^2}\right] \, . \tag{3.15}$$

Wisely adding the identity $1 = Z_0^{-1}\int_{-\infty}^{\infty} dx' \exp(-\kappa\beta x^2/2)$, we get in a compact notation with all integration limits going from $-\infty$ to ∞

$$F^{(2)} = -\frac{\beta\,\varepsilon^2}{2Z_0^2}\iint dx'dx'' \exp\left[-\frac{1}{2}\kappa\beta(x'^2 + x''^2)\right]\left[R(0) - R(x' - x'')\right] \, . \tag{3.16}$$

Evaluating for the Gaussian correlation (1.3) of the toy model yields the expression

$$F^{(2)} = -\frac{\beta\,\varepsilon^2}{2\lambda\sqrt{2\pi}}\left[1 - \frac{\kappa\,\beta\,\lambda}{\sqrt{\kappa\,\beta(2 + \kappa\,\beta\,\lambda^2)}}\right] \, . \tag{3.17}$$

The second non-vanishing coefficient $F^{(4)}$ involves the computation and averaging of the 4$^{\text{th}}$ cumulant (3.11) which yields

$$F^{(4)} = -\frac{\beta^3\,\varepsilon^4}{24 Z_0^4}\iiiint dx'dx''dx'''dx'''' \exp\left[\frac{1}{2}\kappa\beta(x'^2+x''^2+x'''^2+x''''^2)\right]\left[3R(0)R(x'-x'')\right.$$
$$\left.+24R(x'-x'')R(x'-x''')-6R(x'-x'')^2-18R(x'-x'')R(x'''-x'''')\right]\,. \tag{3.18}$$

For the toy model at stake the coefficients result in

$$F^{(4)} = -\frac{\varepsilon^4\kappa\beta^4}{16\pi}\left[-\frac{6}{2+\kappa\beta\lambda^2}+\frac{8}{\sqrt{3+4\kappa\beta\lambda^2+\kappa^2\beta^2\lambda^4}}+\frac{1}{\lambda\sqrt{\kappa\,\beta(2+\kappa\,\beta\,\lambda^2)}}\right.$$
$$\left.-\frac{2}{\lambda\sqrt{\kappa\,\beta(4+\kappa\,\beta\,\lambda^2)}}\right]\,. \tag{3.19}$$

The free energy can now be approximated by (3.13) with the corrections (3.17) and (3.19). First- and second-order perturbation expansion of the free energy are compared with computer simulations in Fig. 3.1. We notice that the second order turns out to be a worse approximation in comparison with the numeric curve for small temperatures. To verify this impression, we investigate the limit $T \to 0$ of the obtained expressions:

$$\lim_{T\to 0} F^{(0)} = 0\,, \tag{3.20}$$

$$\lim_{T\to 0} F^{(1)} = -\frac{\varepsilon^2}{\sqrt{2\pi}}\frac{1}{2\kappa\lambda^3}\,, \tag{3.21}$$

$$\lim_{T\to 0} F^{(2)} = -\infty\,. \tag{3.22}$$

In our derivation, we performed an expansion for small coupling ε^2. We did expect the first-order expansion to approximate the system's free energy reasonably well for very small coupling parameters, i.e., large κ. The second order correction produces a divergent term and, thus, cannot describe the behavior of the system for small temperatures. As illustrated by the Fig. 3.1, the first-order result does indeed aproximate the expected curve well for large κ. Only in the case $\kappa = 0.01$ one recognizes a visible deviation from numerical results. For $T = 0$ and $\kappa = 0.01$, the first-order free energy is about 20 times the value of the simulated free energy.

3.1.3 Mean Square Displacement

To be able to compare with experimental data, we will investigate a physical quantity which is accessible by experiments namely the mean square displacement of the particle. The angle brackets without subscript denote the thermal average of the original system (1.6)

$$\langle\bullet\rangle = \frac{1}{Z}\int_{-\infty}^{\infty} dx\,\exp\left[-\beta\,H(x)\right]\bullet\,. \tag{3.23}$$

One has to keep in mind, that the disorder averaging processes does not commute with (3.23). Taking the average over all realizations of the random potential has to occur after thermal averaging. Thus, the mean square displacement writes

$$\overline{\langle x^2\rangle} = \overline{\frac{1}{Z}\int_{-\infty}^{\infty} dx\,x^2\exp\left[-\beta\,H(x)\right]}\,. \tag{3.24}$$

Closely looking at the toy model Hamilton function (1.6), one can use a mathematical trick often used in statistical physics: one differentiates with respect to the parameter κ and rewrites the resulting expression in form of a logarithm. Doing so, we get

$$\overline{\langle x^2 \rangle} = -\frac{2}{\beta}\overline{\frac{1}{Z}\frac{d}{d\kappa}Z} = -\frac{2}{\beta}\frac{d}{d\kappa}\overline{\log Z} \ . \tag{3.25}$$

With help of the definition for the free energy (1.8), this reduces to

$$\overline{\langle x^2 \rangle} = 2\,\frac{d}{d\kappa}F \ . \tag{3.26}$$

Now the mean square displacement can be obtained from the perturbation expansion of the free energy (3.13) and (3.26).

3.1.4 First- and Second-Order Mean Square Displacement

To calculate the first- and second-order corrections of the perturbation series for weak correlation strength ε of the mean square displacement, we just have to differentiate the first- and second-order free energy with respect to κ according to (3.26). The calculation yields

$$\overline{\langle x^2 \rangle}^{(0)} = \frac{1}{\kappa\beta} \tag{3.27}$$

for the unperturbed mean square displacement. In first order one finds the correction

$$\overline{\langle x^2 \rangle}^{(1)} = \beta^{3/2}\frac{\varepsilon^2}{\sqrt{2\pi}}\frac{1}{\sqrt{\kappa(2+\beta\lambda^2\kappa)^3}} \ . \tag{3.28}$$

The second-order correction of the mean square displacement expansion for small correlation length writes

$$\begin{aligned}\overline{\langle x^2 \rangle}^{(2)} = \quad & \frac{\beta^4}{4}\frac{\varepsilon^4}{2\pi}\Bigg[-\frac{12}{(2+\kappa\beta\lambda^2)^2} + \frac{12}{2+\kappa\beta\lambda^2} - \frac{8}{\sqrt{3+4\kappa\beta\lambda^2+\kappa^2\beta^2\lambda^4}} \\ & -\frac{1}{\lambda}\frac{1}{\sqrt{\kappa\beta(2+\kappa\beta\lambda^2}} + \frac{1}{\lambda}\frac{2}{\sqrt{\kappa\beta(4+\kappa\beta\lambda^2)}} + \kappa^2\beta^2\lambda\Bigg(\frac{1}{[\kappa\beta(2+\kappa\beta\lambda^2)]^{3/2}} \\ & -\frac{2}{[\kappa\beta(4+\kappa\beta\lambda^2)]^{3/2}} + \frac{8\lambda^3}{(3+4\kappa\beta\lambda^2+\kappa^2\beta^2\lambda^4)^{3/2}}\Bigg)\Bigg] \ . \end{aligned} \tag{3.29}$$

These results are shown and compared to numerical simulations in Fig. 3.2. Again, the respective expressions for small T are investigated. One finds

$$\lim_{T\to 0}\overline{\langle x^2 \rangle}^{(0)} = 0 \tag{3.30}$$

$$\lim_{T\to 0}\overline{\langle x^2 \rangle}^{(1)} = \frac{\varepsilon^2}{\sqrt{2\pi}}\frac{1}{\kappa^2\lambda^3} \tag{3.31}$$

$$\lim_{T\to 0}\overline{\langle x^2 \rangle}^{(2)} = -\infty \ . \tag{3.32}$$

As was the case for the free energy expansion, one finds again a divergent contribution from the second-order correction.

In the following part of this chapter, we will mainly be concerned with finding a better approximation in the small temperature regime.

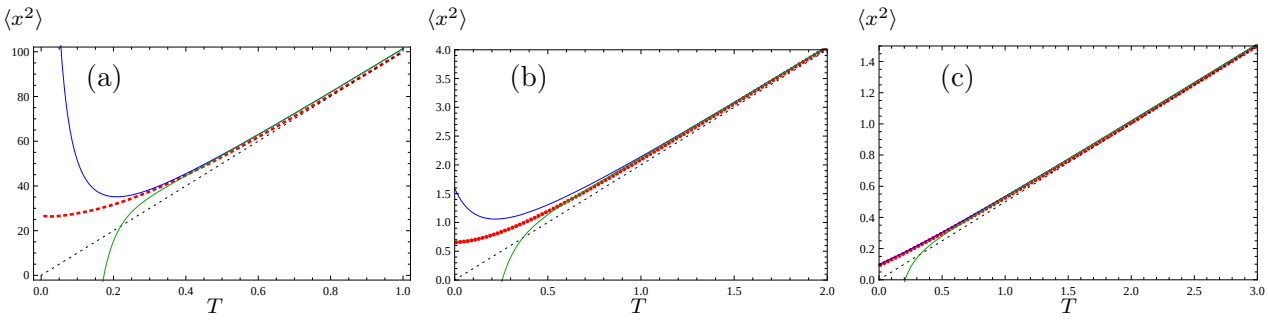

Figure 3.2: Zeroth (dotted, black), first (solid, blue) and second (solid, green) order approximation of the mean square displacement with paremeters $\varepsilon = 1$, $\lambda = 1$, and (a) $\kappa = 0.01$, (b) $\kappa = 0.5$, (c) $\kappa = 2$, respectively, compared to computer simulations (dashed, red).

3.2 Variational Perturbation Theory

Improved results are expected to be given by variational perturbation theory (VPT), which has already been shown to be a useful tool to handle divergencies in many physical problems [12]. In the following, this method will be introduced. As well, a shortcut will be shown to resum weak-coupling perturbation series. We will at first discuss the variational perturbation approach in a standard way using the frequency ω instead of the spring constant κ, which has been used in our toy model (1.6). This will help to gain more physical insight. Then just small adjustments have to be made to apply VPT to the original problem.

A simple Hamilton function is given by

$$H(x) = \frac{M}{2}\,\omega^2\,x^2 + \varepsilon V(x)\,, \tag{3.33}$$

where ε is a small parameter. Now, the partition function is calculated by (1.7) and the free energy by taking its logarithm and multiplying by $-T$ as in (1.8). We assume that both, the partition function and the free energy of this problem, cannot be calculated exactly. Therefore, one is in need of a good approximation to extract the system's physical information.

At first, we will introduce artificially a harmonic oscillator with trial frequency Ω by adding and substracting a term in the Hamilton function:

$$H(x) = \frac{M}{2}\,(\omega^2 + \Omega^2)\,x^2 - \frac{M}{2}\,\Omega^2 x^2 + \varepsilon\,V(x)\ . \tag{3.34}$$

The idea of variational perturbation theory is to treat the deviation from the harmonic oscillator with trial frequency as a perturbation or, to put it simple, to approximate the original system by a harmonic oscillator. The problem breaks down to the task of finding the optimal frequency. To do this in detail, one defines the trial Hamilton function

$$H_t(x) = \frac{M}{2}\,(\omega^2 + \Omega^2)\,x^2\ . \tag{3.35}$$

As well, one defines an expectation value of the trial system (3.35) to prepare the cumulant expansion:

$$\langle \bullet \rangle_{H_t} = \frac{1}{Z_t}\int_{-\infty}^{\infty} dx\,\exp[-\beta H_t(x)]\ \bullet\ . \tag{3.36}$$

Furthermore, we calculate the partition function

$$Z_t = \int_{-\infty}^{\infty} dx \exp[-\beta H_t(x)] = \sqrt{\frac{2\pi}{\beta M(\omega^2 + \Omega^2)}} \; . \tag{3.37}$$

Now the free energy can be approximated by the truncated series of the cumulant expansion (3.7) as

$$F_N = F_0 - \frac{1}{\beta} \sum_{k=1}^{N} \frac{(-\varepsilon\,\beta)^k}{k!} \left\langle \left[\varepsilon\, V(x) - \frac{M}{2}\,\Omega^2\, x^2 \right]^k \right\rangle_{H_t}^{c} \tag{3.38}$$

with $\varepsilon \to 1$. Note that the free energy in the limit $N \to \infty$ does not depend on the trial frequency Ω. The truncated series F_N, however, does. This is the central point of the variational perturbation method. The new parameter Ω provides a tool to optimize the approximated expression for the free energy. For the optimal parameter one requires

$$\frac{dF_N}{d\Omega} = 0 \; . \tag{3.39}$$

This strategy is referred to as *principle of minimal sensitivity* [46]. If no minimum exists, one needs to carefully investigate higher derivates with respect to the variational paramter Ω [12]. The idea is quite intriguing: Since the infinite series does not depend on the variational parameter, one searches for a solution which depends least on it. A special case is $N = 1$, which can be shown to give an optimal upper bound. This is referred to as the Jensen-Peierls inequality:

$$F \leq F_0 + \langle H(x) - H_t(x) \rangle_{H_t} \; . \tag{3.40}$$

Thus, in first order we search for a minimum of the trial free energy F_1 depending on the variational parameter Ω to obtain an optimal upper bound.

3.2.1 Square Root Substitution

If the first coefficients are already calculated in standard perturbation theory, Kleinert's square root substitution comes in handy to optimize the approximation [12, 47]. It is a clever shortcut to obtain (3.38). The idea is to rewrite the Hamilton function (3.34) as

$$H(x) = \frac{M}{2} \left(\Omega \sqrt{1 + \varepsilon\, r} \right)^2 x^2 + \varepsilon\, V(x) \tag{3.41}$$

with the newly defined auxiliary parameter

$$r = \frac{\omega^2 - \Omega^2}{\varepsilon\, \Omega^2} \; . \tag{3.42}$$

Formally treating the parameter r as being independent of ε, one expands the free energy for small coupling ε up to the considered order. We remark that this corresponds to performing the formal square root substitution

$$\omega \to \Omega \sqrt{1 + \varepsilon\, r} \tag{3.43}$$

into the standard perturbation series and a subsequent expansion in powers of ε. Then (3.42) is resubstituted. Again, it is to note that the full expansion does not depend on the parameter Ω. whereas the truncated series does.

Underlying the square root substitution is a harmonic oscillator with trial frequency Ω. Artificially, a dependence of this frequency is introduced. As the free energy is independent of this variational parameter, one searches for the expression which least depends on it. It is quite tempting to move away from the physical view and to see the square root expansion as a mere mathematical tool. In a given function $f(\omega)$ which is expanded in terms of a coupling parameter ε the identity (3.42) is inserted. Accordingly, a dependence of the variational parameter Ω is introduced by an expansion in ε to the respective order N. With this, we get a new function $f_N(\omega, \Omega)$. Then the optimal approximation to the exact result is the one least sensitive to the artificial parameter [46].

3.2.2 Resummation of Perturbation Expansion

We will use the square root substitution (3.43) in order to try to improve the result for the free energy and the mean square displacement. For practical reasons we used the spring constant $\kappa = m\,\omega^2$ to describe the harmonic oscillator in (1.6). Therefore, a tiny adaption of (3.43) has to be made. In terms of the spring constant κ and coupling ε^2, the substitution writes

$$\kappa \to \sigma(1 + \varepsilon^2 r) \tag{3.44}$$

with the parameter r given by

$$r = \frac{\kappa - \sigma}{\varepsilon^2\,\sigma} \ . \tag{3.45}$$

As discussed at the end of Sect. 3.2.1, we could simply treat this as a mathematical trick and differentiate the expanded expression with respect to κ. However, to emphasize the physical idea behind the square root substitution, we will relate the appearing conditional equations. Substituting (3.44) into the free energy and expanding in orders of ε^2, one gets an expression

$$F_N(\kappa, \sigma) = F_N(\omega^2, \Omega^2) \ . \tag{3.46}$$

Due to (3.39), the corresponding conditional equation calculates with the chain rule

$$\frac{d\,F_N(\omega^2, \Omega^2)}{d\Omega} = \frac{d\,F_N(\omega^2, \Omega^2)}{d\Omega^2} \cdot 2\,\Omega = 2\sqrt{\sigma}\,\frac{d\,F_N(\kappa, \sigma)}{d\sigma} = 0 \ . \tag{3.47}$$

Accordingly, the conditional equation

$$\frac{d\,F_N(\kappa, \sigma)}{d\sigma} = 0 \tag{3.48}$$

is going to be used. The solution $\sigma = \kappa$ reproduces the perturbation expansion and, thus, one does not expect new or better approximations. We keep this case in mind as a solution of the conditional equation, but it will be excluded from the discussion to follow.

3.2.3 Resummation of First-Order Free Energy

At first, we will apply the variational method to the first-order free energy. Substituting (3.45) into F_1 and expanding to first order coupling ε^2 leads to

$$F_1(\kappa, \sigma) = -\frac{1}{\beta}\log\sqrt{\frac{2\pi}{\sigma\beta}} + \frac{1}{2\sigma\beta}(\kappa - \sigma) + \frac{\beta}{2}\frac{\varepsilon^2}{\sqrt{2\pi}}\left[-\frac{1}{\lambda} + \frac{\sigma\beta}{\sqrt{\sigma\beta(2 + \sigma\beta\lambda^2)}}\right] \ . \tag{3.49}$$

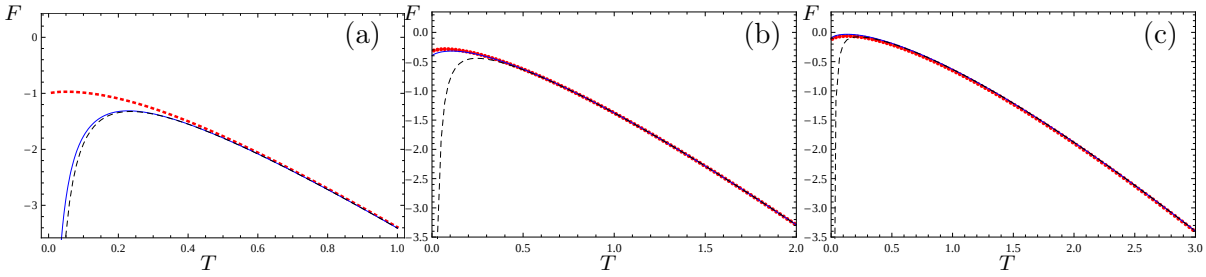

Figure 3.3: Resummation of first-order free energy (solid, blue) with parameters $\varepsilon = 1$, $\lambda = 1$, and (a) $\kappa = 0.01$, (b) $\kappa = 0.5$, (c) $\kappa = 2$, respectively, compared to computer simulations. The dashed black line represents the resummation result. The result $\sigma = \kappa$ was explicitly excluded.

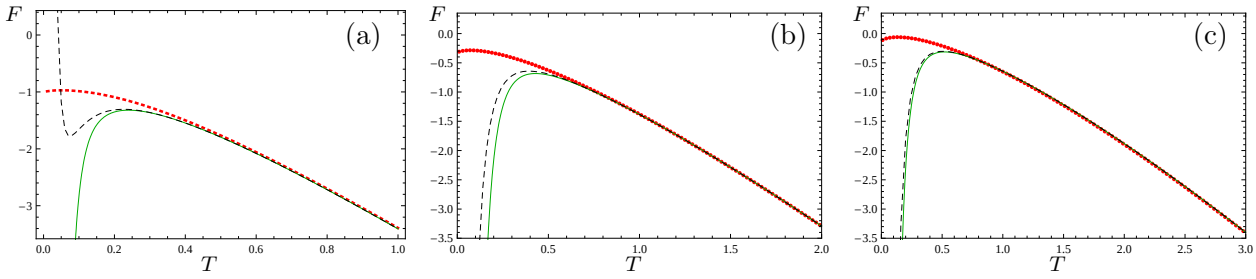

Figure 3.4: Resummation of second-order free energy (solid, green) with parameters $\varepsilon = 1$, $\lambda = 1$, and (a) $\kappa = 0.01$, (b) $\kappa = 0.5$, (c) $\kappa = 2$, respectively, compared to computer simulations (dashed, red). The dashed black line represents the resummation result. The result $\sigma = \kappa$ was explicitly excluded.

Differentiating with respect to σ yields the conditional equation

$$0 = \frac{1}{2\sigma\beta} + \frac{\beta}{2}\frac{\varepsilon^2}{\sqrt{2\pi}}\left\{\frac{\beta}{\sqrt{\sigma\beta(2+\sigma\beta\lambda^2)}} - \frac{\sigma(1+\sigma\beta\lambda^2)}{\beta^2[\sigma\beta(2+\sigma\beta\lambda^2)]}\right\} - \frac{2\kappa}{\sigma^2\beta^2}\ , \tag{3.50}$$

which has to be solved numerically. All numerical results are plotted in Fig. 3.3. No improvement of the perturbative correction is visible and, therefore, in first order no non-perturbative contributions can be added.

3.2.4 Resummation of Second-Order Free Energy

To obtain the second-order result of the free energy, we have to follow the same steps. In second order the free energy writes

$$\begin{aligned} F_2(\kappa,\sigma) = \quad & -\frac{1}{2\beta}\log\left(\frac{2\pi}{\beta\sigma}\right) - \frac{1}{4\beta}\frac{\kappa^2-4\kappa\sigma+3\sigma^2}{\sigma^2} + \frac{\varepsilon^2}{2\pi}\frac{\beta}{2\gamma\sqrt{2\beta\sigma+\beta^2\gamma^2\sigma^2}}\left[\sqrt{\beta\sigma(2+\beta\gamma^2\sigma)}\right. \\ & \left.-\frac{\beta\gamma(\kappa+\sigma+\beta\gamma^2\sigma^2}{2+\beta\gamma^2\sigma}\right] + \frac{\varepsilon^4}{2\pi}\beta^5\sigma\left[\frac{12}{2+\beta\gamma^2\sigma} - \frac{16}{\sqrt{3+4\beta\gamma^2\sigma+\beta^2\gamma^4\sigma^2}}\right. \\ & \left.-\frac{2}{\gamma\sqrt{\beta\sigma(2+\beta\gamma^2\sigma)}} + \frac{4}{\gamma\sqrt{\beta\sigma(4+\beta\gamma^2\sigma)}}\right]. \end{aligned} \tag{3.51}$$

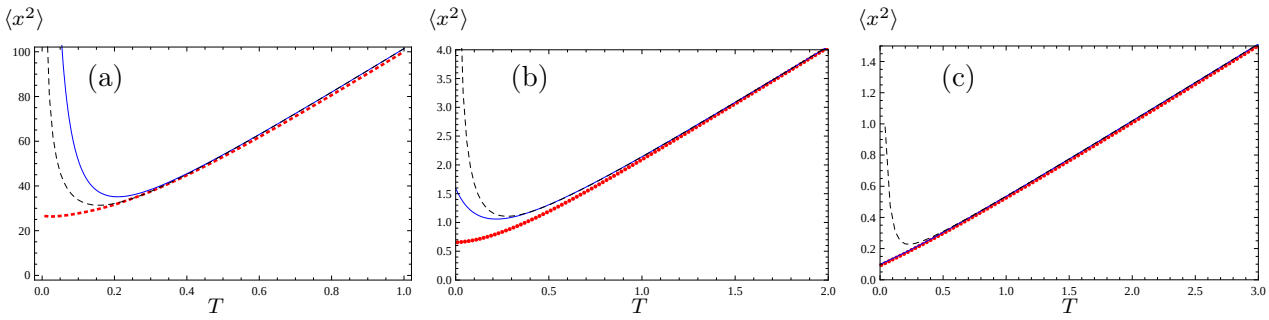

Figure 3.5: Resummation of first-order mean square displacement (solid, blue) with parameters $\varepsilon = 1$, $\lambda = 1$, (a) $\kappa = 0.01$, (b) $\kappa = 0.5$, and (c) $\kappa = 2$, respectively, compared to computer simulations. The dashed black line represents the resummation result. The result $\sigma = \kappa$ was explicitly excluded.

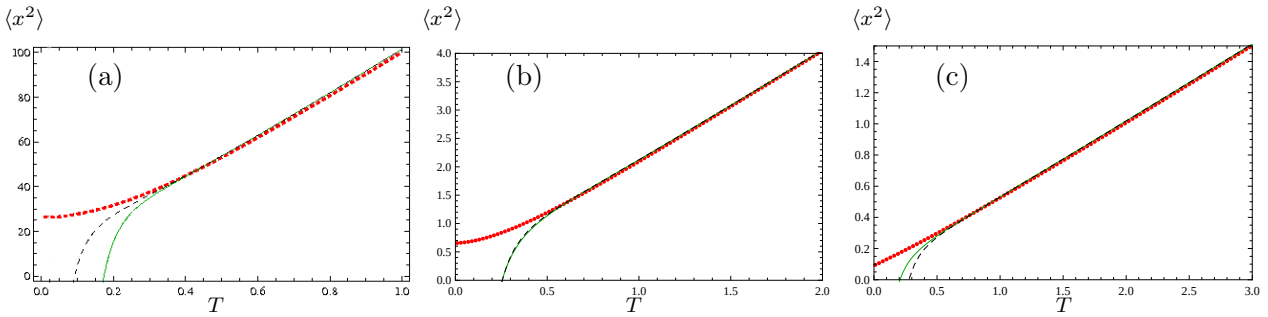

Figure 3.6: Resummation of second-order mean square displacement (solid, green) with parameters $\varepsilon = 1$, $\lambda = 1$, and (a) $\kappa = 0.01$, (b) $\kappa = 0.5$ and (c) $\kappa = 2$, respectively, compared to computer simulations (dashed, red). The dashed black line represents the resummation result. The result $\sigma = \kappa$ was explicitly excluded.

To find the optimal σ we numerically solve

$$\frac{\partial F_2(\kappa,\sigma)}{\partial \sigma} = 0 \ . \tag{3.52}$$

The result is plotted in Fig. 3.4. One does not see an improvement in the overall approximation. The second-order expansion, however, is slightly corrected. Because of its divergence in the $T \to 0$ limit, it cannot be considered as a better approximation as the first-order standard perturbation theory.

3.2.5 Resummation of Mean Square Displacement

In the variational perturbation expansion, the free energy depends on both the parameter κ and the variational parameter σ. The variational parameter is a result of the saddle point equation (3.48), and, therefore, can depend on κ. To calculate the mean square displacement, however, we need to differentiate with respect to κ:

$$\frac{dF_N(\kappa,\sigma)}{d\kappa} = \frac{\partial F_N(\kappa,\sigma)}{\partial \kappa} + \frac{\partial F_N(\kappa,\sigma)}{\partial \sigma}\frac{\partial \sigma}{\partial \kappa} \ . \tag{3.53}$$

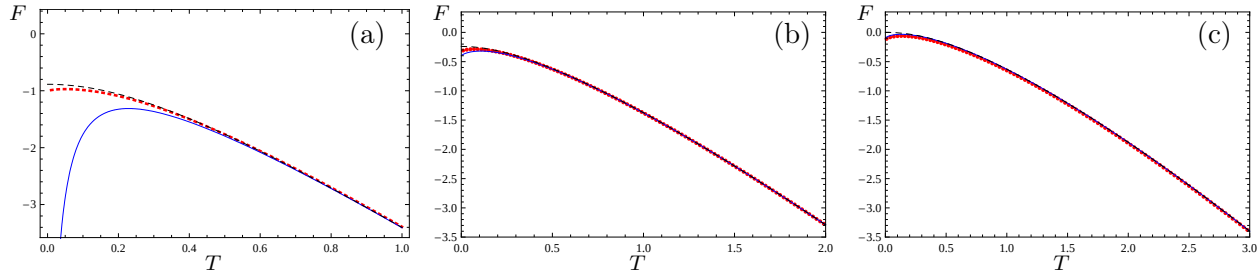

Figure 3.7: Temperature resummation of first-order free energy (solid, blue) with parameters $\varepsilon = 1$, $\lambda = 1$, and (a) $\kappa = 0.01$, (b) $\kappa = 0.5$, (c) $\kappa = 2$, respectively, compared to computer simulations (dashed, red). The dashed black line represents the resummation result.

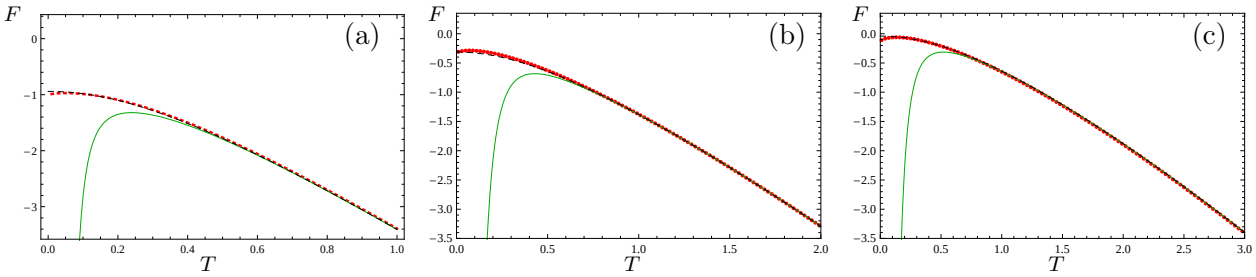

Figure 3.8: Temperature resummation of second-order free energy (solid, green) with parameters $\varepsilon = 1$, $\lambda = 1$, and (a) $\kappa = 0.01$, (b) $\kappa = 0.5$, (c) $\kappa = 2$, respectively, compared to computer simulations (dashed, red). The dashed black line represents the resummation result.

The second term vanishes because of (3.48) and, thus, we just need to calculate the partial derivative with respect to κ. Thus, the mean square displacement is computed to be

$$\overline{\langle x^2 \rangle}_N = 2\frac{\partial F_N(\kappa,\sigma)}{\partial k} \ . \tag{3.54}$$

We find the expression for the mean square displacement in first order to be

$$\overline{\langle x^2 \rangle}_1(\kappa,\sigma) = -\frac{\kappa}{\beta\sigma^2} + \frac{2}{\beta\sigma} + \frac{\varepsilon^2}{\sqrt{2\pi}}\frac{\beta\sigma^3}{\beta\sigma(2+\beta\gamma^2\sigma)^{3/2}} \ . \tag{3.55}$$

The variational parameter σ in (3.55) is the solution of (3.50). The numerical results are plotted in Fig. 3.5. The analog discussion can be made for the second-order corrections. We just show the results in Fig. 3.6. As already noticed in the free energy VPT expansion, no improvement is found.

3.3 Temperature Resummation

In the previous section, we have seen that Kleinert's method to treat the frequency of the harmonic oscillator as a variational parameter does not lead to any improvment. Therefore, we have to leave the usual route. In order to find an analytic for small T that sufficiently well resembles the Monte Carlo simulations, we apply the square root substitution (3.42) rather

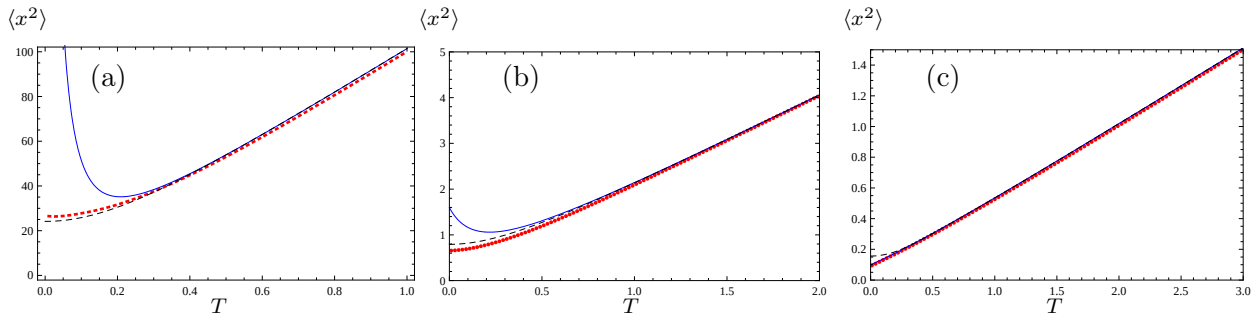

Figure 3.9: Temperature resummation of first-order mean square displacement (solid, blue) with parameters $\varepsilon = 1$, $\lambda = 1$, and (a) $\kappa = 0.01$, (b) $\kappa = 0.5$, (c) $\kappa = 2$, respectively, compared to computer simulations (dashed, red). The dashed black line represents the resummation result.

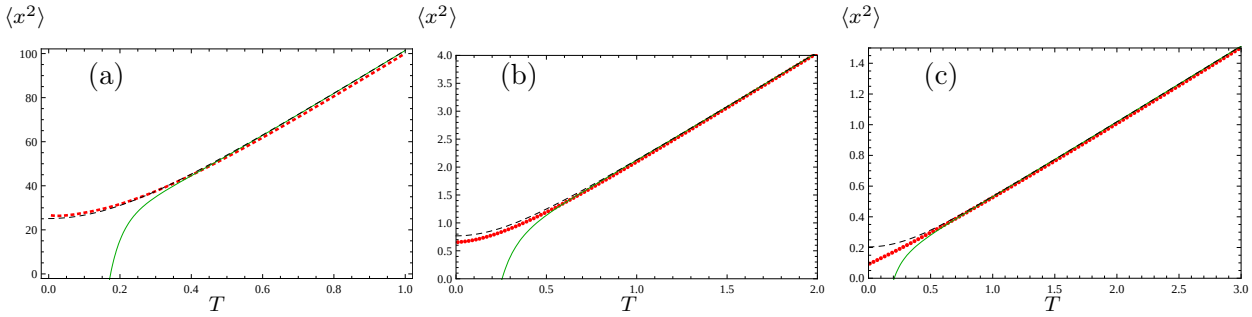

Figure 3.10: Temperature resummation of second-order mean square displacement (solid, green) with parameters $\varepsilon = 1$, $\lambda = 1$, and (a) $\kappa = 0.01$, (b) $\kappa = 0.5$, (c) $\kappa = 2$, respectively, compared to computer simulations (dashed, red). The dashed black line represents the resummation result.

unconventionally. We suggest a new resummation of the perturbation series by treating the temperature instead of the frequency as variational parameter. Therefore, we substitute

$$T \to \tau\sqrt{1+\varepsilon^2 r} \tag{3.56}$$

with the parameter

$$r = \frac{T^2-\tau^2}{\varepsilon^2\tau^2} \ . \tag{3.57}$$

3.3.1 Free Energy

Substituting (3.56) in the expression for the free energy $F_N(T)$ and expanding with respect to the coupling ε^2 to the first order yields the expression

$$F_1(T,\tau) = -\frac{T^2}{4\tau} - \frac{1}{4\tau} + (T^2+\tau^2)\log\left(\frac{2\pi\tau}{\kappa}\right) - \frac{\varepsilon^2}{\sqrt{2\pi}}\frac{2\kappa}{\gamma^2\kappa^2+2\kappa\tau} \ . \tag{3.58}$$

We search the solution which least depends on the variational parameter τ. Thus, we demand

$$\frac{\partial F_1(T,\tau)}{\partial\tau} = 0 \tag{3.59}$$

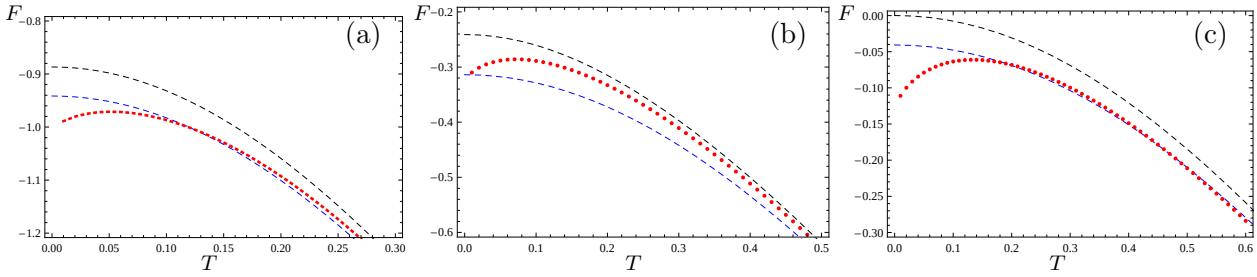

Figure 3.11: Zoomed plot of the temperature resummation of the free energy with parameters $\varepsilon = 1$, $\lambda = 1$, (a) $\kappa = 0.01$, (b) $\kappa = 0.5$ and (c) $\kappa = 2$ respectively. The first order (black, dashed) and the second order (blues ,dashed) compared to computer simulations (red, dotted).

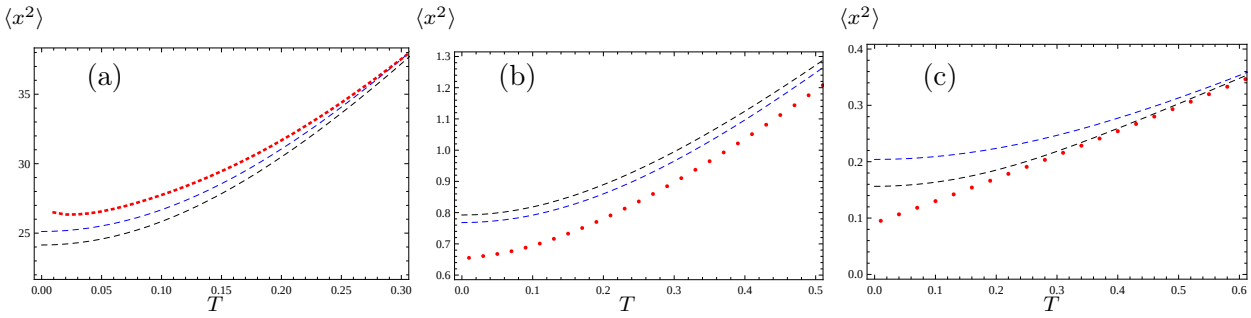

Figure 3.12: Zoomed plot of temperature resummation of the mean square displacement with parameters $\varepsilon = 1$, $\lambda = 1$, (a) $\kappa = 0.01$, (b) $\kappa = 0.5$ and (c) $\kappa = 2$ respectively. The first order (black, dashed) and second order (blue, dashed) are compared to computer simulations (red, dotted).

and get in consequence the conditional equation

$$\begin{aligned} 0 = \quad & \gamma\sqrt{\kappa}(\gamma^2\kappa + 2\tau)^{3/2}(T^2 - \tau^2)\log\left(\frac{2\pi\tau}{\kappa}\right) + 2\frac{\varepsilon^2}{2\pi}\Big[-\gamma^3\kappa^2 - 3\gamma\kappa\tau \\ & +\gamma^2\kappa\sqrt{\kappa(\gamma^2\kappa + 2\tau)} + 2\tau\sqrt{\kappa(\gamma^2\kappa + 2\tau)}\Big] . \end{aligned} \tag{3.60}$$

The numerical results can be seen in Fig. 3.7 and the corresponding one in second order in Fig. 3.8. Even in first order the numerical curve represents extremely well the simulation results.

3.3.2 Mean Square Displacement

With the same argumentation as in Sect. 3.2.5, we calculate the mean square displacement as the partial derivative with respect to κ. With the saddle point equation (3.60), we find a solution which least depends on the varitional parameter. Results are plotted in Fig. 3.9 in first order and in Fig. 3.10 for second. As for the free energy, the results resembles the simulation curves quite well.

3.3.3 Comparison of First and Second Order

It is quite surprising that both, first- and second-order temperature resummation, resemble the simulation curve extremeley well. In Fig. 3.11 and Fig. 3.12 we zoom into the problematic

region near $T = 0$ to get a feeling for the quality of the approximation. The case of large κ can be described quite accurate by standard perturbation theory. For small κ and small temperatures non-perturbative contributions of the disorder potential play a decisive role. In this case, the temperature resembles the simulations with increasing accuracy in second order. For the problematic case $\kappa = 0.01$ in the limit $T = 0$, the deviation to numerical results is an estimated 10% for first order of the free energy, and about 6% in second. For the mean square displacement the picture is quite similar: the difference are about 9% and 8%, respectively. In the case of large κ, however, the resummation is slightly worse than standard perturbation expansion.

Chapter 4

Replica Symmetry

In this chapter, we will apply a different method often used to describe the physics of disordered systems. The replica method is used to rewrite the toy model in form of a many-particle problem. This has the advantage of stating the problem in terms of its correlation function instead of the random potentials. The replica-symmetric solution and its limits will be discussed. In the following, we will describe the problem in the language of Ch. 3. This makes it easy for the reader to proceed to higher orders in variational perturbation theory. This, for instance, has been done to describe the phase diagrams for vortices in certain superconductors in Ref. [24]. We, however, will stop with the calculations of first-order VPT as starting point for the discussion of the replica solutions.

4.1 Replica Trick

A standard method to solve (1.8) is the replica trick [12]

$$\overline{\log Z} = \lim_{n\to 0} \frac{1}{n} \left(\overline{Z^n} - 1\right) , \tag{4.1}$$

which follows directly from the Taylor expansion of the logarithm if the limit and the averaging process commutate. Hence, the disorder-averaged partition function $\overline{Z^n}$ of a system of n identical replicas is calculated for all integer parameters n. Having done this, one has to analytically continue Z^n with respect to n and study it in the limit $n \to 0$. The replicated partition function is given by

$$\overline{Z^n} = \overline{\left\{ \int_{-\infty}^{\infty} dx \, \exp\left[-\beta H(x)\right] \right\}^n} . \tag{4.2}$$

Inserting the Hamilton function (1.6) yields

$$\overline{Z^n} = \int_{-\infty}^{\infty} d^n x \, \overline{\exp\left\{ -\beta \sum_{a=1}^{n} \left[\frac{1}{2} \kappa \, x_a^2 + \varepsilon \, U(x_a) \right] \right\}} . \tag{4.3}$$

Here, the volume element $d^n x$ is an abbreviation for $\prod_{a=1}^{n} dx_a$. Because of Wick's Theorem (2.12), odd moments vanish in the averaging process. Thus, we get

$$\overline{Z^n} = \int_{-\infty}^{\infty} d^n x \, \exp\left[-\frac{\beta}{2} \kappa \sum_{a=1}^{n} x_a^2 \right] \overline{\exp\left[-\beta \, \varepsilon \sum_{a=1}^{n} U(x_a) \right]} . \tag{4.4}$$

The random functions $U(x_a)$ are Gaussian distributed. Therefore, one can use (2.9) and (2.10) to write

$$\overline{\exp\left[-\beta\,\varepsilon\sum_{a=1}^{n}U(x_a)\right]}=\exp\left[\frac{1}{2}\beta^2\varepsilon^2\sum_{a,b}\overline{U(x_a)U(x_b)}\right]=\exp\left[\frac{1}{2}\beta^2\varepsilon^2\sum_{a,b}R(x_a-x_b)\right]\;. \quad (4.5)$$

This allows to calculate the replicated partition function according to

$$\overline{Z^n}=\int d^nx\;\exp\left[-\frac{\beta}{2}\,\kappa\,\sum_{a=1}^{n}x_a^2+\frac{1}{2}\beta^2\varepsilon^2\sum_{a,b}R(x_a-x_b)\right]\;. \quad (4.6)$$

Expression (4.6) can now be reinterpreted as the partition function of a non-random system with the Hamilton function

$$H_r(\boldsymbol{x})=\frac{1}{2}\,\kappa\sum_{a=1}^{n}x_a^2-\frac{1}{2}\beta\,\varepsilon^2\sum_{a,b}R(x_a-x_b) \quad (4.7)$$

with $\boldsymbol{x}=(x_1,x_2,...,x_n)$. Thus, the correlation function $R(x_a-x_b)$ represents a non-linear potential involving two arbitrary replica coordinates a and b. Note that the minus sign in (4.6) indicates that the disorder in the replica formalism is always attractive.

4.2 Variational Perturbation Approach for Replicated Partition Function

Due to the highly nonlinear term in the exponent, it is not possible to calculate (4.6) exactly. Therefore, appropriate approximation methods are needed. In order to include non-perturbative contributions, the approach presented here will be based on variational perturbation theory as introduced in Sect. 3.2. We start with defining a new Hamilton function as [19]

$$H_t(\boldsymbol{x})=\frac{1}{2}\,\kappa\sum_{a=1}^{n}x_a^2-\frac{1}{2}\sum_{a,b}x_a\,\sigma_{ab}\,x_b\,. \quad (4.8)$$

It depends on $n(n-1)/2$ parameters $\sigma_{ab}=\sigma_{ba}$. Later on these parameters will be chosen according to an extremalization condition for the free energy. Furthermore, a matrix G^{-1} is defined in analogy to the covariance of a Gaussian integral

$$G^{-1}_{ab}:=(\kappa\mathbb{I}-\sigma)_{ab}. \quad (4.9)$$

With this matrix G^{-1} the Hamilton function (4.8) is rewritten as

$$H_t(\boldsymbol{x})=\frac{1}{2}\sum_{a,b}x_a\,G^{-1}_{ab}\,x_b\,. \quad (4.10)$$

For the system (4.10) the partition function Z_t reads

$$Z_t=\int d^nx\,\exp\big[-\beta\,H_t(\boldsymbol{x})\big]=\left(\frac{2\pi}{\beta}\right)^{n/2}\frac{1}{\sqrt{\det G^{-1}}}\,, \quad (4.11)$$

which yields the corresponding free energy

$$F_t = -T \log Z_t = -\frac{n}{2\beta} \log \frac{2\pi}{\beta} + \frac{1}{2\beta} \log \det G^{-1} \,. \tag{4.12}$$

It is left to define an expectation value for the system with the new Hamilton function (4.10), which will turn out to be useful in the following discussion:

$$\langle \bullet \rangle_{H_t} = \frac{1}{Z_t} \int d^n x \, \exp\left[-\beta \, H_t(\boldsymbol{x})\right] \bullet \;\; . \tag{4.13}$$

In this formalism, the advantages of the newly introduced Hamilton function become obvious. Evaluating the expectation value means solving averages with a Gaussian weight. The idea is to rewrite (4.6) in a different manner

$$\overline{Z^n} = \int_{-\infty}^{\infty} d^n x \, \exp\Big(-\beta \Big\{ H_t(\boldsymbol{x}) + \left[H_r(\boldsymbol{x}) - H_t(\boldsymbol{x})\right] \Big\}\Big) \;\; . \tag{4.14}$$

We assume the difference of replicated and trial Hamilton function to be small and denote this by an artificial parameter η. The replicated partition function (4.14) is rephrased in terms of the expectation value (4.13):

$$\overline{Z^n} = Z_t \, \big\langle \exp\big\{ -\beta \, \eta \left[H_r(\boldsymbol{x}) - H_t(\boldsymbol{x})\right] \big\} \big\rangle_{H_t} \;\; . \tag{4.15}$$

Of course, we have in mind that the parameter η is evaluated in the limit $\eta \to 1$ at the end, but for the time being, we expand the replicated partition function with respect to η, which will be formally considered a small parameter.

Using (4.15) and the cumulant expansion (3.13) the free energy of the replicated system is given in the N^{th} order by

$$F_n^{(N)} = F_t - \frac{1}{\beta} \sum_{k=1}^{N} \frac{(-\beta)^k}{k!} \Big\langle \left[H_r(\boldsymbol{x}) - H_t(\boldsymbol{x})\right]^k \Big\rangle_{H_t}^{c} \;, \tag{4.16}$$

where η was already set to 1. Note that the replicated free energy does not depend on the parameters σ_{ab} at all. The N-th order expansion, however, does depend on these variational parameters. Therefore, they provide a tool to improve the approximation of the free energy for the replicated system. The optimal σ_{ab} extremize $F_n^{(N)}$ according to the *principle of minimal sensitivity* [12, 46]. Thus, one requires

$$\frac{\partial F_n^{(N)}}{\partial \sigma_{ab}} = 0 \;. \tag{4.17}$$

Especially important will be the optimal upper bound given by the Jensen-Peierls inequality (3.40) in the many-particle case:

$$F_n = F_n^{(\infty)} \leq F_t + \big\langle H_r(\boldsymbol{x}) - H_t(\boldsymbol{x}) \big\rangle_{H_t} \;. \tag{4.18}$$

It is, in fact, the starting point of the usual replica symmetry technique and its successor, the broken replica symmetry [17, 19]. We aspire a safe upper bound approximation of the system's free energy.

4.2.1 A Clever Choice

Handling the cumulant expansion (4.16) involves quite lengthy calculations of the moments of the interaction potential. Therefore, a mathematical trick will be adopted here. First of all, we focus once again on a rewritten version of the replicated partition function (4.13) or (4.15). An apparently trivial transformation is given by

$$\overline{Z^n} = \int d^n x \, \exp\left\{ -\beta \left[\frac{\kappa}{2} \sum_{a=1}^{n} x_a^2 - \frac{1}{2} \sum_{a,b} x_a (1-\eta)\, \sigma_{ab}\, x_b + \eta \, \frac{\beta\, \varepsilon^2}{2} \sum_{a,b} R(x_a - x_b) \right] \right\} \ . \tag{4.19}$$

As it often happens, the tricky part begins with renaming a certain parameter:

$$(1-\eta)\sigma_{ab} = \tilde{\sigma}_{ab} \ . \tag{4.20}$$

This leads straight to the new Hamilton function

$$\tilde{H}_t = \frac{\kappa}{2} \sum_{a=1}^{n} x_a^2 - \frac{1}{2} \sum_{a,b} x_a \, \tilde{\sigma}_{ab} \, x_b \tag{4.21}$$

and the corresponding expectation value

$$\langle \bullet \rangle_{\tilde{H}_t} = \frac{1}{\tilde{Z}_t} \int d^n x \, \exp(-\beta \, \tilde{H}_t) \bullet \ . \tag{4.22}$$

Just for the sake of completeness, it is pointed out that $\tilde{Z}_t = \int d^n x \, \exp(-\beta \, \tilde{H}_t)$ represents the normalization factor. Thus, the replicated partition function (4.15) is now written as

$$\overline{Z^n} = \tilde{Z}_t \left\langle \exp\left\{ -\eta \, \frac{\beta^2 \varepsilon^2}{2} \sum_{a,b} R(x_a - x_b) \right\} \right\rangle_{\tilde{H}_t} \ . \tag{4.23}$$

In analogy to (4.16), one gets the free energy in form of the series

$$\tilde{F}_n^{(N)} = \tilde{F}_t - \frac{1}{\beta} \sum_{k=1}^{N} \frac{(\eta \, \beta^2 \varepsilon^2)^k}{2^k \, k!} \left\langle \left[\sum_{a,b} R(x_a - x_b) \right]^k \right\rangle_{\tilde{H}_t}^{c} \ . \tag{4.24}$$

Here, one has to be careful to perform the limit $\eta \to 1$ after the final step, as it is left to insert (4.20) into the final result and to expand it up to order N in η.

To describe the expansion in powers of η a new notation is introduced. We will expand

$$\tilde{F}_n^{(N)} = \tilde{F}_n^{(N,0)}\Big|_{\eta=0} + \tilde{F}_n^{(N,1)}\Big|_{\eta=0} \eta + \tilde{F}_n^{(N,2)}\Big|_{\eta=0} \eta^2 + \ldots \ , \tag{4.25}$$

with the coefficients of the Taylor series given by

$$\tilde{F}_n^{(N,i)} = \frac{\partial^i}{\partial \eta^i} \tilde{F}_n^{(N)} \ . \tag{4.26}$$

Furthermore, we denote the operation $\ldots\Big|_{\eta=0}$ by omitting the tilde:

$$\tilde{F}_n^{(N,i)}\Big|_{\eta=0} = F_n^{(N,i)} \ . \tag{4.27}$$

As discussed before, one can now obtain the free energy series (4.16) in a recursive manner. For fixed N, it can be obtained of the $(N-1)^{\text{th}}$ expression for the free energy by just adding the corresponding terms. After setting $\eta = 1$ it reads

$$F_n^{(N)} = F_n^{(N-1)} + \sum_{i=0}^{N} F_n^{(i,N-i)} \ . \tag{4.28}$$

4.2.2 What to Gain?

One has to keep in mind that the replicated partition function formally describes a non-random system. The free energy F of the toy system can be obtained directly from the free energy of the replicated system F_n. To see this, we first calculate

$$\lim_{n\to 0} n^{-1} F_n = -\frac{1}{\beta} \lim_{n\to 0} \frac{1}{n} \log \overline{Z^n} \ . \tag{4.29}$$

Using the Taylor expansion for the logarithm near $x = 1$ yields

$$\lim_{n\to 0} n^{-1} F_n = -\frac{1}{\beta} \lim_{n\to 0} \frac{1}{n} (\overline{Z^n} - 1) \ . \tag{4.30}$$

In the limit $n \to 0$ the Taylor expansion for small n is intrinsically exact. The replicated partition is assumed to be a continuous function of the number of the replicas n. Accordingly, one may use the replica trick (4.1) and obtains

$$\lim_{n\to 0} n^{-1} F_n = F \ . \tag{4.31}$$

Thus, with the same arguments underlying (3.26), it is possible to write the mean square displacement (3.24) as

$$\overline{\langle x^2 \rangle} = \lim_{n\to 0} \frac{2}{n} \frac{d}{d\kappa} F_n \ . \tag{4.32}$$

With this, the N^{th} order approximation for (4.32) can be obtained from the cumulant expansion (4.16) for $n = 0$:

$$\overline{\langle x^2 \rangle}^{(N)} = \lim_{n\to 0} \frac{2}{n} \frac{d}{d\kappa} F_n^{(N)} \ . \tag{4.33}$$

We know $F_n^{(N)}$ to be a function of κ and $\sigma_{ab}(\kappa)$, such that differentiating with respect to κ yields with the chain rule

$$\frac{d}{d\kappa} F_n^{(N)}(\kappa, \sigma(\kappa)) = \frac{\partial F_n^{(N)}}{\partial \kappa} + \sum_{a,b} \frac{\partial F_n^{(N)}}{\partial \sigma_{ab}} \frac{\partial \sigma_{ab}}{\partial \kappa} \ . \tag{4.34}$$

The second term vanishes because of the saddle point equation (4.17). Hence, one just has to consider the explicit dependence on the parameter κ:

$$\overline{\langle x^2 \rangle}^{(N)} = \lim_{n\to 0} \frac{2}{n} \frac{\partial}{\partial \kappa} F_n^{(N)} \ . \tag{4.35}$$

4.2.3 Toolbox

After going through all this secondary considerations, one is almost prepared to attack the variational perturbation expansion. To proceed with the calculations, one will need further mathematical tools to do the explicit calculation. First of all, the matrix σ in (4.8) is symmetric: $\sigma_{ab} = \sigma_{ba}$. Since it will pop up quite some times, one has to handle the consequences of differentiating quantities with respect to a matrix element of a symmetric matrix. It helps to know [48]

$$\frac{\partial \sigma_{ab}}{\partial \sigma_{cd}} = \frac{1}{2} \left(\delta_{ac}\delta_{bd} + \delta_{ad}\delta_{bc} \right) \ , \tag{4.36}$$

which takes care of the two equal components, respectively. The *principle of minimal sensitivity* asks to differentiate the free energy so that one must know the derivative of a determinant. Let $A(t)$ be a matrix with components $a_{ij}(t)$ which depend on a parameter t. Then $A^{-1}(t)$ is the inverse with matrix elements $a_{ij}^{-1}(t)$, which are characterized by the property $\sum_j a_{ij}^{-1} a_{jk} = \delta_{ik}$. Then we have [49]

$$\frac{\partial \det A(t)}{\partial t} = \det A \sum_{i,j} a_{ij}^{-1} \frac{\partial a_{ji}(t)}{\partial t} \ . \tag{4.37}$$

Because it will be often used in the following, we will restate the inverse relation for G, the inverse of (4.9):

$$\sum_{b=1}^{n} G_{ab}^{-1} G_{bc} = \delta_{ac} \ . \tag{4.38}$$

This helps us to differentiate G, with respect to σ_{ab}:

$$\frac{\partial G_{ab}}{\partial \sigma_{cd}} = -\sum_{e,f} G_{ae} \left(\frac{\partial G_{ef}^{-1}}{\partial \sigma_{cd}} \right) G_{fb} \ . \tag{4.39}$$

With inserting the definition of G_{ab}^{-1} and (4.36), we calculate

$$\frac{\partial G_{ab}}{\partial \sigma_{cd}} = \frac{1}{2} \Big[G_{ac} G_{bd} + G_{bc} G_{ad} \Big] \ . \tag{4.40}$$

In the following, the difference between (4.16) and (4.24) becomes essential. Therefore, quantities depending on $\tilde{G}_{ab}$ and $\tilde{\sigma}_{ab}$, respectively, will be marked by a tilde itself. This will mean that the definition of symbols labeled with a tilde stay, in principle, the same, i.e. one just changes $G_{ab} \to \tilde{G}_{ab}$ and $\sigma_{ab} \to \tilde{\sigma}_{ab}$.

Finding the optimized parameters σ_{ab} of (4.10) will not pose any fundamental problems. It can be done just by using the tools of this and the previous chapters. Because of (4.26), derivatives with respect to the parameter η will appear. It will therefore be helpful to state the chain rule of differentiation in the special form

$$\frac{\partial}{\partial \eta} = \sum_{c,d} \left(\frac{\partial \tilde{\sigma}_{cd}}{\partial \eta} \right) \frac{\partial}{\partial \tilde{\sigma}_{cd}} = -\sum_{c,d} \sigma_{cd} \frac{\partial}{\partial \tilde{\sigma}_{cd}} \ . \tag{4.41}$$

In the calculations to follow, expressions involving terms of elements of σ multiplied with matrix elements of G will appear because of the chain rule (4.41). To handle these terms more elegantly, we will apply the definition (4.9) to the property (4.38). This leads to the identity

$$\sum_{b} \sigma_{ab} G_{bc} = \kappa G_{ac} - \delta_{ac} \ . \tag{4.42}$$

4.3 Explicit Expansion

With the help of the mathematical tools introduced in Sec. 4.2.3, the explicit calculations will be done in the following part of this chapter. Everything will be set up, so the more passionate and brave calculator can compute the variational perturbation series of this problem to higher orders in order to approximate the system better. We, however, will stay in the safe haven of the Jensen-Peierls inequality. We therefore just calculate the first-order free energy and try different choices for the variational parameters.

4.3.1 Zeroth Order

The 0^{th} order of (4.24) poses no further problems. It reads

$$\tilde{F}_n^{(0)} = \frac{1}{2\beta} \log\det \tilde{G}^{-1} - \frac{n}{2\beta} \log\left(\frac{2\pi}{\beta}\right) \ . \tag{4.43}$$

Applying the chain rule (4.41), the expansion coefficients (4.26) and (4.27) for $\eta = 0$ are given as

$$F_n^{(0,0)} = \frac{1}{2\beta} \log\det G^{-1} - \frac{n}{2\beta} \log\left(\frac{2\pi}{\beta}\right) \ , \tag{4.44}$$

$$F_n^{(0,1)} = \frac{1}{2\beta} \sum_{c,d} \sigma_{cd} G_{cd} \ , \tag{4.45}$$

$$F_n^{(0,2)} = -\frac{1}{2\beta} \sum_{c,d} \sum_{e,f} \sigma_{ef} \sigma_{cd} G_{ec} G_{fd} \ , \tag{4.46}$$

$$\vdots$$

Applying (4.42) simplifies the higher orders to

$$F_n^{(0,1)} = \frac{\kappa}{2\beta} \mathrm{Tr}\, G - \frac{n}{2\beta} \ , \tag{4.47}$$

$$F_n^{(0,2)} = -\frac{\kappa^2}{2\beta} \sum_{e,f} G_{ef}^2 + \frac{\kappa}{\beta} \mathrm{Tr}\, G - \frac{n}{2\beta} \ , \tag{4.48}$$

$$\vdots$$

The free energy of the replicated system in zeroth order (4.16) reads

$$F_n^{(0)} = F_n^{(0,0)} \ . \tag{4.49}$$

4.3.2 First Order

To calculate the first order of the free energy series (4.16), we apply the recursive relation (4.28):

$$F_n^{(1)} = F_n^{(0)} + F_n^{(0,1)} + F_n^{(1,0)} \ . \tag{4.50}$$

The only new term arises from the first order of (4.24) and reads

$$\tilde{F}_n^{(1)} = -\frac{\beta\, \varepsilon^2}{2} \sum_{a_1, b_1} \Big\langle\, R(x_{a_1} - x_{b_1}) \,\Big\rangle_{\tilde{H}_t} \ . \tag{4.51}$$

Expectation values of correlation functions have been calculated in App. C with the smearing formula [50, 51]. We use Eq. (C.25) to get

$$\tilde{f}[q(a,b)] = \varepsilon^2 \Big\langle\, R(x_a - x_b) \,\Big\rangle_{\tilde{H}_t} \;, \tag{4.52}$$

which is just a function of

$$q(a,b) = \frac{1}{\beta}(G_{aa} + G_{bb} - 2G_{ab})\,. \tag{4.53}$$

The analog expression without tilde quantities writes according to (4.27)

$$f[q(a,b)] = \varepsilon^2 \Big\langle\, R(x_a - x_b) \,\Big\rangle_{H_t} \;. \tag{4.54}$$

For the toy model (1.6), the function (4.54) can be calculated explicitly by (C.31):

$$f(\xi) = \frac{\varepsilon^2}{\sqrt{2\pi}} \left[\xi + \lambda^2\right]^{-1/2} \;. \tag{4.55}$$

The coefficients of the expansion in η can be calculated by elementary transformations. They read with (4.40), (4.41) and renaming the summation indices:

$$F_n^{(1,0)} = -\frac{\beta}{2} \sum_{a,b} f[q(a,b)] \;, \tag{4.56}$$

$$F_n^{(1,1)} = \sum_{a,b} \sum_{e,f} \sigma_{ef} f_\xi[q(a,b)] \left[G_{ae}G_{af} - G_{ae}G_{bf}\right] \;, \tag{4.57}$$

$$\vdots$$

The subscript ξ denotes differentiation with respect to the argument. In a nutshell, the first order free energy writes using the identity Trlog = logdet:

$$F_n^{(1)} = -\frac{n}{2\beta} \log\left(\frac{2\pi e}{\beta}\right) + \frac{1}{2\beta}\mathrm{Trlog}\, G^{-1} + \frac{\kappa}{2\beta}\mathrm{Tr}\, G - \frac{\beta}{2}\sum_{a,b} f[q(a,b)] \;. \tag{4.58}$$

It is left to point out, that calculating the mean square displacement, one has to partially differentiate with respect to κ according to (4.35). Thus, it computes

$$\overline{\langle\, x^2 \,\rangle}^{(1)} = \lim_{n\to 0} \frac{1}{n\beta}\mathrm{Tr}\, G \;. \tag{4.59}$$

Now the extremalization of the free energy can be done. Differentiating (4.50) with respect to the variational parameter σ_{cd} yields

$$\frac{\partial}{\partial \sigma_{cd}} F_n^{(1)} = -\frac{1}{2\beta}G_{cd} + \frac{\kappa}{2\beta}\sum_e G_{ec}G_{ed} - \sum_{a,b} f_\xi[q(a,b)]\Big[G_{ac}G_{ad} - G_{ac}G_{bd}\Big]. \tag{4.60}$$

The *principle of minimal sensitivity* (4.17) demands

$$\frac{\partial}{\partial \sigma_{cd}} F_n^{(1)} = 0 \;. \tag{4.61}$$

From the structure of the terms in (4.60), we read off that the application of the identity (4.38) can lead to a conditional equation for the elements of σ. After a straightforward calculation just using (4.38), one obtains

$$\sigma_{cd} = 2\beta \sum_a f_\xi[q(a,c)]\delta_{cd} - 2\beta f_\xi[q(c,d)] \; . \tag{4.62}$$

The result (4.62) can be rewritten as

$$c \neq d \quad \Rightarrow \quad \sigma_{cd} = -2\beta f_\xi[q(c,d)] \, , \tag{4.63}$$

$$c = d \quad \Rightarrow \quad \sigma_{cc} = -\sum_{a \neq c} \sigma_{ac} \, . \tag{4.64}$$

4.4 Replica-Symmetric Ansatz

In this section a special ansatz for the matrix σ will be discussed: the replica-symmetric ansatz (RSA). It is taken to be the simplest ansatz' possible - a highly symmetric matrix is assumed with just two elements [19]:

$$\sigma_{ab} = \tilde{\sigma}\delta_{ab} + \sigma_0(1 - \delta_{ab}) \; . \tag{4.65}$$

So now the matrix in G^{-1} (4.9) is given as

$$G^{-1}_{ab} = (\kappa - \tilde{\sigma})\delta_{ab} - \sigma_0(1 - \delta_{ab}) \, . \tag{4.66}$$

Given this structure of G^{-1}, it is reasonable to make for its inverse G the corresponding ansatz

$$G_{ab} = A\delta_{ab} + B \, . \tag{4.67}$$

Using the relation of inverse matrices (4.38), one obtains two conditional equations for A and B:

$$A = \frac{1}{\kappa - \tilde{\sigma} + \sigma_0} \; , \tag{4.68}$$

$$B = \frac{\sigma_0}{\kappa - (n-1)\sigma_0 - \tilde{\sigma}} \cdot \frac{1}{\kappa - \tilde{\sigma} + \sigma_0} \; . \tag{4.69}$$

Within the RSA, we get for the quantity (4.53)

$$q(a,b) = \frac{2A}{\beta}(1 - \delta_{ab}) \; . \tag{4.70}$$

4.4.1 Zeroth-Order Result

As seen in the Sec. 4.3.1, no physical conditional equation for the variational parameters could be found. Despite this, it is possible to calculate quantities in zeroth order cumulant expansion as the mean square displacement (4.35).

The free energy has been calculated for the case of a general matrix G_{ab}. In the RSA an explicit formula can be derived straightforwardly. The only real problem is to calculate the determinant of a $n \times n$ matrix G as demanded in (4.44). With the help of the considerations of App. C.2 and especially equation (C.39), the free energy calculates in zeroth order

$$F^{(0)} = \lim_{n \to 0} \frac{1}{n} F_n^{(0)} = \frac{1}{2\beta} \log \frac{\kappa\beta}{2\pi} \; . \tag{4.71}$$

It is no suprise, that this is exactly (3.3), the result disregarding the random potentials. Furthermore, the corresponding mean square displacement calculates

$$\overline{\langle x^2 \rangle}^{(0)} = \frac{1}{\kappa\beta} \ . \tag{4.72}$$

4.4.2 First-Order Result

Via variational perturbation theory and the *principle of minimal sensitivity*, we obtained for the matrix elements σ_{ab} the conditional equation (4.62). Using (4.63) and (4.64), we find

$$\tilde{\sigma} = -(n-1)\sigma_0 \ . \tag{4.73}$$

Now, one can state (4.67) with (4.68), (4.69) in a very comfortable way:

$$G_{ab} = \frac{1}{\kappa + n\sigma_0}\delta_{ab} + \frac{\sigma_0}{\kappa(\kappa + n\sigma_0)} \ . \tag{4.74}$$

Inserting into (4.63) yields

$$\sigma_0 = -2\beta f_\xi \left(\frac{2}{\beta(\kappa + n\sigma_0)} \right) . \tag{4.75}$$

In the limit $n \to 0$ this expression reduces to

$$\sigma_0 = -2\beta f_\xi \left(\frac{2}{\beta\kappa} \right) \ , \tag{4.76}$$

leaving the left-hand side independent of σ. In the case (4.55), we obtain

$$\sigma_0 = \frac{\varepsilon^2}{\sqrt{2\pi}}\beta \left[\frac{2}{\beta\kappa} + \lambda^2 \right]^{-3/2} . \tag{4.77}$$

4.4.3 Free Energy and Mean Square Displacement

The free energy of the random system is calculated by (4.31). Having obtained the zeroth order contribution to the free energy (4.71), we are left to calculate $F_n^{(0,1)}/n$ and $F_n^{(1,0)}/n$ in the limit $n \to 0$, which poses no further problem. Using the expression (4.47) and inserting the matrix (4.67) with coefficients (4.68) and (4.69) yields in the limit $n \to 0$

$$\frac{1}{n} F_n^{(0,1)} \to 0 \ . \tag{4.78}$$

With (4.56), (4.74), and (4.75) we get correspondingly

$$\frac{1}{n} F_n^{(1,0)} \to -\frac{\beta}{2} f(0) + \frac{\beta}{2} f\left(\frac{2}{\kappa\beta} \right) \ . \tag{4.79}$$

We note that the free energy in the replica-symmetric ansatz in the limit $n \to 0$ does not depend on the variational parameter. Thus, no non-perturbative correction is achieved for any correlation function. The free energy turns out to be

$$F^{(1)} = \frac{1}{2\beta} \log \frac{\kappa\beta}{2\pi} - \frac{\beta}{2} f(0) + \frac{\beta}{2} f\left(\frac{2}{\kappa\beta} \right) \ , \tag{4.80}$$

which, comparing with (3.3) and (3.17), is exactly the same result as within first-order perturbation theory. This will be seen more direct in the general case that will be discussed in the next chapter. By (4.33) or (4.59) it is possible to calculate now the mean square displacement to

$$\overline{\langle x^2\rangle}^{(1)} = \frac{1}{\kappa\beta} - \frac{2}{\kappa^2} f_\xi\left(\frac{2}{\kappa\beta}\right) \ . \tag{4.81}$$

As said before, the first-order result is especially important. Because of the Jensen-Peierls inequality (4.18), it gives an upper bound to the free energy. At low temperatures the accuracy of the approximation can decrease. This will be investigated in the following section by calculating the Hessian.

4.4.4 Stability Analysis

The stability analysis of the system is extremely delicate. Because of the Jensen-Peierls inequality (4.18), it is quite clear that in the case $n > 1$ one has to find the minimum of the first order variational free energy to find the optimal upper bound. Analytically continuing the free energy to $n < 1$, the corrections come from the maxima and not from the minima of the system (4.58). Naively speaking, all dimensional factors in the partition function become negative in the limit $n \to 0$. This artifact of the model is commented on in Refs. [11, 52] and will not be discussed further in this work. To avoid further problems, the stability for the solutions is shown for $n > 1$. One calculates the Hessian and the stability depends on it being positive definite.

The Hessian is computed as the second derivative of the free energy with respect to the variational parameters:

$$H_{ab,cd} = \frac{\partial^2}{\partial\sigma_{ab}\partial\sigma_{cd}} F_n^{(N)} \ . \tag{4.82}$$

The intermediary results are given in App. C. The Hessian of the replicated system in general is given in (C.41). Furthermore, using (C.46) makes it possible to calculate the Hessian in the replica-symmetric ansatz straightforwardly. Using (4.65)–(4.70) and the first-order result (4.75), one gets after a cumbersome calculation the expression

$$\begin{aligned} H_{ab,cd} = & -\frac{1}{2\beta}B^2 + \frac{2AB^2\kappa}{\beta} + 2A^2 B f_\xi\left(\frac{2A}{\beta}\right) + (\delta_{ac}+\delta_{ad}+\delta_{bc}+\delta_{bd})\Big[-\frac{AB}{4\beta} \\ & + \frac{\kappa}{4\beta}(3A^2B + nAB^2) - \frac{1}{2}(nA^2B - A^3) f_\xi\left(\frac{2A}{\beta}\right)\Big] + (\delta_{ac}\delta_{bd} + \delta_{ad}\delta_{bc}) \\ & \times\Big[-\frac{1}{4\beta}A^2 + \frac{\kappa}{2\beta}A^3 - nA^3 - \frac{1}{\beta}A^4 f_{\xi\xi}\left(\frac{2A}{\beta}\right)\Big] - (n\delta_{ab}\delta_{ac}\delta_{cd} + \delta_{ab}\delta_{cd} \\ & - \delta_{ac}\delta_{ad} - \delta_{bc}\delta_{bd} - \delta_{ab}\delta_{ac} - \delta_{ab}\delta_{ad})\frac{A^4}{\beta} f_{\xi\xi}\left(\frac{2A}{\beta}\right) \ . \end{aligned} \tag{4.83}$$

The eigenvectors have to satisfy the relation

$$\sum_{a,b} H_{ab,cd}\, v_{ab} \stackrel{!}{=} \lambda\, v_{cd} \, . \tag{4.84}$$

The most natural ansatz

$$v_{ab} = v + u\delta_{ab} \ . \tag{4.85}$$

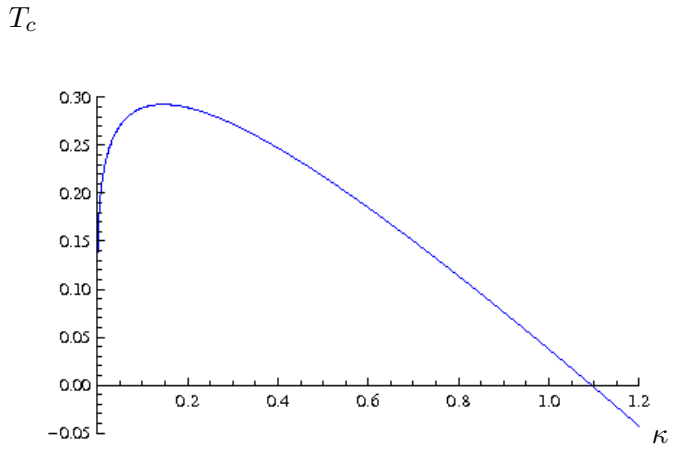

Figure 4.1: Almeida-Thouless line for Gaussian correlation with $\lambda = 1,\ \varepsilon = 1$.

reproduces the critical eigenvalue. Two solutions can be found, which coincide in the limit $n = 0$. In this limit the coefficient u vanishes and, therefore, the eigenvector is a matrix with constant entries. The critical eigenvalue reads

$$\lambda_c = \frac{1}{\kappa^2\beta} - \frac{4}{\kappa^4\beta} f_{\xi\xi}\left(\frac{2}{\kappa\beta}\right) \ . \tag{4.86}$$

Further eigenvalues of those so-called ultrametric matrices are calculated in [17, 19, 53]. In the limit $n \to 0$, there are three different eigenvalues, two of which are positive for all temperatures.

To get the optimal upper bound of the free energy, one has to demand that

$$\lambda_c \geq 0 \ . \tag{4.87}$$

The line $\lambda_c = 0$ is called the Almeida-Thouless line and is plotted in Fig. 4.1. In our case of Gaussian correlation, we arrive at the inequality

$$T \leq \frac{1}{2}\left(\frac{9\varepsilon^4\kappa}{2\pi}\right)^{1/5} - \frac{\lambda^2\kappa}{2} \ . \tag{4.88}$$

The right-hand side is plotted in Fig. 4.1. If the confinement parameter satisfies the condition

$$\kappa \geq \frac{\sqrt{3}\,\varepsilon}{(2\pi)^{1/4}}\lambda^{5/2} \ , \tag{4.89}$$

the replica-symmetric solution is an optimal bound for the free energy for all temperatures. Otherwise, it does not give satisfying results below a critical temperature.

Although the replica-symmetric ansatz does not provide a better approximation than first-order standard perturbation theory, we can understand Fig. 3.1 better. For $\kappa = 2$ we obtain almost no difference between the first order free energy and numerical results, whereas for $\kappa = 0.01$, one notices huge deviations. This, however, agrees perfectly with the expectations gained by the discussion of the Almeida-Thouless line. For the problem of a harmonic oscillator within a disorder environment, the replica-symmetric solution is, indeed, a good approximation in cases of κ bigger than approximately 1.1. However, it ceases to resemble the simulation results for smaller parameter values, as visualized in Fig. 3.1.

Since by using the replica-symmetric approach no further improvement in the approximation has been achieved, one needs to find a better method. This gives rise to the breaking of replica symmetry. To this end, the Parisi method and its formalism will be presented in the following chapter.

Chapter 5

Replica-Symmetry Breaking

In this chapter we will overcome the limits of the replica-symmetric ansatz, which does not yield satisfying results in the small temperature regime. Therefore, we will break the replica symmetry according to Giorgio Parisi. Originally developed to describe spin glasses, the replica-symmetry breaking (RSB) method has shown to be very successful in many other systems as well [10, 15, 53].

5.1 Idea

In the RSA a symmetric matrix of the form $G_{ab} = \tilde{g}\delta_{ab} + g_0(1-\delta_{ab})$ was used, which is invariant under the permutation of the replica indices. With this choice of the matrix all replicas are equivalent. A natural suggestion to improve the approximations obtained is to introduce additional independent variational parameters. Unfortunately, it is not possible to invert an arbitrary $n \times n$ matrix in a general way as needed to calculate the free energy expression (4.58). Hence, we will restrict ourselves to a special type of matrices called Parisi matrices, for which one can calculate the free energy (4.58) explicitly. Physical motivations for this choice of matrix can be found for instance in Ref. [11].

One starts by dividing the n replicas into n/m groups of replicas [10, 11]. Of course, n/m must be an integer as well. Then all diagonal elements are set to constant values $G_{aa} = \tilde{g}$. Further on, one sets the other matrix elements $G_{ab} = g_1$, if the indices a and b belong to the same group and $G_{ab} = g_0$, if they do not. Mathematically speaking (assuming $a \neq b$):

$$G_{aa} = \tilde{g} \tag{5.1}$$

$$G_{ab} = g_1 \quad \text{if} \quad \lceil a/m \rceil = \lceil b/m \rceil \tag{5.2}$$

$$G_{ab} = g_0 \quad \text{if} \quad \lceil a/m \rceil \neq \lceil b/m \rceil \,. \tag{5.3}$$

The bracket $\lceil \cdot \rceil$ denotes the ceiling function:

$$\lceil x \rceil = \min\{n \in \mathbb{Z} | n \geq x\} \,. \tag{5.4}$$

With this ansatz, one adds one more independent variational parameter. The method of replica-symmetry breaking can further be generalized by dividing the groups of replicas into groups of replicas and so on. In order to describe this recursive procedure a set of integers m_i with $i \in \mathcal{I}$ is introduced. The set $\mathcal{I}$ contains $k+1$ integer values:

$$\mathcal{I} = \{0, 1, 2, ..., k\} \,. \tag{5.5}$$

One will later speak of a k-step RSB. If not said otherwise, all summations in the discussion to follow will go over all $i \in \mathcal{I}$. In this formalism the replica symmetric approach can be named a 0-step RSB. These integers have the following properties:

$$m_{k+1} = 1 \tag{5.6}$$
$$m_0 = n \tag{5.7}$$
$$m_i/m_{i+1} \in \mathbb{Z}, \quad \forall\, i \in \mathcal{I} \tag{5.8}$$

and, thus, they obey the inequalities

$$1 = m_{k+1} \leq m_k \leq ... \leq m_1 \leq m_0 = n \ . \tag{5.9}$$

Furthermore, we introduce a set of real valued constants $\{g_0, g_1, ..., g_k\}$. The aim is to divide the n replicas into n/m_k groups of replicas. These groups are subdivided into m_k/m_{k-1} groups and so on. Thus, the elements of the Parisi matrix are given by (again assuming $a \neq b$);

$$G_{aa} \quad = g_0 \,, \tag{5.10}$$
$$G_{ab} \quad = g_i \quad \text{if} \quad \lceil a/m_i \rceil \neq \lceil b/m_i \rceil \quad \text{and} \quad \lceil a/m_{i+1} \rceil = \lceil b/m_{i+1} \rceil \quad \text{for} \quad i \in \mathcal{I}. \tag{5.11}$$

The concept of Parisi matrices can further be generalized. To keep track of the parameters g, we define the piecewise constant function $g(u)$ by

$$g(u) = g_i \quad \text{if} \quad m_{i+1} \leq u \leq m_i \ . \tag{5.12}$$

Note that this expression is just a reparametrization. We are still looking at a $n \times n$ matrix for the integer n. However, the aim is to formulate a language in which it is possible to analytically continue the results, like the Trace or the Tracelog, to the limit $n \to 0$. A complete discussion of properties and methods to deal with Parisi matrices is given in the following sections.

5.2 Parisi Matrices

The treatment of replica-symmetry breaking can be quite cumbersome and scientific publications often just mention the basic equation referring mostly to the original papers of Giorgio Parisi that can be found in the book Ref. [10] or in the work with Marc Mézard and Miguel A. Virasoro in Ref. [16]. The core equations of the formalism were first mentioned in full in their article Ref. [54]. In the following, the basic ideas of the mathematical treatment of RSB will be presented. The discussion can also be found in the lecture notes of Ref. [55] in a similar manner. In particular, one has to be careful with the analytic continuation. In the case $n < 1$, the inequality (5.9) formally goes over into [10, 11, 15]

$$1 = m_{k+1} \geq m_k \geq ... \geq m_1 \geq m_0 = n \ . \tag{5.13}$$

Whenever this plays a decisive role, we will refer to this equation explicitly.

5.2.1 Definitions

The set $\mathcal{P}$ of all Parisi matrices forms a closed algebra. In order to show this, we will introduce a practical way to construct a Parisi matrix. At first we will introduce the $n \times n$ matrix $\mathbb{I}_{i,n} = \mathbb{I}_{m_i,n}$.

It can be most intuitively described by the following example for $m_i = 3$ and $n = 12$:

$$\mathbb{I}_{i,12} = \begin{pmatrix} 1 & 1 & 1 & 0 & 0 & 0 & 0 & 0 & 0 & 0 & 0 & 0 \\ 1 & 1 & 1 & 0 & 0 & 0 & 0 & 0 & 0 & 0 & 0 & 0 \\ 1 & 1 & 1 & 0 & 0 & 0 & 0 & 0 & 0 & 0 & 0 & 0 \\ 0 & 0 & 0 & 1 & 1 & 1 & 0 & 0 & 0 & 0 & 0 & 0 \\ 0 & 0 & 0 & 1 & 1 & 1 & 0 & 0 & 0 & 0 & 0 & 0 \\ 0 & 0 & 0 & 1 & 1 & 1 & 0 & 0 & 0 & 0 & 0 & 0 \\ 0 & 0 & 0 & 0 & 0 & 0 & 1 & 1 & 1 & 0 & 0 & 0 \\ 0 & 0 & 0 & 0 & 0 & 0 & 1 & 1 & 1 & 0 & 0 & 0 \\ 0 & 0 & 0 & 0 & 0 & 0 & 1 & 1 & 1 & 0 & 0 & 0 \\ 0 & 0 & 0 & 0 & 0 & 0 & 0 & 0 & 0 & 1 & 1 & 1 \\ 0 & 0 & 0 & 0 & 0 & 0 & 0 & 0 & 0 & 1 & 1 & 1 \\ 0 & 0 & 0 & 0 & 0 & 0 & 0 & 0 & 0 & 1 & 1 & 1 \end{pmatrix} . \tag{5.14}$$

We remember that we read off from (5.9)

$$i < j \Rightarrow m_i \geq m_j \ , \tag{5.15}$$

which will become important in the continuous case. In the special cases of $i = 0$ and $i = k + 1$, we get the $n \times n$ matrices

$$\mathbb{I}_{0,n} = \begin{pmatrix} 1 & \dots & 1 \\ \vdots & \ddots & \vdots \\ 1 & \dots & 1 \end{pmatrix} \quad , \qquad \mathbb{I}_{k+1,n} = \mathbb{I}_n = \begin{pmatrix} 1 & & 0 \\ & \ddots & \\ 0 & & 1 \end{pmatrix} , \tag{5.16}$$

a matrix with constant elements equal to 1 and the unity matrix, respectively. An arbitrary $\mathbb{I}_{i,n}$ can be written in terms of (5.16) as

$$\mathbb{I}_{i,n} = \begin{pmatrix} \mathbb{I}_{0,i} & & 0 \\ & \ddots & \\ 0 & & \mathbb{I}_{0,i} \end{pmatrix} . \tag{5.17}$$

Before we go on to demonstrate how to write Parisi matrices in a convenient form, we calculate the matrix product $\mathbb{I}_{i,n}\mathbb{I}_{j,n}$. This calculation crucially depends on the assumptions (5.6)–(5.9). For $i = j$, the situation is quite clear. The multiplication yields

$$\mathbb{I}_{i,n}\mathbb{I}_{i,n} = \begin{pmatrix} \mathbb{I}_{0,i}\mathbb{I}_{0,i} & & 0 \\ & \ddots & \\ 0 & & \mathbb{I}_{0,i}\mathbb{I}_{0,i} \end{pmatrix} = m_i \mathbb{I}_{i,n} \, . \tag{5.18}$$

Otherwise, we assume $i < j$ without loss of generality. Because of (5.8), we may calculate

$$\begin{pmatrix} \mathbb{I}_{0,j} & & 0 \\ & \ddots & \\ 0 & & \mathbb{I}_{0,j} \end{pmatrix} \mathbb{I}_{0,i} = m_j \mathbb{I}_{0,i} \, . \tag{5.19}$$

This leads to

$$\mathbb{I}_{j,n}\mathbb{I}_{i,n} = \begin{pmatrix} m_j\mathbb{I}_{0,i} & & 0 \\ & \ddots & \\ 0 & & m_j\mathbb{I}_{0,i} \end{pmatrix} = m_j \mathbb{I}_{i,n} \, . \tag{5.20}$$

Summarizing both cases (5.18) and (5.20), we find the general product to be

$$\mathbb{I}_{i,n}\mathbb{I}_{j,n} = m_{\max\{i,j\}}\mathbb{I}_{\min\{i,j\},n} \ . \tag{5.21}$$

Having derived the multiplication properties of the matrices $\mathbb{I}_{i,n}$, we are going to drop the second index n, which refers to the size of the matrix as we will just deal with $n \times n$ matrices. With this notation (5.21) goes over into

$$\mathbb{I}_i\mathbb{I}_j = m_{\max\{i,j\}}\mathbb{I}_{\min\{i,j\}} \ . \tag{5.22}$$

Now a Parisi matrix is constructed as follows. It is convenient to define the matrices

$$\overline{\mathbb{I}}_i \equiv \mathbb{I}_i - \mathbb{I}_{i+1} \tag{5.23}$$

in order to write a general Parisi matrix as

$$\mathbf{P} = \tilde{p}\,\mathbb{I} + \sum_i p_i\,\overline{\mathbb{I}}_i \ . \tag{5.24}$$

An example is a Parisi matrix with parameter values $n = 12$, $k = 1$ and $m_1 = 3$. This is the so-called one-step replica-symmetry breaking case. The form of the matrix is

$$\mathbf{P} = \left(\begin{array}{ccc|ccc|ccc|ccc}
\tilde{p} & p_1 & p_1 & p_0 & p_0 & p_0 & p_0 & p_0 & p_0 & p_0 & p_0 & p_0 \\
p_1 & \tilde{p} & p_1 & p_0 & p_0 & p_0 & p_0 & p_0 & p_0 & p_0 & p_0 & p_0 \\
p_1 & p_1 & \tilde{p} & p_0 & p_0 & p_0 & p_0 & p_0 & p_0 & p_0 & p_0 & p_0 \\
\hline
p_0 & p_0 & p_0 & \tilde{p} & p_1 & p_1 & p_0 & p_0 & p_0 & p_0 & p_0 & p_0 \\
p_0 & p_0 & p_0 & p_1 & \tilde{p} & p_1 & p_0 & p_0 & p_0 & p_0 & p_0 & p_0 \\
p_0 & p_0 & p_0 & p_1 & p_1 & \tilde{p} & p_0 & p_0 & p_0 & p_0 & p_0 & p_0 \\
\hline
p_0 & p_0 & p_0 & p_0 & p_0 & p_0 & \tilde{p} & p_1 & p_1 & p_0 & p_0 & p_0 \\
p_0 & p_0 & p_0 & p_0 & p_0 & p_0 & p_1 & \tilde{p} & p_1 & p_0 & p_0 & p_0 \\
p_0 & p_0 & p_0 & p_0 & p_0 & p_0 & p_1 & p_1 & \tilde{p} & p_0 & p_0 & p_0 \\
\hline
p_0 & p_0 & p_0 & p_0 & p_0 & p_0 & p_0 & p_0 & p_0 & \tilde{p} & p_1 & p_1 \\
p_0 & p_0 & p_0 & p_0 & p_0 & p_0 & p_0 & p_0 & p_0 & p_1 & \tilde{p} & p_1 \\
p_0 & p_0 & p_0 & p_0 & p_0 & p_0 & p_0 & p_0 & p_0 & p_1 & p_1 & \tilde{p}
\end{array}\right) . \tag{5.25}$$

From (5.24) we see that

$$\sum_{b=1}^{n} \mathbf{P}_{ab} = \tilde{p} + \sum_i p_i(m_i - m_{i+1}) \, . \tag{5.26}$$

To be able to deal with the Parisi matrices, we derive from (5.22), (5.23) the relations

$$\overline{\mathbb{I}}_i\overline{\mathbb{I}}_j = \begin{cases} (m_i - m_{i+1})\mathbb{I}_i - m_{i+1}\overline{\mathbb{I}}_i & \text{for } i = j \\ (m_j - m_{j+1})\overline{\mathbb{I}}_i & \text{for } i < j \\ (m_i - m_{i+1})\overline{\mathbb{I}}_j & \text{for } j < i \, . \end{cases} \tag{5.27}$$

Note that because of (5.27), the matrices $\overline{\mathbb{I}}_i$ commute:

$$\overline{\mathbb{I}}_i\overline{\mathbb{I}}_j = \overline{\mathbb{I}}_j\overline{\mathbb{I}}_i \, . \tag{5.28}$$

5.2.2 Algebra

Now we will finally prove that the set of Parisi matrices forms a closed algebra. To this end, we take two Parisi matrices $\mathbf{P}, \mathbf{Q} \in \mathcal{P}$ and define their product $\mathbf{R} = \mathbf{PQ}$. Using the construction scheme of a Parisi matrix (5.24), we get

$$\mathbf{R} = \left(\tilde{p}\, \mathbb{I} + \sum_i p_i\, \overline{\mathbb{I}}_i \right) \left(\tilde{q}\, \mathbb{I} + \sum_j q_j\, \overline{\mathbb{I}}_j \right) , \tag{5.29}$$

which yields

$$\mathbf{R} = \tilde{p}\tilde{q}\, \mathbb{I} + \sum_i (\tilde{q} p_i + \tilde{p} q_i)\, \overline{\mathbb{I}}_i + \sum_{i,j} p_i q_j\, \overline{\mathbb{I}}_i \overline{\mathbb{I}}_j \, . \tag{5.30}$$

Due to the commutativity (5.28) and the identity

$$\sum_{i,j<i} = \sum_{j,i>j} \tag{5.31}$$

one can rewrite the product of two Parisi matrices (5.30) as

$$\mathbf{R} = \tilde{p}\tilde{q}\, \mathbb{I} + \sum_i (\tilde{q} p_i + \tilde{p} q_i)\, \overline{\mathbb{I}}_i + \sum_{i,j>i} (p_i q_j + p_j q_i)\, \overline{\mathbb{I}}_i \overline{\mathbb{I}}_j + \sum_i p_i q_i\, \overline{\mathbb{I}}_i \overline{\mathbb{I}}_i \, . \tag{5.32}$$

Using (5.27) yields

$$\begin{aligned} \mathbf{R} \quad &= \tilde{p}\tilde{q}\, \mathbb{I} + \sum_i (\tilde{q} p_i + \tilde{p} q_i)\, \overline{\mathbb{I}}_i + \sum_{i,j>i} (p_i q_j + p_j q_i)(m_j - m_{j+1})\, \overline{\mathbb{I}}_i - \sum_i p_i q_i m_{i+1} \overline{\mathbb{I}}_i \\ &\quad + \sum_i p_i q_i (m_i - m_{i+1}) \mathbb{I}_i \, . \end{aligned} \tag{5.33}$$

To get the correct form of $\mathbf{R}$, we make use of the identity

$$\mathbb{I}_i = \mathbb{I} + \sum_{j \geq i} \overline{\mathbb{I}}_j \, , \tag{5.34}$$

which follows from the summation of (5.23) and taking into account (5.16). By changing the summation indices and using (5.34), we get from (5.33) the form

$$\begin{aligned} \mathbf{R} = \quad &\left[\tilde{p}\tilde{q} + \sum_i q_i p_i (m_i - m_{i+1}) \right] \mathbb{I} + \sum_i (\tilde{q} p_i + \tilde{p} q_i)\, \overline{\mathbb{I}}_i + \sum_{i,j>i} (p_i q_j + p_j q_i)(m_j - m_{j+1})\, \overline{\mathbb{I}}_i \\ &- \sum_i^k p_i q_i m_{i+1} \overline{\mathbb{I}}_i + \sum_{i,j \leq i} p_j q_j (m_j - m_{j+1}) \overline{\mathbb{I}}_i \, . \end{aligned} \tag{5.35}$$

For the last term, we used the identity $\sum_{i,j \geq i} = \sum_{j,i \geq j}$. Hence, Eq. (5.35) corresponds to a Parisi matrix (5.24) with the parameters

$$\tilde{r} \; = \tilde{p}\tilde{q} + \sum_i q_i p_i (m_i - m_{i+1}) \, , \tag{5.36}$$

$$r_i \; = \tilde{q} p_i + \tilde{p} q_i - p_i q_i m_{i+1} + \sum_{j>i} (p_i q_j + p_j q_i)(m_j - m_{j+1}) + \sum_{j \leq i} p_j q_j (m_j - m_{j+1}) \, . \tag{5.37}$$

5.2.3 Analytic Continuation

In order to prepare the analytic continuation, one prefers to describe the matrix elements as a piecewise linear function (5.12). In this way, the sums go over into integrals:

$$\sum_j (m_j - m_{j+1}) \to \int_1^n dv \ . \tag{5.38}$$

Because of the convention (5.15), one has to be careful with the integration limits:

$$\sum_{j\le i} (m_j - m_{j+1}) \quad \to \int_u^n dv \,, \tag{5.39}$$

$$\sum_{j>i} (m_j - m_{j+1}) \quad \to \int_1^u dv \,. \tag{5.40}$$

Thus, we get for the respective coefficients of the Parisi matrix (5.36) and (5.37)

$$\tilde{r} = \tilde{q}\tilde{p} + \int_1^n dv\, p(v)q(v) \,, \tag{5.41}$$

$$r(u) = \tilde{p}q(u) + \tilde{q}p(u) - up(u)q(u) + \int_u^n dv\, p(v)q(v) + \int_1^u dv\, [p(u)q(v) + q(u)p(v)] \,. \tag{5.42}$$

The latter equation can be rewritten as

$$r(u) = (\tilde{p} - \langle p\rangle_n)q(u) + (\tilde{q} - \langle q\rangle_n)p(u) - np(u)q(u) - \int_n^u dv\, [p(v) - p(u)][q(v) - q(u)] \,, \tag{5.43}$$

where we introduced the abbreviation

$$\langle p\rangle_n = \int_n^1 dv\, p(v) \ . \tag{5.44}$$

Now there remains no further problem to continue the function analytically for all n. We will be mostly interested in the case $n = 0$. Writing $\langle p\rangle_0 = \langle p\rangle$ and taking the limit $n \to 0$ of the expressions (5.41) and (5.43) yields the final expressions

$$\tilde{r} \ = \tilde{p}\tilde{q} - \int_0^1 dv\, p(v)q(v) = \tilde{p}\tilde{q} - \langle pq\rangle \,, \tag{5.45}$$

$$r(u) \ = (\tilde{p} - \langle p\rangle)q(u) + (\tilde{q} - \langle q\rangle)p(u) - \int_0^u dv\, [p(v) - p(u)][q(v) - q(u)] \,. \tag{5.46}$$

5.2.4 Inverse Matrix

With help of the results of the previous section, it is possible to calculate the inverse of a Parisi matrix in a quite general way. The aim is to find for a given matrix $\mathbf{P}$ a corresponding matrix $\mathbf{Q}$ such that $\mathbf{PQ} = \mathbb{I}$. In the limit $n \to 0$, this matrix can be obtained via Eqs. (5.45) and (5.46). We just set $\tilde{r} = 1$ and $r(u) = 0$ and solve for $\tilde{q}$ and $q(u)$, respectively. In order to do that, a further new abbreviation will be introduced

$$[q]_n(u) := \int_n^u dv\, [q(u) - q(v)] \ , \tag{5.47}$$

which basically measures the deviation of $q(u)$ from a constant. Again we will write $[q]_0 = [q]$. It is easy to see that

$$[q]'(u) = uq'(u) \ . \tag{5.48}$$

Calculating the derivative of $r(u)$ with respect to u for $n = 0$ yields from (5.46)

$$r'(u) = q'(u)\big\{\tilde{p} - [p](u) - \langle p\rangle\big\} + p'(u)\big\{\tilde{q} - [q](u) - \langle q\rangle\big\} \ . \tag{5.49}$$

Because of (5.48) this writes

$$r'(u) = -\frac{1}{u}\frac{d}{du}\big\{\tilde{p} - \langle p\rangle - [p](u)\big\}\big\{\tilde{q} - \langle q\rangle - [q](u)\big\} = 0 \ . \tag{5.50}$$

Therefore, we know that

$$\big\{\tilde{p} - \langle p\rangle - [p](u)\big\}\big\{\tilde{q} - \langle q\rangle - [q](u)\big\} = 1 \ . \tag{5.51}$$

The constant 1 on the right-hand side of the equation can be determined via Eq. (5.43) by calculating $r(1)$ and setting it equal to 0. The unknown integral can be substituted because (5.45) is equal to 1. Comparing with (5.51) at $u = 1$ leads to the given result.

On the other hand, for $u = 0$ Eq. (5.51) reads because of $[q](0) = 0$ as

$$\big[\tilde{p} - \langle p\rangle\big]\big[\tilde{q} - \langle q\rangle\big] = 1 \ . \tag{5.52}$$

The case $u = 1$ yields the similar expression

$$\big[\tilde{q} - q(1)\big]\big[\tilde{p} - p(1)\big] = 1 \ . \tag{5.53}$$

Now using (5.51) and (5.52), we arrive at

$$[q](u) = -\frac{1}{\tilde{p} - \langle p\rangle}\frac{[p](u)}{\tilde{p} - \langle p\rangle - [p](u)} \ . \tag{5.54}$$

Differentiating with respect to u yields with (5.48)

$$q'(u) = -\frac{1}{\tilde{p} - \langle p\rangle}\frac{1}{u}\frac{d}{du}\frac{[p](u)}{\tilde{p} - \langle p\rangle - [p](u)} \ . \tag{5.55}$$

To solve this equation for $q(u)$, we are in need of an initial value. Evaluating (5.46) at $u = 0$ and using (5.52) to simplify the result yields

$$q(0) = -\frac{p(0)}{(\tilde{p} - \langle p\rangle)^2} \ . \tag{5.56}$$

Now we can solve (5.55) for the function $q(u)$ by integration and get

$$q(u) = q(0) - \frac{1}{\tilde{p} - \langle p\rangle}\int_0^u dv\,\frac{1}{v}\frac{d}{dv}\frac{[p](v)}{\tilde{p} - \langle p\rangle - [p](v)} \ . \tag{5.57}$$

Thus, we get the coefficient function of the inverse Parisi matrix to be

$$q(u) = -\frac{1}{\tilde{p} - \langle p\rangle}\left(\frac{[p](u)}{u\{\tilde{p} - \langle p\rangle - [p](u)\}} + \frac{p(0)}{\tilde{p} - \langle p\rangle} + \int_0^u \frac{dv}{v^2}\frac{[p](v)}{\tilde{p} - \langle p\rangle - [p](v)}\right) \ . \tag{5.58}$$

It remains to compute the diagonal element $\tilde{q}$ of the inverse matrix. In order to do that, we make use of (5.53), (5.58) and calculate straightforwardly

$$\tilde{q} = \frac{1}{\tilde{p} - p(1)} + q(1) = \frac{1}{\tilde{p} - \langle p \rangle} \left(1 - \frac{p(0)}{\tilde{p} - \langle p \rangle} - \int_0^1 \frac{dv}{v^2} \frac{[p](v)}{\tilde{p} - \langle p \rangle - [p](v)} \right) . \tag{5.59}$$

As we see, the inverse of a Parisi matrix is of the Parisi form with coefficients (5.58) and (5.59). We end this section by mentioning an equation that can be calculated straightforwardly. It will turn out to be useful throughout the calculation of the toy model (1.6) to take into account

$$\tilde{q} - q(u) = \frac{1}{u\{\tilde{p} - \langle p \rangle - [p](u)\}} - \int_u^1 \frac{dv}{v^2} \frac{1}{\tilde{p} - \langle p \rangle - [p](v)} , \tag{5.60}$$

which follows directly from (5.58) and (5.59).

5.2.5 Eigenvalues of Parisi Matrix

To determine the eigenvalues of a Parisi matrix, we first construct projectors. We introduce the matrices

$$\mathbb{P}_i := \frac{1}{m_i} \mathbb{I}_i \, , \text{for } i \in \mathcal{I} \quad \text{and} \quad \mathbb{P}_{-1} := 0 . \tag{5.61}$$

Because of the property (5.27) of the matrices $\mathbb{I}_i$, we get the multiplication rule

$$\mathbb{P}_i \mathbb{P}_j = \mathbb{P}_{\min\{i,j\}} . \tag{5.62}$$

Similar to (5.23), we now define the actual projector as

$$\overline{\mathbb{P}}_i := \mathbb{P}_i - \mathbb{P}_{i-1} . \tag{5.63}$$

Because of (5.62), they are idempotent and orthogonal

$$\overline{\mathbb{P}}_i \overline{\mathbb{P}}_j = \delta_{ij} \overline{\mathbb{P}}_i , \tag{5.64}$$

and with (5.16), (5.61) and (5.63) one finds a completeness relation

$$\mathbb{I} = \sum_{i=0}^{k+1} \overline{\mathbb{P}}_i . \tag{5.65}$$

Hence, the matrices $\overline{\mathbb{P}}_i$ are, indeed, orthogonal projection operators. The rank of the matrices (5.61), i.e., the number of linear independent rows or columns, follows from symmetry reasons:

$$\operatorname{rank}(\mathbb{P}_i) = \frac{n}{m_i} . \tag{5.66}$$

The rank of the projector (5.63) accordingly calculates for $i \geq 1$

$$\operatorname{rank}(\overline{\mathbb{P}}_i) = \frac{n}{m_i} - \frac{n}{m_{i-1}} . \tag{5.67}$$

The case $i = 0$ has to be treated independently as m_{-1} is not a well-defined quantity. It will be discussed later in this section.

Due to the identity (5.65), we can decompose any vector $\mathbf{y}$ as

$$\mathbf{y} = \sum_{i=0}^{k+1} \mathbf{y}_i \ , \tag{5.68}$$

with the coefficients

$$\mathbf{y}_i = \overline{\mathbb{P}}_i \mathbf{y} \ . \tag{5.69}$$

In the following, we will show that the coefficients $\mathbf{y}_i$ are eigenvectors of the Parisi matrix $\mathbf{P}$. To this end, we use (5.22), (5.61) and write the matrix (5.24) in terms of the projectors

$$\mathbf{P} = \tilde{p}\,\mathbb{I} + \sum_i p_i \left(m_i \mathbb{P}_i - m_{i+1}\mathbb{P}_{i+1}\right) \ . \tag{5.70}$$

Multiplication of the Parisi matrix $\mathbf{P}$ with the vector $\mathbf{y}_i$ leads to

$$\mathbf{P}\,\mathbf{y}_j = \left[\tilde{p}\,\mathbb{I} + \sum_i p_i \left(m_i \mathbb{P}_i - m_{i+1}\mathbb{P}_{i+1}\right)\right] \left(\mathbb{P}_j - \mathbb{P}_{j-1}\right) \mathbf{y} \,, \tag{5.71}$$

where the index j runs from $j = 0$ to $j = k+1$. Applying the properties (5.62) yields

$$\begin{aligned} \mathbf{P}\,\mathbf{y}_j = \ & \tilde{p}\mathbf{y}_j + \sum_i \Big[p_i m_i \left(\mathbb{P}_{\min\{i,j\}} - \mathbb{P}_{\min\{i,j-1\}}\right) \\ & - p_i m_{i+1} \left(\mathbb{P}_{\min\{i+1,j\}} - \mathbb{P}_{\min\{i+1,j-1\}}\right)\Big] \mathbf{y} \,, \end{aligned} \tag{5.72}$$

which reduces to

$$\mathbf{P}\,\mathbf{y}_j = \tilde{p}\,\mathbf{y}_j + \sum_{i \geq j} p_i (m_i - m_{i+1}) \mathbf{y}_j - p_{j-1} m_j \mathbf{y}_j \ . \tag{5.73}$$

The corresponding eigenvalues can thus be read off as

$$\lambda_j = \tilde{p} + \sum_{i \geq j} (m_i - m_{i+1}) p_i - m_j p_{j-1} \ . \tag{5.74}$$

In the parameterization in terms of the continuous functions (5.12) we get

$$\lambda(u) = \tilde{p} - u p(u) + \int_1^u dv\, p(v) = \tilde{p} - \langle p \rangle_n - [p]_n(u) - n p(u) \ . \tag{5.75}$$

Their multiplicities can be derived from (5.67) as

$$\frac{n}{m_i} - \frac{n}{m_{i-1}} = n \frac{m_{i-1} - m_i}{m_i m_{i-1}} \to n \frac{du}{u^2} \ . \tag{5.76}$$

Now we return to the case $j = 0$ and take a look at the projector $\overline{\mathbb{P}}_0$. From (5.16) and (5.61) follows that it is a matrix with constant coefficients $P_{ij} = 1/n \ \forall i, j$. Accordingly, applying the projector $\overline{\mathbb{P}}_0$ to any vector leads to a new vector with constant entries. Because of the general considerations (5.72), it is also an eigenvector with a multiplicity that is obviously equal to 1. The corresponding eigenvalue can be obtained from (5.74). One has to be careful with the quantity

p_{-1}. It has to be defined as 0 in accordance with the definition of the Parisi matrix (5.24) and (5.72). The eigenvalue then results to be

$$\lambda_0 = \tilde{p} + \sum_i p_i(m_i - m_{i+1})\,. \tag{5.77}$$

This eigenvalue already could have been read off directly from Eq. (5.26) for an eigenvector $\mathbf{e} = (1, 1, ..., 1)^T$.

In the continuous case, the eigenvalue can by found with (5.38). One finds

$$\lambda_0 = \tilde{p} - \langle p \rangle_n\,. \tag{5.78}$$

Now we will go over to the case $n < 1$. However, we will defer the limiting process $n \to 0$ to the next section. There it will be shown that a term vanishing in this limit will give a nonzero contribution to the Tracelog. This is, in fact, the first time we have to be careful with small n. Moreover, the inequality (5.13) becomes important for the first time as the multiplicity of the eigenvalues changes its sign because of $m_{i-1} - m_i \to -du$ for small n. Hence, we obtain instead of (5.76)

$$\frac{n}{m_i} - \frac{n}{m_{i-1}} \to -n\frac{du}{u^2}\ . \tag{5.79}$$

5.2.6 Tracelog of Parisi Matrix

In order to avoid any confusion, we will state right at the beginning of this section that all following considerations are done for $n < 1$. To calculate the Tracelog of a Parisi matrix, we first investigate the logarithm of a Parisi matrix. Via the Taylor expansion of the logarithm $\log A = \log[\mathbb{I} + (A - \mathbb{I})]$, one can show that for every diagonizable matrix A

$$\log A = T(\log A')T^{-1}\ , \tag{5.80}$$

where the matrix $A' = T^{-1}AT$ is the matrix with the eigenvalues as entries on the diagonal. Each column vector of T is an eigenvector of A. It is convenient that eigenvalues are invariant under this transformation as

$$\det(A' - \lambda\mathbb{I}) = \det T^{-1}(A - \lambda\mathbb{I})T = \det(A - \lambda\mathbb{I})\ . \tag{5.81}$$

Therefore, the trace of a matrix, i.e., the sum of all diagonal elements, is invariant and equal to the sum of all eigenvalues

$$\mathrm{Tr}A = \sum_i \lambda_i^{\alpha_i}\ . \tag{5.82}$$

The exponent α_i denotes the multiplicity of the corresponding eigenvalue. It follows that the Tracelog of a diagonizable matrix A calculates according to

$$\mathrm{Trlog}A = \sum_i \log \lambda_i^{\alpha_i}\ . \tag{5.83}$$

Considering this, one finds via the results (5.75), (5.76), and (5.78) of the previous section the expression for the continuous case

$$\begin{aligned}\mathrm{Trlog}\,\mathbf{P} &= \log\left\{\tilde{p} - \langle p\rangle_n\right\} + \int_n^1 dv\ \log\left\{\tilde{p} - \langle p\rangle_n - [p]_n(v) - np(v)\right\}^{-n/v^2} \\ &= \log\left\{\tilde{p} - \langle p\rangle_n\right\} - n\int_n^1 \frac{dv}{v^2}\ \log\left\{\tilde{p} - \langle p\rangle_n - [p]_n(v) - np(v)\right\}.\end{aligned} \tag{5.84}$$

In view of the limit $n \to 0$, one has to account for all terms up to order n. Because the second term is already of that order, the first one for will be expanded for small n to get

$$\log\left\{\tilde{p} - \langle p\rangle_n\right\} = \log\left\{\tilde{p} - \langle p\rangle\right\} + n\frac{p(0)}{\tilde{p} - \langle p\rangle} + O(n^2)\ . \tag{5.85}$$

With this, it follows that the whole Tracelog can be written as

$$\mathrm{Trlog}\,\mathbf{P} = \log\left\{\tilde{p} - \langle p\rangle\right\} + n\frac{p(0)}{\tilde{p} - \langle p\rangle} - n\int_n^1 \frac{dv}{v^2}\,\log\left\{\tilde{p} - \langle p\rangle - [p](v)\right\} + O(n^2)\ . \tag{5.86}$$

Furthermore noticing the identity

$$\frac{1}{n} - 1 = \int_n^1 \frac{dv}{v^2}\ , \tag{5.87}$$

we may simplify the whole expression and get

$$\mathrm{Trlog}\,\mathbf{P} = n\log\left\{\tilde{p} - \langle p\rangle\right\} + n\frac{p(0)}{\tilde{p} - \langle p\rangle} - n\int_n^1 \frac{dv}{v^2}\log\left\{\frac{\tilde{p} - \langle p\rangle - [p](v)}{\tilde{p} - \langle p\rangle}\right\} + O(n^2). \tag{5.88}$$

Now one is able to take the well-defined limit $n \to 0$

$$\lim_{n\to 0}\frac{1}{n}\mathrm{Trlog}\,\mathbf{P} = \log\left\{\tilde{p} - \langle p\rangle\right\} + \frac{p(0)}{\tilde{p} - \langle p\rangle} - \int_0^1 \frac{dv}{v^2}\log\left\{\frac{\tilde{p} - \langle p\rangle - [p](v)}{\tilde{p} - \langle p\rangle}\right\}\ . \tag{5.89}$$

This is exactly the result found by Mézard and Parisi in Ref. [54].

5.3 Application to Model

Having developed the formalism of Parisi matrices, we can finally tackle our key problem. At first, we rewrite (4.53) in terms of the new formalism:

$$q(a,b) = \frac{2}{\beta}(\tilde{g} - g(u))\,, \tag{5.90}$$

with $\tilde{g}$ being the diagonal and $g(u)$ describing the non-diagonal part of the matrix G. Similar, the conditional equation (4.64) for the diagonal elements $\sigma_{aa} = \tilde{\sigma}$ reads using (5.26) and (5.38):

$$\tilde{\sigma} = \int_0^1 dv\,\sigma(v) = \langle\sigma\rangle\,. \tag{5.91}$$

Note that $\tilde{\sigma}$ can be expressed in terms of the non-diagonal elements. It is, thus, no independent degree of freedom. Accordingly, one proceeds for the non-diagonal elements. The conditional equation (4.63) translates into

$$\sigma(u) = -2\beta f_\xi\left(\frac{2}{\beta}[\tilde{g} - g(u)]\right)\ . \tag{5.92}$$

The inverse G^{-1} of G is defined in (4.9). A Parisi matrix in the limit $n \to 0$ is described by the diagonal element

$$\tilde{g}^{-1} = \kappa - \tilde{\sigma} \tag{5.93}$$

and a function on the interval $[0,1]$ describing the non-diagonal elements

$$g^{-1}(u) = -\sigma(u) \ . \tag{5.94}$$

Therefore, (5.44) and (5.47) give

$$\langle g^{-1} \rangle \quad = -\langle \sigma \rangle = -\tilde{\sigma} \tag{5.95}$$

$$[g^{-1}](u) \quad = -[\sigma](u) \ . \tag{5.96}$$

Furthermore, we find from (5.60) the expression

$$\tilde{g} - g(u) = \frac{1}{u\{\kappa + [\sigma](u)\}} - \int_u^1 \frac{dv}{v^2} \frac{1}{\kappa + [\sigma](v)} \ . \tag{5.97}$$

The central point is to calculate the free energy (4.58). In order to this, we need the expressions for $\mathrm{Tr}\, G$ and $\mathrm{Trlog}\, G^{-1}$. From Eq. (5.59), we find

$$\lim_{n\to 0} n^{-1} \,\mathrm{Tr}\, G = \tilde{g} = \frac{1}{\kappa} + \frac{\sigma(0)}{\kappa^2} + \frac{1}{\kappa} \int_0^1 \frac{dv}{v^2} \frac{[\sigma](v)}{\kappa + [\sigma](v)} \ . \tag{5.98}$$

The mean square displacement was derived to be (4.59) and, thus, it is given in the Parisi formalism as

$$\overline{\langle x^2 \rangle}^{(1)}_{(k)} = \frac{1}{\beta} \left[\frac{1}{\kappa} + \frac{\sigma(0)}{\kappa^2} + \frac{1}{\kappa} \int_0^1 \frac{dv}{v^2} \frac{[\sigma](v)}{\kappa + [\sigma](v)} \right] \ . \tag{5.99}$$

The index k denotes the indirect dependence of the step parameter in (5.5).

Looking at the expression, we have to be careful near $u = 0$ as the integrand is multiplied by a factor $1/v^2$. Thus, one naively expects the remaining part of the integrand to have to go in leading order with v^2 as to make sure that the integral does not diverge. We have to keep in mind, though, that sometimes we have to be careful with the limit $n \to 0$. Hence, we conclude that if we have $[\sigma](u) = 0$ in an interval $[0, c]$ with $c \leq 1$, no further problems arise in the integra. In the case of finite-step RSB, this is exactly what happens. Also it is possible to have a continuous function $\sigma(u)$ starting as constant on the interval $[0, c]$. Now we use (5.89) to compute

$$\lim_{n\to 0} n^{-1} \,\mathrm{Trlog}\, G = \log \kappa - \frac{\sigma(0)}{\kappa} - \int_0^1 \frac{dv}{v^2} \log \left\{ \frac{\kappa + [\sigma](v)}{\kappa} \right\} \ . \tag{5.100}$$

The last term missing is the double sum. Due to the fact that one separates the diagonal case from the non-diagonal one, we get

$$\begin{aligned} \sum_{a,b} f \left[\frac{2}{\beta} (G_{aa} + G_{bb} - 2G_{ab}) \right] \ &= n f(0) - n \int_0^1 dv \, f \left[\frac{2}{\beta} (\tilde{g} - g(v)) \right] \\ &= n f(0) - n \int_0^1 dv \, f \left[\frac{2}{\beta} \left(\frac{1}{u\{\kappa + [\sigma](u)\}} - \int_u^1 \frac{dv}{v^2} \frac{1}{\kappa + [\sigma](v)} \right) \right] . \end{aligned} \tag{5.101}$$

The minus sign in front of the integral results from the case $n < 1$. With the help of (5.98)–(5.101), we find the free energy under replica-symmetry breaking to be

$$\begin{aligned} F^{(1)}_{(k)} = \lim_{n\to 0} n^{-1} F^{(1)}_n = &-\frac{1}{2\beta} \log \left(\frac{2\pi}{\kappa\beta} \right) + \frac{1}{2\beta} \int_0^1 \frac{dv}{v^2} \frac{[\sigma](v)}{\kappa + [\sigma](v)} - \frac{1}{2\beta} \int_0^1 \frac{dv}{v^2} \log \left\{ \frac{\kappa + [\sigma](v)}{\kappa} \right\} \\ &- \frac{\beta}{2} f(0) + \frac{\beta}{2} \int_0^1 du \, f \left[\frac{2}{\beta} \left(\frac{1}{u\{\kappa + [\sigma](u)\}} - \int_u^1 \frac{dv}{v^2} \frac{1}{\kappa + [\sigma](v)} \right) \right] . \end{aligned} \tag{5.102}$$

Again the index k indicates the step number of RSB. One notices that the free energy (5.102) just depends on the function $[\sigma](u)$.

After all this preparation, it is easy to reproduce the replica-symmetric result. In this specific ansatz, all non-diagonal elements are equal

$$\sigma_{\mathrm{RSA}}(u) = \sigma_0 = \text{const.} \tag{5.103}$$

According to (5.47), the quantity $[\sigma_{\mathrm{RSA}}](u)$ is seen to be 0 for all values $u \in [0,1]$. Hence, the free energy (5.102) does not depend on the variational parameter. This is the reason why the replica-symmetric ansatz does not include non-perturbative contributions as mentioned in Sect. 4.4.3. As expected, this case is easily seen to reproduce (4.80).

5.3.1 Infinite-Step Symmetry Breaking

Inspired by its success in spin glasses, we search for continuous functions $\sigma(u)$ and $[\sigma](u)$, respectively, as a solution of the saddle point equation. In order to find it, we differentiate the conditional equation (5.92) with respect to u. We get

$$\beta\sigma'(u)\left\{\kappa + [\sigma](u)\right\}^2 = 4f_{\xi\xi}\left[\frac{2}{\beta}(\tilde{g} - g(u))\right]\sigma'(u)\ . \tag{5.104}$$

Thus, one has either $\sigma'(u) = 0$, which is the case for a piecewise constant function, or

$$\beta\left\{\kappa + [\sigma](u)\right\}^2 = 4f_{\xi\xi}\left[\frac{2}{\beta}(\tilde{g} - g(u))\right]\ . \tag{5.105}$$

According to (5.97), this equation depends just on $[\sigma](u)$. In our toy model, the function f is defined in (4.55). Using this definition, we rewrite

$$\frac{2}{\beta}[\tilde{g} - g(u)] + \lambda^2 = \left(\frac{9\varepsilon^4}{2\pi}\right)^{1/5}\left\{\kappa + [\sigma](u)\right\}^{-4/5}. \tag{5.106}$$

Differentiating yet another time with respect to the variable u and simplifying the resulting expression yields

$$\left(\frac{5}{2\beta}\right)^5 \frac{2\pi}{9\varepsilon^4}\frac{1}{u^5} = \kappa + [\sigma](u)\,. \tag{5.107}$$

Note that (5.107) cannot be used in the limit $u \searrow 0$, as the definition (5.47) guarantees the boundary condition $[\sigma](0) = 0$. Keeping in mind, that solutions with $\sigma'(u) = 0$ also satisfy the conditional equation (5.92), the most general continuous solution is

$$[\sigma](u) = \begin{cases} 0 & \text{for } 0 \le u \le u_1 \\ Au^{-5} - \kappa & \text{for } u_1 < u < u_2 \\ Au_2^{-5} - \kappa & \text{for } u_2 \le u \le 1\ , \end{cases} \tag{5.108}$$

with the definition

$$A = \left(\frac{5}{2\beta}\right)^5 \frac{2\pi}{9\varepsilon^4}\,. \tag{5.109}$$

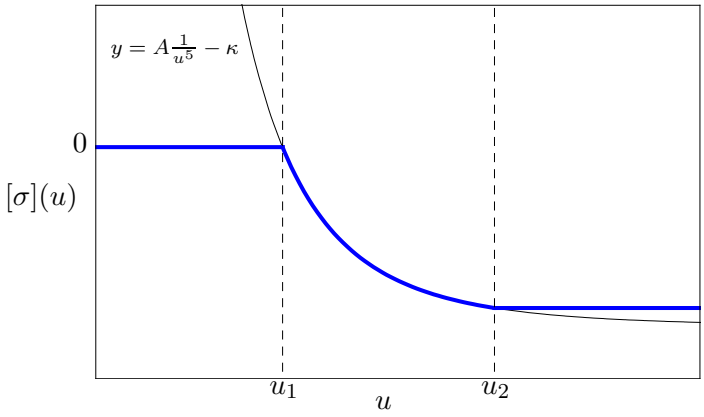

Figure 5.1: Sketch of the function $[\sigma](u)$ as defined in (5.108).

The function (5.108) is sketched in Fig. 5.1. The parameter u_1 is defined by $Au_1^{-5} - \kappa = 0$ and, thus, is

$$u_1 = \left(\frac{A}{\kappa}\right)^{1/5} , \tag{5.110}$$

if this solution u_1 is less or equal to 1. Otherwise, the replica-symmetric solution is reproduced. The second parameter u_2 is either equal to 1 or can be obtained from (5.97) and (5.106) in order to get a continuous solution. Inserting $[\sigma](u)$ for $u = u_2$ leads to the conditional equation

$$4u_2^5 - 5u_2^4 + 2\beta A\lambda^2 = 0\,. \tag{5.111}$$

The solution of Eq. (5.111) has to be in the interval $[u_1, 1]$. Otherwise, the parameter u_2 is chosen to be equal to 1, if a solution is greater than 1. In this case, just the function $[\sigma](u)$ is defined by just two regions. If all solutions $u_2 \leq u_1$, one is back at the replica-symmetric case with $[\sigma](u) = 0$. The parameter function $[\sigma](u)$ is decreasing monotonously. Accordingly, the parameter $\sigma(u)$ is also a decreasing function, as can bee seen from Eq. (5.48). This, however, crucially depends on the correlation function. For other choices of derived function f, the parameter $\sigma(u)$ may be described by an increasing function [19]. In this case, the infinite-step replica-symmetry breaking solution is shown to be stable for all temperatures [56]. As an assumption the proof uses the argument that $\sigma(u)$ is increasing to show that the eigenvalues of the Hessian are non-negative.

Although the infinite step is not proven to be stable for all temperatures, we can compare the free energy solution to numerical simulation. Knowing (5.108), there remains no further problem to calculate the free energy (5.102)

$$\begin{aligned} F_{(\infty)}^{(1)} = & -\frac{1}{2\beta}\log\left(\frac{2\pi}{\kappa\beta}\right) + \frac{1}{2\beta}\left[\frac{1}{u_1} - 1 + \frac{\kappa}{4A}(u_1^4 - 5u_2^4 + 4u_2^5)\right] - \frac{1}{2\beta}\left[\log\left(\frac{A}{\kappa}\right)\left(\frac{1}{u_1} - 1\right)\right. \\ & \left. +5\log u_2 - 5\frac{\log u_1}{u_1} + \frac{1}{u_1} - \frac{1}{u_2}\right] - \frac{\beta}{2}f(0) + \frac{\beta}{2}\left\{u_1 f\left[\frac{2}{\beta}\left(\frac{1}{\kappa u_1} + \frac{u_1^4 + 4u_2^5 - 5u_2^4}{4A}\right)\right]\right. \\ & \left. +(1-u_2)f\left[\frac{2}{\beta}\left(\frac{u_2^5}{A}\right)\right] + \int_{u_1}^{u_2} du\, f\left[\frac{2}{\beta}\left(\frac{5u^4 + 4u_2^5 - 5u_2^4}{4A}\right)\right]\right\}. \end{aligned} \tag{5.112}$$

It is left to calculate the remaining integral. If one finds an u_2 such that Eq. (5.111) is satisfied, the integration is simple. The integrand in case of the Gauss correlator (1.3) then simplifies to

$$f\left(\frac{5}{2A\beta}u^4-\lambda^2\right)=\varepsilon^2\sqrt{\frac{A\beta}{5\pi}}\frac{1}{u^2}\,. \tag{5.113}$$

Thus, the integration yields

$$\int_{u_1}^{u_2}du\,f\left[\frac{2}{\beta}\left(\frac{5u^4+4u_2^5-5u_2^4}{4A}\right)\right]=\varepsilon^2\sqrt{\frac{A\beta}{5\pi}}\left(\frac{1}{u_1}-\frac{1}{u_2}\right)\,. \tag{5.114}$$

If no solution of (5.111) can be found, then $u_2=1$. In this case, the integration is more complicated. One finds the remaining integral to be

$$\begin{aligned}\int_{u_1}^{u_2}du\,f\left[\frac{1}{2A\beta}(5u^4-1)\right]=\;&\varepsilon^2\sqrt{\frac{A\beta}{5\pi}}\Bigg\{\frac{1}{u_1}{}_2F_1\left[\frac{1}{4},\frac{1}{2};\frac{5}{4};\frac{1-2\beta A\lambda^2}{5u_1^4}\right]\\&+{}_2F_1\left[\frac{1}{4},\frac{1}{2};\frac{5}{4};\frac{1-2\beta A\lambda^2}{5}\right]\Bigg\}\,.\end{aligned} \tag{5.115}$$

The function ${}_2F_1$ is the hypergeometric function. It is defined by

$${}_2F_1[a,b;c;x]=\sum_{n=0}^{\infty}\frac{(a)_n(b)_n}{(c)_n}\frac{x^n}{n!}\,, \tag{5.116}$$

with the Pochhammer symbol $(a)_n=a(a+1)(a+2)...(a+n-1)$.

5.3.2 Finite-Step RSB

In this section, we will improve the approximation results by apllying finite-step RSB. The easiest non-symmetric choice of a Parisi matrix is

$$\sigma(u)=\begin{cases}\sigma_0 & \text{for } 0\le u\le u_c\\ \sigma_1 & \text{for } u_c\le u\le 1\,.\end{cases} \tag{5.117}$$

It corresponds to the parameter $k=1$ and $m_k=m\to u_c$ for $n\to 0$. Furthermore, we use the definition (5.47) to calculate

$$[\sigma](u)=\begin{cases}0 & \text{for } 0\le u\le u_c\\ \Sigma=u_c(\sigma_1-\sigma_0) & \text{for } u_c\le u\le 1\,.\end{cases} \tag{5.118}$$

For this one-step RSB, the free energy (5.102) writes

$$\begin{aligned}F_{(1)}^{(1)}=\;&-\frac{1}{2\beta}\log\left(\frac{2\pi}{\kappa\beta}\right)+\frac{1}{2\beta}\left(1-\frac{1}{u_c}\right)\left[\log\left(\frac{\kappa+\Sigma}{\kappa}\right)-\frac{\Sigma}{\kappa+\Sigma}\right]-\frac{\beta}{2}f(0)\\&+\frac{\beta}{2}\Bigg\{u_c f\left[\frac{2}{\beta(\kappa+\Sigma)}\left(1+\frac{\Sigma}{u_c\kappa}\right)\right]+(1-u_c)f\left[\frac{2}{\beta(\kappa+\Sigma)}\right]\Bigg\}.\end{aligned} \tag{5.119}$$

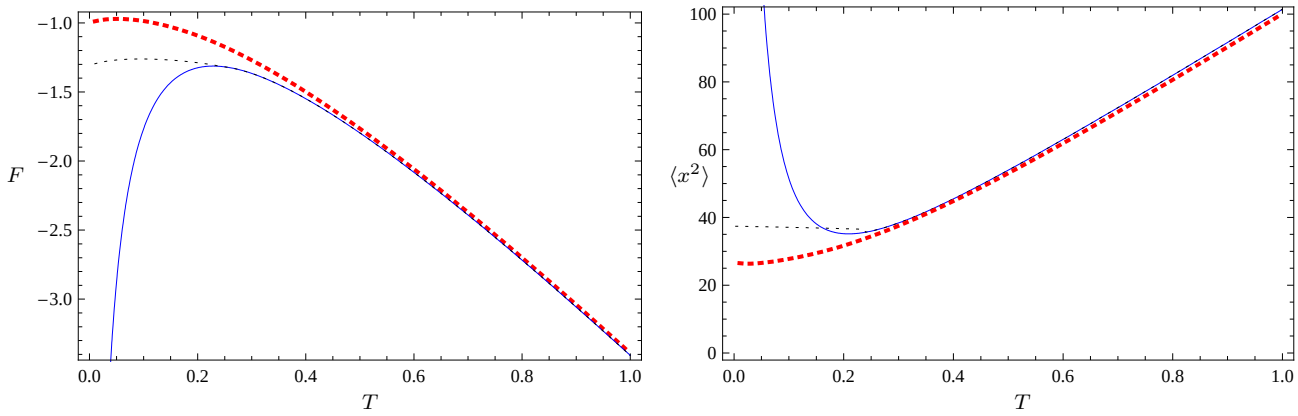

Figure 5.2: The dotted black line represents the free energy and mean square displacement, respectively, in one-step replica symmetry breaking with parameters $\varepsilon = 1$, $\lambda = 1$, and $\kappa = 0.01$. The results are compared to the replica-symmetric solution (solid, blue) and computer simulations (dashed, red).

For completeness reasons, we state the expression for the mean square displacement resulting from (5.99):

$$\overline{\langle x^2 \rangle}^{(1)}_{(1)} = \frac{1}{\kappa\beta}\left[1 + \frac{\sigma_0}{\kappa} + \frac{\Sigma}{\kappa+\Sigma}\left(\frac{1}{u_c} - 1\right)\right] . \tag{5.120}$$

It is left to determine $\tilde{\sigma}$, σ_0, σ_1 and u_c via conditional equations. For practical reasons, we will find equations in terms of Σ instead of σ_1, which can be computed by the definition from Σ in (5.118) with the help of σ_0 and u_c. In the following, we are going to set up four conditional equations for the four unknown variables. By using (5.92), one gets the first equation

$$\sigma_0 = -2\beta f_\xi\left[\frac{2}{\beta(\kappa+\Sigma)}\left(1 + \frac{\Sigma}{u_c\kappa}\right)\right] . \tag{5.121}$$

The parameter σ_1 is calculated analogously. However, we will make use of an indirect conditional equation. For practical reasons, we concentrate on

$$\Sigma = u_c(\sigma_1 - \sigma_0) = -2\beta u_c\left\{f_\xi\left[\frac{2}{\beta(\kappa+\Sigma)}\right] - f_\xi\left[\frac{2}{\beta(\kappa+\Sigma)}\left(1 + \frac{\Sigma}{\kappa u_c}\right)\right]\right\} . \tag{5.122}$$

Furthermore, we get by the definition (5.96) and further using (5.91) the diagonal element

$$\tilde{\sigma} = \sigma_0 + \left(\frac{1}{u_c} - 1\right)\Sigma . \tag{5.123}$$

Until now, we did not account for the fact, that the free energy depends on the parameter u_c. Applying the *principle of minimal sensitivity*, we have to demand

$$\frac{\partial}{\partial u_c} F_n^1 = 0 . \tag{5.124}$$

Thus, we find the last equation to be

$$\begin{aligned} 0 = {} & \beta^2 u_c^2\left\{f\left[\frac{2}{\beta(\kappa+\Sigma)}\right] - f\left[\frac{2}{\beta(\kappa+\Sigma)}\left(1 + \frac{\Sigma}{u_c\kappa}\right)\right]\right\} - 2\beta u_c \frac{\Sigma}{\kappa(\kappa+\Sigma)} f_\xi\left[\frac{2}{\beta(\kappa+\Sigma)}\right] \\ & - \frac{\Sigma}{\kappa} + \log\left(\frac{\kappa+\Sigma}{\kappa}\right) . \end{aligned} \tag{5.125}$$

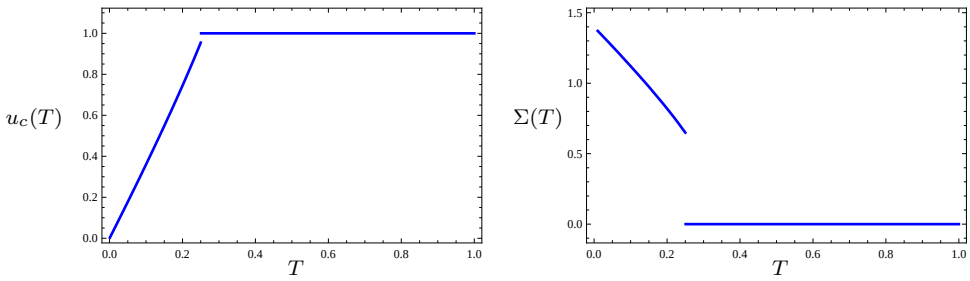

Figure 5.3: Parameters of one-step RSB u_c and Σ with parameter values $\varepsilon = 1$, $\lambda = 1$ and $\kappa = 0.01$ as function of the temperature. Both parameters are not continuous. They jump discontinuously from the replica-symmetric solution $u_c = 1$ and $\Sigma = 0$ to a new solution beneath a certain temperature.

As a matter of fact, these are the equations found in Ref. [19]. Numerically solving sets of multidimensional nonlinear equations is complicated and a convergence of any algorithm cannot be guaranteed. We can, however, avoid this problem. The conditional equations are set up to find the optimal upper bound of the free energy. Extremalization of a function is computationally much simpler. Hence, we make use of optimization algorithms to find the extrema of the free energy. Mainly, we employ the Simplex Method developed by Nelder and Mead [57]. The Eqs. (5.122) and (5.125) may then be used to verify the results.

As seen in the discussion of the Almeida-Thouless line (4.89), the replica-symmetric solution breaks down for small κ at small temperatures. Thus, we will concentrate on this problematic case and show in Fig. 5.3 the case $\kappa = 0.01$. We notice that the symmetry-breaking improves the approximation both for the free energy and the mean square displacement. Still, the deviation from the numerical simulations is about 30% for the free energy and approximately 40% for the mean square displacement.

The one-step solution branches continuously off the replica-symmetric curve. The parameter u_c, however, jumps from the replica-symmetric solution $u_c = 1$ to the replica-broken solution beneath a small temperature slightly higher than the critical instability point (4.89). This becomes clearer from Fig. 5.3.

It is natural to expect further corrections of higher step replica-symmetry breaking. There is no fundamental problem using piecewise constant functions $\sigma(u)$ with more steps. With every new step two parameters are introduced and, accordingly, the number of conditional equation will raise. Also, the free energy expression (5.102) will contain three additional summands. We numerically maximized the free energy for step parameters up to $k = 6$. No additional corrections could be found.

Chapter 6

Overview

Describing nature, one has to face the facts: it is impossible to have information about all details of any physical system. The awareness of nescience has entered the domain of physical modelling via the concept of randomness and disorder. By means of several examples, the importance of disorder theory in modern physics was illuminated in **Chapter 1**. However, many problems containing randomness cannot be solved exactly. Thus, the introduction was devoted to establish a guinea pig model in order to test different approximation techniques. The use of our specific model was motivated on the one hand with classical statistics. Although the toy model of a harmonic oscillator in a random environment seemed very simple at first, numerous applications and generalizations were presented [20, 21, 22, 23, 24, 25, 26]. On the other hand, we approached the model via the theory of continuous-time stochastic processes: from the Fokker-Planck equation we proceeded to the Kramers and Smoluchowski equations. Our testing ground for disorder was the stationary probability distribution of an overdamped Brownian motion exposed to a conservative random force. In this thesis, we concentrated on the thermodynamic problem of finding the free energy of a harmonic oscillator in a random potential, which was already studied in depth in Ref. [19].

In **Chapter 2**, we introduced the idea of Gaussian distributed random fields and we presented the Randomization Method (2.13). The parameters were chosen according to (2.15) and (2.16). This led to the calculation of the generating functional (2.26). We showed that the algorithm generates, indeed, Gaussian distributed random functions with controllable accuracy. As examples, a Gaussian correlation and a Cauchy-type correlation were discussed in Figs. 2.1–2.4.

In the following, we approached the actual toy model. In the beginning of **Chapter 3**, we calculated the perturbation expansion for small correlation strength. The unperturbed state was taken to be a harmonic oscillator without disorder. The corrections for the free energy in first and second order were given in (3.17) and (3.18) and were plotted in Fig. 3.1. To compare our approximations with quantities accessible to experiments, we calculated the width of the probability distribution, i.e., the mean square displacement. The corrections were computed in (3.28) and (3.29) and the results, plotted in Fig. 3.2, were shown to be unsatisfactory for small temperatures. The deviation for $\kappa = 0.01$ was about $2000\,\%$ at $T = 0$. Hence, we tried to improve the approximations by introducing in a variational parameter in a naïve approach using the square root substitution (3.43) for the restoring force κ. The obtained results were plotted in Figs. 3.3–3.6 and we showed that no improvement was gained. We thus went on using a square root like method (3.56) to introduce a variational parameter via the temperature dependence of the system. The free energy is then computed in (3.58) and the results are plotted in Figs. 3.7–3.10. To our astonishment, the results even in first order reproduced the numerical simulations

extremely well. The deviation for the investigated parameter $\kappa = 0.01$ in the small temperature regime could be reduced to a maximal 10 %.

Chapter 4 was devoted to the replica trick, which is the standard method to treat systems with quenched disorder. By rewriting the toy model system as a many-particle system introducing n copies, the problem could be formulated in terms of a non-random system in (4.7). Due to the identity Eq. (4.31), the free energy of the replicated system could be shown to be equal to the real system's free energy in the limit $n \to 0$. This system, however, was not solvable analytically. Therefore, we employed a variational principle by introducing a $n \times n$ matrix $G_{ab}^{-1} = \kappa\delta_{ab} - \sigma_{ab}$ in (4.9), in which the variational parameters were stored. The first-order expansion (4.15) was the basis of all approaches to follow because the Jensen-Peierls inequality (4.18) provided us with the result that the first-order free energy in the variational perturbation expansion is a safe upper bound for the free energy of the system. It was calculated in (4.58) and the variational parameter could be determined in (4.62). As a canonical ansatz for the variational matrix σ we chose the approach (4.65) where all replicated systems are interchangeable. In this special ansatz the free energy was calculated in (4.80) and the mean square displacement, thus, resulted in (4.81). In this way, the results of Ref. [19] could be reproduced. However, we showed that the free energy did not depend on the variational parameter and, therefore, no non-perturbative correction was found. This conclusion, that one just derived the first-order standard perturbation expansion in an extremely complicated way was overlooked in Ref. [19]. Additional information was given by the Almeida-Thouless line (4.89), though, plotted in Fig 4.1 and found in Ref. [19] as well. It provided a criterion to test the stability of the system by evaluating the eigenvalues of the Hessian. In order to have a stable bound for the free energy, it has to be positive definite. Although no non-perturbative corrections could be included, we nevertheless gained a method to decide when non-perturbative contributions do play a decisive role. Thus, the stability analysis manifests the scope of perturbation theory.

For small restoring constants κ and small temperatures the perturbation expansion of the system breaks down and it does not provide a good approximation of the system. Therefore, in **Chapter 5** we investigated the method of replica-symmetry breaking [54]. This method has shown to be successful in many disorder problems. The basic formalism was introduced in Sects. 5.1–5.2. The method is based on stepwise raising the number of variational parameters. The free energy was given in (5.102) and the mean square displacement in (5.98). The first step correction was plotted in Fig. 5.3 and, in fact, improved the perturbation approach to a certain extent as also shown in Ref. [19]. The obtained curve, however, did not resemble the simulation results. For the smallest confinement parameter $\kappa = 0.01$, the deviation at $T = 0$ was still an estimated 30 %. It was seen that, by numerical optimization, even higher step parameters up to $k = 6$ did not provide further corrections.

The overall aim of this work was to test approximation techniques on a guinea pig model. The simple disorder problem of a harmonic oscillator in a random environment turned out to be quite tricky. The standard approach for systems with quenched disorder, the replica method, did not provide a satisfying approximation. It turns out that the canonical replica-symmetric approach could not include non-perturbative corrections. Also, the stability of the infinite-step replica-symmetry breaking, a method that has been extremely successful in describing spin glasses, could not be proved to give a stable solution for all temperatures. Small corrections were found by the finite-step replica-symmetry breaking. However, they did not reproduce the numerics and it still remains to investigate the stability of the finite-step RSB solutions. Within this thesis, a satisfactory approximation of the simulated results could only be obtained by a variational principle based on the temperature as variational parameter. This approach, however,

yet remains to be put onto a solid mathematical basis.

The most important result of this thesis was to expose the shortcomings of the replica-symmetry breaking method in the investigated model. Parisi's approach is the standard tool in disorder problems. It is based on the first order of a systematic variational perturbation expansion, which is convenient because of the Jensen-Peierls inequality. However, previous VPT results for the anharmonic oscillator [12, 58, 59] suggest that higher orders of RSB may improve the results considerably. Thus, combining higher corrections of the variational perturbation expansion with the symmetry breaking scheme is expected to be very useful. The idea is to improve the approximation for a fixed representative of the ensemble of random potentials by VPT and to additionally include the effects of locally stable extrema by breaking the symmetry. This procedure was already applied to investigate the disappearance of a saddle point solution in higher order VPT leading to a second order phase transition in certain high-temperature superconductors [24].

The applications of variational methods in disorder problems are numerous. These methods play an integral role in disorder models not only of physical systems, but they are used in the theory of neural networks and, quite recently, they even made an impact on economics, e.g., describing emerging properties in heterogeneous agent models [11, 18, 60, 61]. As a representative for the countless possibilities opened up by strong variational techniques, I want to come back to the Brownian motion. It can be described as a passive movement. A small particle suspended in a liquid moves just because of collisions with thermally moving molecules. Many biological systems, however, exhibit driven motion. Cells or microorganisms, for instance, can be modeled as active particles with an inner energy depot. This reserve depot can be converted into kinetic energy and refilled by interaction with the environment. In more complicated models, also the dissipation of internal energy is included. This active motion is superposed with the effect of colliding molecules and, consequently, is called *active Brownian movement* [62, 63, 64]. Energy is pumped into the system via an external potential. To make the model realistic, it is inevitable to include disorder. Together with a potent approximation procedure, realistic active particle models constitute a useful description. Especially in the small temperature regime where the correlation strength is of the order of magnitude of the thermal movement, interesting results are to be expected.

Appendix A

Solution of Fokker-Planck Equation for Brownian Motion

The Fokker-Planck equation (1.19) has the form of a continuity equation. It can be written as

$$\frac{\partial}{\partial t}P(x,t) + \frac{\partial}{\partial x}S(x,t) = 0 \tag{A.1}$$

with the probability current

$$S(x,t) = K(x,t)P(x,t) - \frac{1}{2}\frac{\partial}{\partial x}\left[D(x,t)P(x,t)\right] \ . \tag{A.2}$$

As the Fokker-Planck equation describes the time evolution of the probability density, we require natural boundary conditions, i.e., the probability density vanishes for $x \to \pm\infty$. Therefore, the probability current (A.2) has to vanish as well. It follows that

$$0 = S(\infty,t) - S(-\infty,t) = \int_{-\infty}^{\infty} dx \frac{\partial}{\partial x}S(x,t) = \int_{-\infty}^{\infty} dx \frac{\partial}{\partial t}P(x,t) = \frac{\partial}{\partial t}\int_{-\infty}^{\infty} dx\, P(x,t) \ . \tag{A.3}$$

Conveniently, this allows a normalization of the probability density which we choose to be

$$\int_{-\infty}^{\infty} dx\, P(x,t) = 1 \ . \tag{A.4}$$

A.1 Stationary Solution

First of all, we try to find the stationary solution of the Fokker-Planck equation by requiring

$$\frac{\partial}{\partial t}P_{\mathrm{st}}(x) = 0 \ . \tag{A.5}$$

Further, assuming time independent drift and diffusion coefficients, this leads to the ordinary differential equation

$$\frac{d}{dx}\left\{K(x)P_{\mathrm{st}}(x) - \frac{1}{2}\frac{d}{dx}\left[D(x)P_{\mathrm{st}}(x)\right]\right\} = 0 \ . \tag{A.6}$$

Integrating yields

$$K(x)P_{\mathrm{st}}(x) - \frac{1}{2}\frac{d}{dx}\left[D(x)P_{\mathrm{st}}(x)\right] = \mathrm{const} \ . \tag{A.7}$$

With natural boundary conditions, the integration constants is equal to 0. So, (A.7) can be rewritten as

$$\frac{d}{dx}P_{\rm st}(x) + \frac{\frac{d}{dx}D(x) - 2K(x)}{D(x)}P_{\rm st}(x) = 0 \ . \tag{A.8}$$

As can be verified quite easily, the solution of (A.8) is

$$P_{\rm st}(x) = \frac{N}{D(x)} \exp\left[2\int^x \frac{K(\xi)}{D(\xi)}d\xi\right] \ . \tag{A.9}$$

The parameter N is the normalization constant. It is chosen according to the normalization condition (A.4). Assuming a constant diffusion coefficient $D(x) = D$, we get as a result the stationary solution

$$P_{\rm st}(x) = \frac{N}{D} \exp\left[-\frac{2}{D}V(x)\right] \ , \tag{A.10}$$

with the newly introduced potential

$$V(x) = -\int^x K(\xi)d\xi \tag{A.11}$$

and the normalization constant

$$N = \frac{D}{\int_{-\infty}^{\infty} dx \exp\left[-\frac{2}{D}V(x)\right]} \ . \tag{A.12}$$

A.2 Dynamic Solution

For Brownian motion we have the Kramers-Moyal coefficients

$$K(x) = -\gamma x \qquad \text{and} \qquad D(x) = D \ . \tag{A.13}$$

Additionally, we have the initial condition

$$P(x, t_0) = \delta(x - x_0) \, . \tag{A.14}$$

Thus, we easily find with (A.9) the stationary solution to be a Gaussian distribution

$$P_{\rm st}(x) = \sqrt{\frac{\gamma}{\pi D}} \exp\left(-\frac{\gamma}{D}x^2\right) \ . \tag{A.15}$$

With the Einstein-Smoluchowski relation (1.18), we identify (A.15) to be the Maxwell distribution

$$P(x) = \sqrt{\frac{m}{2\pi k_B T}} \exp\left(-\frac{m}{2k_B T}x^2\right) \ . \tag{A.16}$$

Knowing the stationary solution of the Fokker-Planck equation, the time dependent solution can be found in a heuristic manner [35]. Knowing the stationary distribution to be Gaussian, one uses as ansatz a Gaussian distribution with time dependent variance and mean value. We write

$$P(x, t) = N(t) \exp\left[\frac{-x^2 + 2H_1(t)x}{2H_2(t)}\right] \ . \tag{A.17}$$

Inserting (A.17) into the Fokker-Planck equation (1.19) with corresponding Krames-Moyal coefficients and dividing by $P(x,t)$ to get rid of the exponentials yields a polynom of second order in x:

$$x^2\left[\frac{\dot{H}_2(t)}{2H_2(t)^2}+\frac{\gamma}{H_2(t)}-\frac{D}{2H_2(t)^2}\right]+x\left[\frac{\dot{H}_1(t)}{2H_2(t)}-\frac{H_1(t)\dot{H}_2(t)}{2H_2(t)^2}-\frac{\gamma H_1(t)}{2H_2(t)}+\frac{DH_1(t)}{2H_2(t)^2}\right]$$
$$+\frac{\dot{N}(t)}{N(t)}-\gamma-D\frac{H_1(t)^2}{8H_2(t)^2}+\frac{D}{2H_2(t)}=0. \tag{A.18}$$

Equating coefficients we get equations for the functions $H_2(t)$, $H_1(t)$ and $N(t)$. As $H_2(t)\neq 0$ the first one is the coefficient of x^2

$$\dot{H}_2(t)=-2\gamma H_2(t)+D\ . \tag{A.19}$$

With help of (A.19), we find the second conditional equation via the x cofficient to be

$$\dot{H}_1(t)=-\gamma H_1(t)\ . \tag{A.20}$$

Furthermore, we find

$$\frac{\dot{N}(t)}{N(t)}=\gamma+D\frac{H_1(t)^2}{8H_2(t)^2}-\frac{D}{2H_2(t)}\ . \tag{A.21}$$

The solutions of (A.19) and (A.20) can easily found to be

$$H_2(t)=\frac{D}{2\gamma}\left[1-e^{-2\gamma(t-t_0)}\right], \tag{A.22}$$
$$H_1(t)=H_1(t_0)e^{-\gamma(t-t_0)}. \tag{A.23}$$

The solution of (A.21) is not calculated that simply. Luckily, we might as well use the normalization conditon (A.4) to find $N(t)$, giving

$$N(t)=\frac{1}{\sqrt{2\pi H_2(t)}}\exp\left[\frac{-H_1(t)^2}{2H_2(t)}\right]\ . \tag{A.24}$$

This result can be easily verified by inserting into (A.21). Now we can state as final solution the time evolution of the probability density of Brownian motion as

$$P(x,t)=\frac{1}{\sqrt{2\pi H_2(t)}}\exp\left\{-\frac{[x-H_1(t)]^2}{2H_2(t)}\right\}\ . \tag{A.25}$$

From this solution, we can identify $H_1(t_0)=x_0$ due to (A.14). It is important to see, that the functions H_1 and H_2 do depend on the initial values $x(t_0)=x_0$ and $t=t_0$. To point out this dependence, we therefore could equivalently use the notation $H_1(t)=H_1(x_0,t_0;t)$ and $H_2(t)=H_2(x_0,t_0;t)$. Moreover, one sees that the time-dependent solution quickly tends toward the stationary one (A.15). For progressing fixed time steps, this is plotted in Fig. A.14.

Appendix B

Numerical Appendix

In addition to the external parameters like correlation length and variance, the Randomization Method is in need of an integer constant N. In this appendix, we show quantitatively, that the choice of this parameter allows to tune the accuracy. Furthermore, an example for a source code will be given to show how the algorithm can be implemented.

B.1 Algorithm Parameter

As the Randomization Method will be used to calculate expectation values, one has to accept that computing the complete average over all realizations via sampling pseudo-randomly generated functions is numerically impossible. But although Monte Carlo methods converge slowly, they can produce a good accuracy, which has been visualized in Figs. 2.2 and 2.4. The Randomization Method produces an additional error, though. It does not depend on the number of samples used, but of the choice of the parameter N. For the considerations to follow we will introduce the following abbreviation:

$$\langle \bullet \rangle_k = \int_{-\infty}^{\infty} dk\, p(k)\ \bullet\ . \tag{B.1}$$

Now, we obtain for even spectral density (2.2) and probability distribution (2.15)

$$\langle e^{ikx} \rangle_k = \langle e^{-ikx} \rangle_k = R(x)/\alpha^2\ . \tag{B.2}$$

This additional error does not occur for approximating the 2-point correlation. Calculating the correlation, we get with definition (2.13)

$$\begin{aligned}\langle U(x)U(x') \rangle_k =& \frac{1}{N} \sum_{n=0}^{N-1} \sum_{m=0}^{N-1} \big[\langle A_n A_m \cos(k_n x) \cos(k_m x') \rangle_k + \langle B_n B_m \sin(k_n x) \sin(k_m x') \rangle_k \\ &+ \langle A_n B_m \cos(k_n x) \sin(k_m x') \rangle_k + \langle B_n A_m \sin(k_n x) \cos(k_m x') \rangle_k \big]\end{aligned} \tag{B.3}$$

Using the property (2.14) this simplifies to

$$\langle U(x)U(x') \rangle_k = \frac{\alpha^2}{N} \sum_{n=0}^{N-1} \big[\langle \cos(k_n x) \cos(k_n x') \rangle_k + \langle \sin(k_n x) \sin(k_n x') \rangle_k \big] \tag{B.4}$$

Using addition theorems and (B.2), we finally get as result

$$\langle U(x)U(x') \rangle_k = \frac{\alpha^2}{N} \frac{\alpha^2}{N} \sum_{n=0}^{N-1} \langle \cos[k_n (x - x')] \rangle_k = R(x - x')\ . \tag{B.5}$$

To get a visible deviation from the imposed properties of the random functions one has to calculate the 4-point correlation. As normal distributed functions, Wick's Theorem (2.12) should be satisfied.

It is left to compute the 4-point correlation. Inserting (2.13) using (2.14) yields after a direct but somewhat involved calculation

$$\begin{aligned}\overline{U(x_1)U(x_2)U(x_3)U(x_4)} &= \tfrac{\alpha^4}{N^2}\textstyle\sum_{n,m}\langle\cos[k_n(x_1-x_2)]\cos[k_m(x_3-x_4)]+\cos[k_n(x_1-x_3)]\\ &\quad\times\cos[k_m(x_2-x_4)]+\cos[k_n(x_1-x_4)]\cos[k_m(x_2-x_3)]\rangle. \qquad \text{(B.6)}\end{aligned}$$

To calculate the expectation values, one has to carefully distinguish between two cases. For the $N(N-1)$ terms in the sum with $n \neq m$, one gets

$$\begin{aligned}\langle\cos(k_n x)\cos(k_m x')\rangle &= \langle\cos(k_n x)\rangle_{k_n}\langle\cos(k_m x')\rangle_{k_m}\\ &= \langle e^{ik_n x}\rangle_{k_n}\langle e^{ik_m x'}\rangle_{k_m}\\ &= R(x)R(y)/\alpha^4\ . \qquad \text{(B.7)}\end{aligned}$$

For the N terms with $n = m$, however, the average looks slightly different:

$$\begin{aligned}\langle\cos(k_n x)\cos(k_n x')\rangle &= \frac{1}{2}\langle\cos\left[k_n(x-x')\right]+\cos\left[k_n(x+x')\right]\rangle_{k_n}\\ &= \frac{1}{2}\langle e^{ik_n(x+x')}+e^{ik_n(x-x')}\rangle_{k_n}\\ &= \Big[R(x-x')+R(x+x')\Big]/2\alpha^4\ . \qquad \text{(B.8)}\end{aligned}$$

Therefore, Eq. (B.6) yields a form that is easily comparable with (2.12)

$$\begin{aligned}\overline{U(x_1)U(x_2)U(x_3)U(x_4)} &= R(x_1-x_2)R(x_3-x_4)+R(x_1-x_3)R(x_2-x_4)\\ &\quad +R(x_1-x_4)R(x_2-x_3)+\tfrac{1}{N}\Delta(x_1,x_2,x_3,x_3) \qquad \text{(B.9)}\end{aligned}$$

In accordance with (2.26), it is seen that Wick's Theorem is satisfied as the deviation

$$\begin{aligned}\Delta(x_1,x_2,x_3,x_4) = \quad &\Big\{R\big[(x_1-x_2)-(x_3-x_4)\big]+R\big[(x_1-x_2)+(x_3-x_4)\big]\\ &+R\big[(x_1-x_3)-(x_2-x_4)\big]+R\big[(x_1-x_3)+(x_2-x_4)\big]\\ &+R\big[(x_1-x_4)-(x_2-x_3)\big]+R\big[(x_1-x_4)+(x_2-x_3)\big]\\ &-R(x_1-x_2)R(x_3-x_4)-R(x_1-x_3)R(x_2-x_4)\\ &-R(x_1-x_4)R(x_2-x_3)\Big\}, \qquad \text{(B.10)}\end{aligned}$$

is suppressed by a factor $1/N$. As seen in Fig. B.1, the deviation of the expected 4-point correlation is small as it scales with $1/N$.

A simple example is provided by a Gaussian correlation function. It can be taken to be (2.27) restated as

$$R(x-y) = \alpha^2\exp\left\{-\frac{(x-y)^2}{2\lambda^2}\right\} \qquad \text{(B.11)}$$

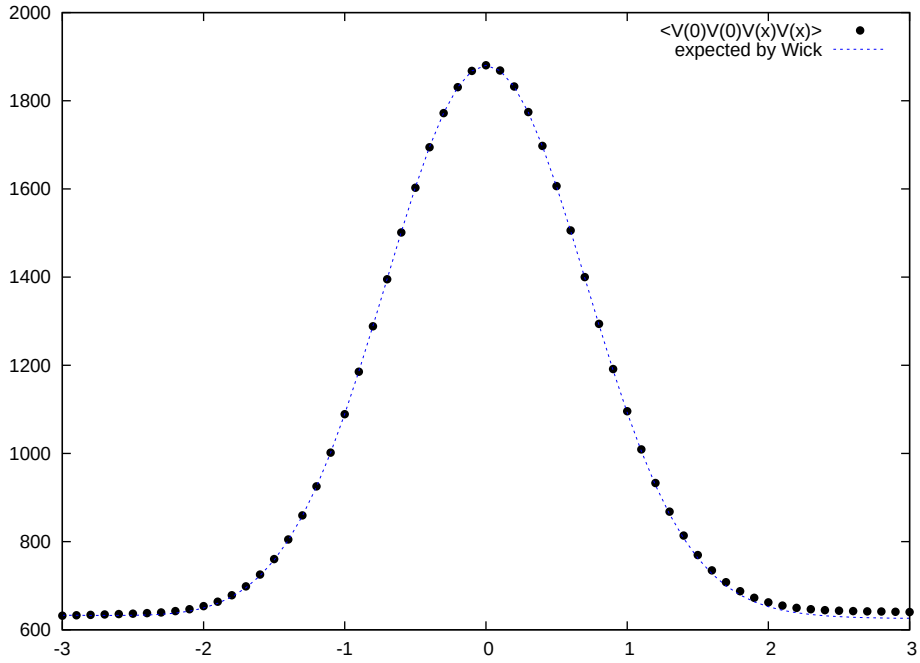

Figure B.1: $\overline{U(0)^2U(x)^2}$ compared to Wick's Theorem for the parameters $\alpha = 5$ and $N = 100$

The computation of the error due to the randomization parameter N is computed as

$$\begin{aligned}\Delta(x_1,x_2,x_3,x_4) = \quad & \Bigg\{ R(x_1-x_2)R(x_3-x_4)\left[\cosh\left(\frac{(x_1-x_2)(x_3-x_4)}{\lambda^2}\right)-1\right] \\ & + R(x_1-x_3)R(x_2-x_4)\left[\cosh\left(\frac{(x_1-x_3)(x_2-x_4)}{\lambda^2}\right)-1\right] \\ & + R(x_1-x_4)R(x_2-x_3)\left[\cosh\left(\frac{(x_1-x_4)(x_2-x_3)}{\lambda^2}\right)-1\right]\Bigg\}. \end{aligned} \tag{B.12}$$

In this section it was shown, that, using the simple ansatz (2.13), it is possible to generate random functions. The numerically generated expressions resemble the imposed properties of normally distributed random functions with given correlation function very well. Thus, we expect simulations of physical quantities due to randomness to be quite accurate.

B.2 Example Source Code

In Ch. 2, the Randomization Method was introduced to generate random potentials. This method was used for comparing analytic results with numerical simulations throughout this diploma thesis. As an example, the source code of the program simulating the free energy of a harmonical oscillator in a random potential is given in this appendix. The program was written in C++. The algorithm is farely simple: A random potential of the form (2.13) is created with help of trigonometric functions defined in the `math.h`-header. Furthermore, the Gnu Scientifc Library provided random number generators [65]. Then, the partition function for the fixed function $U(x)$ is calculated by numerical integration. This can be easily done because the Gaussian prefactor of the integrand ensures a fast enough decay of the integrand. This procedure is done for a number of `numOfRandomPot` functions and then averaged. For the commentated version of the source code of the free energy and the mean square displacement simulations see the webpages [66, 67].
At first, we include the headers used:

```
#include <iostream>
#include <ostream>
#include <fstream>
#include <math.h>
#include <gslgsl_rng.h>
#include <gslgsl_randist.h>
```

Then, we define the functions used in the main program. The first one generates a $N \times 3$ matrix that store the randomly drawn wavenumber k_n and the amplituds A_n and B_n, respectively. The second function uses this matrix to generate a random potential:

```
double coeff(double, double, int, const gsl_rng);
double randomPot(double, int, double**);

   int main(){
```

The parameters of the random number generator are initialized in the following. The `seed` is the starting point for the random number generator, which is allocated in the following. The quantities `alpha, sigma, N` and `numOfRandomPot` are the variances of the probability distributions, the algorithm paramter N and the number of potential averaged over, respectively:

```
       gsl_rng_default_seed =1326752;
       gsl_rng*r = gsl_rng_alloc (gsl_rng_taus);

       double alpha = 0.1/pow(2*3.14159265358979323846,0.25);
       double sigma = 1;
       int N = 100;
       int numOfRandomPot = 100;
```

The parameter `kappa` corresponds to the external paramter κ:

```
double kappa = 0.01;
```

The paramters need for the numerical integration are defined in the following:

```
double pi=3.14159265358979323846;
int numOfTempSteps = 100;
double lowerT =0.01;
double deltaT =0.01;
double dw;
double **matrix;
double T = lowerT;
double helpArray[numOfTempSteps];
for(int i = 0; i<numOfTempSteps; i++){
          helpArray[i]=0;
}
```

The implementation of the numerical integration and the averaging process work as follows. The integration limits can be estimated by looking at the standard deviation of the Gaussian prefactor. The integration routine is a standard integration via Riemann sums:

```
 double Z;
 double freeEnergy;

 for(int i = 0; i<numOfRandomPot; i++){
         matrix = coeff(alpha, sigma,N,r);
         for(int j =0; j<numOfTempSteps; j++){
                  Z = 0;
                  freeEnergy = 0;
                  double lower = -50;
                  double upper = 50;
                  dw = (upper -lower)/10000;
                  double w = lower;

                  while( w < upper){
                            Z += dw*exp(-kappa*w*w/(2*T)
                               -randomPot(w,N,matrix)/(T));
                           w += dw;
                  }
                  w = lower;
                           freeEnergy = -T*log(Z);
                  helpArray[j] += freeEnergy/numOfRandomPot;
                  T+=deltaT;
          }
          T=lowerT;
 }
```

The data output is written into an external file:

```
        std::  ofstream pout("/home/duettman/diplom/cpp/freieEnergie01.txt");
       if(pout) {
                 std::cout « "Cannot open file.\n";
                 return 1;
        }
        T = lowerT;
        for(int q = 0; q < numOfTempSteps; q++){
                pout « T « " "« helpArray[q] «'\n;
                T+=deltaT;
       }
       pout.close();

       return 0;
}
```

After the main function, the above defined functions `coeff` and `randomPot` are implemented with predifined random number generators of the Gnu Scientific Library:

```
  double **coeff(double alpha, double beta, int N, const gsl_rng*r){
       double **out;
       out = (double**) malloc(N*sizeof(double*));
       for(int i=0; i< N; ++i)
       {
                out[i]= (double*)
                malloc(3*sizeof(double));
       }
           for(int i=0; i<N; ++i){
                out[i][0]= gsl_ran_gaussian(r, alpha);
                out[i][1]= gsl_ran_gaussian(r, alpha);
                out[i][2]= gsl_ran_exponential(r, beta);
                }
       return out;
}

double randomPot(double x, int N,double **koeffMatrix){
       double out = 0;
       for(int i=0; i<N; ++i){
                out += koeffMatrix[i][0] * cos(koeffMatrix[i][2] *x)
                            + koeffMatrix[i][1] * sin (koeffMatrix[i][2] * x );
        }
        out = sqrt(N);
        return out;
}
```

Appendix C

Mathematical Tools for Replica Method

In this appendix, we will present mathematical methods used throughout the calculations of Ch. 4. It will be shown how to calculate expectation values of correlation functions. Furthermore, the determinant of a replica-symmetric matrix will be calculated by obtaining its eigenvectors. Then, we will compute the Hessian of the free energy approximation. Finally, we will use a mathematical trick to simplify calculations of functions of Kronecker delta considerably.

C.1 Smearing Formula for Harmonic Expectation Values

Due to (4.24), it is impossible to evade the calculation of harmonic expectation values of powers of the correlation function. A particularly elegant way to do this is to reduce the expectation value to a product of N convolutions of the regarded function with Gaussian functions. This method is presented in first order in Ref. [50] and generalized in Ref. [51] to higher orders. Here, we will derive similar expressions of the harmonic expectation value (4.22) for powers of the correlation function (1.3). For simplicity, the tilde will be omitted in the following discussion.

C.1.1 One Correlation Function

For $N = 1$ just first powers of the correlation function appear. The important quantity therefore is

$$\langle\, R(x_a - x_b)\,\rangle_{H_a} = \frac{1}{Z_a} \int d^n x\, \exp\{-\beta\, H_a(\boldsymbol{x})\} R(x_a - x_b)\ . \tag{C.1}$$

To get a Gaussian-type integral, one carries out a Fourier transform of the correlation function. Introducing the spectral density (2.2), this yields

$$\langle\, R(x_a - x_b)\,\rangle_{H_a} = \frac{1}{Z_a} \int d^n x \int_{-\infty}^{\infty} dk\, S(k)\, \exp\left\{ -\frac{\beta}{2} \sum_{c,d} x_c\, G_{cd}^{-1}\, x_d + ik(x_a - x_b) \right\}\ . \tag{C.2}$$

By introducing currents, one transforms the expression into the standard form

$$\langle\, R(x_a - x_b)\,\rangle_{H_a} = \frac{1}{Z_a} \int d^n x \int_{-\infty}^{\infty} dk\, S(k)\, \exp\left\{ -\frac{\beta}{2} \sum_{c,d} x_c\, G_{cd}^{-1}\, x_d + i \sum_c j_c\, x_c \right\}\ . \tag{C.3}$$

with $j_c = k\,(\delta_{ac} - \delta_{bc})$. The $d^n x$ integral can be solved in analogy to (2.10), but a direct solution can also be found in Ref. [14]. The solution reads

$$\langle\, R(x_a - x_b)\,\rangle_{H_a} = \int_{-\infty}^{\infty} dk\, S(k)\, \exp\left\{ -\frac{1}{2\beta} k^2 \sum_{c,d} j_c\, G_{cd}\, j_d \right\} . \tag{C.4}$$

Inserting the current j_c yields

$$\langle\, R(x_a - x_b)\,\rangle_{H_a} = \int_{-\infty}^{\infty} dk\, S(k)\, \exp\left\{ -\frac{1}{2\beta} k^2\, (G_{aa} + G_{bb} - 2G_{ab}) \right\} . \tag{C.5}$$

Note that similar to the case (2.10) the inverse G of (4.9) appears in the exponent. It is characterized by the property (4.38). Transforming back with (2.2) yields

$$\langle\, R(x_a - x_b)\,\rangle_{H_a} = \int_{-\infty}^{\infty} dk \int_{-\infty}^{\infty} \frac{dx}{2\pi}\, R(x) \exp\left\{ -ikx - \frac{1}{2\beta} k^2\, (G_{aa} + G_{bb} - 2G_{ab}) \right\} . \tag{C.6}$$

Luckily, the k integral can be transformed to a simple Gaussian integral via completing the square. For a more compact notation, yet another abbreviation is introduced:

$$q(a,b) := \frac{1}{\beta}\, (G_{aa} + G_{bb} - 2G_{ab}) \ . \tag{C.7}$$

With this, one finally arrives at the expression

$$\langle\, R(x_a - x_b)\,\rangle_{H_a} = \frac{1}{\sqrt{2\pi\, q(a,b)}} \int_{-\infty}^{\infty} dx\, R(x) \exp\left\{ -\frac{x^2}{2q(a,b)} \right\} . \tag{C.8}$$

C.1.2 Two Correlation Functions

For $N = 2$ terms up to two correlation functions appear. Thus, one needs to calculate

$$\langle\, R(x_{a_1} - x_{b_1})\, R(x_{a_2} - x_{b_2})\,\rangle_{H_a} = \frac{1}{Z_a} \int d^n x\, \exp\{-\beta\, H_a(\boldsymbol{x})\} R(x_{a_1} - x_{b_1})\, R(x_{a_2} - x_{b_2}) \ . \tag{C.9}$$

Introducing the spectral density one gets

$$\begin{aligned} \langle\, R(x_{a_1} - x_{b_1})\, R(x_{a_2} - x_{b_2})\,\rangle_{H_a} = \ & \frac{1}{Z_a} \int d^n x \int_{-\infty}^{\infty} dk_1\, S(k_1) \int_{-\infty}^{\infty} dk_2\, S(k_2) \\ & \times \exp\left\{ -\frac{\beta}{2} \sum_{c,d} x_c\, G^{-1}_{cd}\, x_d + i \sum_c j_c\, x_c \right\} \end{aligned} \tag{C.10}$$

with the current $j_c = k_1(\delta_{a_1 c} - \delta_{b_1 c}) + k_2(\delta_{a_2 c} - \delta_{b_2 c})$. As before, the computation of (C.10) can be performed explicitly. It yields

$$\begin{aligned} \langle\, R(x_{a_1} - x_{b_1})\, R(x_{a_2} - x_{b_2})\,\rangle_{H_a} = \ & \int_{-\infty}^{\infty} dk_1\, S(k_1) \int_{-\infty}^{\infty} dk_2\, S(k_2) \\ & \times \exp\left\{ -\frac{1}{2} \left[q_{11}(a,b) k_1^2 + q_{22}(a,b) k_2^2 + 2k_1 k_2\, q_{12}(a,b) \right] \right\} \end{aligned} \tag{C.11}$$

with the new parameters

$$q_{ij} \equiv q_{ij}(\boldsymbol{a},\boldsymbol{b}) := \frac{1}{\beta}\left(G_{a_i a_j} + G_{b_i b_j} - G_{b_i a_j} - G_{a_i b_j}\right) \ , \tag{C.12}$$

which are functions of the vector components

$$\boldsymbol{a} = (a_1, a_2) \ , \qquad \boldsymbol{b} = (b_1, b_2) \ . \tag{C.13}$$

Obviously, we have $q_{ii} = q(a_i, b_i)$ as in (C.7). As the equations seem to get more and more complex, it seems a good idea to introduce the following vector notation:

$$\boldsymbol{k} := \begin{pmatrix} k_1 \\ k_2, \end{pmatrix}, \qquad \boldsymbol{x} := \begin{pmatrix} x_1 \\ x_2 \end{pmatrix}. \tag{C.14}$$

Furthermore, one defines the matrix

$$Q := \begin{pmatrix} q_{11} & q_{12} \\ q_{12} & q_{22} \end{pmatrix} \tag{C.15}$$

in order to write the exponent in the more convenient form

$$-\frac{1}{2}\left[q_{11}k_1^2 + q_{22}k_2^2 + 2k_1k_2\, q_{12}\right] = -\frac{1}{2}\boldsymbol{k^T} Q \boldsymbol{k} \ . \tag{C.16}$$

Transforming back yields in this new notation

$$\langle\, R(x_a - x_b)\, R(x_c - x_d)\,\rangle_{H_a} = \int d^2k \int \frac{d^2x}{(2\pi)^2}\, R(x_1)R(x_2) \exp\left\{-i\boldsymbol{k^T x} - \frac{1}{2}\boldsymbol{k^T} Q \boldsymbol{k}\right\}. \tag{C.17}$$

And again we find convolutions of Gaussian functions with correlation functions

$$\langle\, R(x_a - x_b)\, R(x_c - x_d)\,\rangle_{H_a} = \frac{1}{\sqrt{(2\pi)^2 \det Q}} \int d^2x\, R(x_1)R(x_2) \exp\left\{-\frac{1}{2}\boldsymbol{x^T} Q^{-1} \boldsymbol{x}\right\} \ . \tag{C.18}$$

C.1.3 M Correlation Functions

Now the general case will be considered. For fixed M the harmonic expectation value of a product of M functions $R(x_a - x_b)$ will be calculated:

$$\langle\, R(x_{a_1} - x_{b_1})\, R(x_{a_2} - x_{b_2}) ... R(x_{a_M} - x_{b_M})\,\rangle_{H_a} = \langle \prod_{n=1}^{M} R(x_{a_n} - x_{b_n})\,\rangle_{H_a} \ . \tag{C.19}$$

Following the same steps as before, one arrives at the similar expression

$$\langle \prod_{n=1}^{M} R(x_{a_n} - x_{b_n})\,\rangle_{H_a} = \prod_{n=1}^{M} \left[\int_{-\infty}^{\infty} dk_n S(k_n)\right] \exp\left\{-\frac{1}{2}\boldsymbol{k^T} Q \boldsymbol{k}\right\} \tag{C.20}$$

with vectors defined as

$$\boldsymbol{k} := \begin{pmatrix} k_1 \\ . \\ . \\ . \\ k_M \end{pmatrix} \ , \qquad \boldsymbol{x} := \begin{pmatrix} x_1 \\ . \\ . \\ . \\ x_M \end{pmatrix} \ . \tag{C.21}$$

With (C.7) and (C.12) the $M \times M$ matrix Q looks a little bit more complicated

$$Q = \begin{pmatrix} q_{11} & q_{12} & q_{13} & \cdots & q_{1M} \\ q_{21} & q_{22} & & & q_{2M} \\ \vdots & & \ddots & & \vdots \\ \vdots & & & \ddots & \vdots \\ q_{M1} & \cdots & \cdots & \cdots & q_{MM} \end{pmatrix} . \tag{C.22}$$

The matrices G_{ab} are assumed to be symmetric, so one can write rather elegantly

$$Q_{ij} = q_{ij} \ . \tag{C.23}$$

As in (C.12) the matrix elements are functions of vector components of

$$\boldsymbol{a} = (a_1, ..., a_M) \ , \qquad \boldsymbol{b} = (b_1, ..., b_M) \ . \tag{C.24}$$

In principle, the multi-dimensional Gaussian integral can be calculated in a straightforward manner

$$\langle \prod_{n=1}^{M} R(x_{a_n} - x_{b_n}) \rangle_{H_a} = \frac{1}{\sqrt{(2\pi)^M \det Q}} \prod_{n=1}^{M} \left[\int_{-\infty}^{\infty} dx_n R(x_n) \right] \exp\left\{ -\frac{1}{2} \boldsymbol{x}^{\boldsymbol{T}} Q^{-1} \boldsymbol{x} \right\} \ . \tag{C.25}$$

Despite this compact expression, calculating the harmonic expectation value remains complicated. To get the M^{th} order result, one has to invert a $M \times M$ matrix and calculate M convolutions of Gaussian functions with the correlation function. Then, it is still left to compute the determinant of the matrix Q.

C.1.4 Specializing to Gaussian Correlation

In this subsection, we return to our toy model. The correlation assumed is of the Gaussian type (1.3). After inserting into (C.25) reads

$$\langle \prod_{n=1}^{N} R(x_{a_n} - x_{b_n}) \rangle_{H_a} = \frac{1}{\sqrt{(2\pi)^{2M} \lambda^M \det Q}} \int d^M x \, \exp\left\{ -\frac{\boldsymbol{x}^2}{2\lambda^2} \right\} \exp\left\{ -\frac{1}{2} \boldsymbol{x}^{\boldsymbol{T}} Q^{-1} \boldsymbol{x} \right\} . \tag{C.26}$$

As this is just the product of two multi-dimensional Gaussian functions, the expression can be written in a natural way. After renaming

$$\mathcal{Q}^{-1} := \frac{1}{\lambda^2} \boldsymbol{I} + Q^{-1} \tag{C.27}$$

we write (C.26) as just one Gaussian integral

$$\langle \prod_{n=1}^{M} R(x_{a_n} - x_{b_n}) \rangle_{H_a} = \frac{1}{\sqrt{(2\pi)^{2M} \lambda^M \det Q}} \int d^M x \exp\left\{ -\frac{1}{2} \boldsymbol{x}^{\boldsymbol{T}} \mathcal{Q}^{-1} \boldsymbol{x} \right\} \ , \tag{C.28}$$

which can be evaluated in general:

$$\langle \prod_{n=1}^{M} R(x_{a_n} - x_{b_n}) \rangle_{H_a} = \left(\frac{1}{\sqrt{2\pi}\lambda} \right)^M \sqrt{\frac{\det \mathcal{Q}}{\det Q}} \ . \tag{C.29}$$

With the properties of the determinant and definition (C.27), we get

$$\det \mathcal{Q}^{-1} \det Q = \det \mathcal{Q}^{-1} Q = \det \frac{1}{\lambda^2} \left(Q + \lambda^2 \boldsymbol{I} \right) = \frac{1}{\lambda^{2M}} \det \left(Q + \lambda^2 \boldsymbol{I} \right) , \tag{C.30}$$

so the expression reads simply

$$\langle \prod_{n=1}^{M} R(x_{a_n} - x_{b_n}) \rangle_{H_a} = \frac{1}{(2\pi)^{M/2}} \Big[\det \Big(Q + \lambda^2 \boldsymbol{I} \Big) \Big]^{-1/2} . \tag{C.31}$$

Thus, in the case of a Gaussian correlation function, the smearing formula for the toy model simplifies considerably. Just an elementary calculation of the determinant of a $M \times M$ matrix remains which, admittedly, can be quite cumbersome.

C.2 Determinant of Replica-Symmetric Matrix

Because of the special form of the replica-symmetric matrices, the determinant can be derived after some general considerations. Let us take a matrix

$$M_{ab} = (A - B)\delta_{ab} + B . \tag{C.32}$$

This special form appears in the RSA in all matrices of concern, namely G_{ab}, G_{ab}^{-1} and σ_{ab}. To calculate $\det M$ we want to find the eigenvalues λ_i, since

$$\det M = \prod_i \lambda_i . \tag{C.33}$$

Thus, we search for solutions of the equation

$$\sum_b M_{ab} \eta_b^{(i)} = \lambda_i \, \eta_a^{(i)} , \tag{C.34}$$

with $\eta^{(i)}$ being the eigenvector to λ_i. Inserting the definition (C.32) yields

$$\sum_b M_{ab} \eta_b^{(i)} = (A - B)\eta_a^{(i)} + B \sum_b \eta_b^{(i)} \stackrel{!}{=} \lambda_i \, \eta_a^{(i)} . \tag{C.35}$$

We see, that the simple form of the matrix M_{ab} makes it possible to just guess the eigenvectors. This equation can be fulfilled easily, if all vector components are equal. Therefore, we choose the first eigentvector

$$\boldsymbol{\eta}^{(1)} = \begin{pmatrix} 1 \\ 1 \\ \vdots \\ 1 \end{pmatrix} \tag{C.36}$$

with the resulting eigenvalue

$$\lambda_1 = A + (n - 1)B . \tag{C.37}$$

Eigenvectors of different eigenvalues are orthogonal. Because of (C.36), we therefore know $\sum_b \eta_b^{(i)} = 0$. But in this case, Eq. (C.34) is automatically satisfied. The easiest way to do

this is to choose vectors with just two nonzero components set to -1 and 1, respectively. The resulting eigenvalues are all equal to $A-B$ and one can construct in total $n-1$ linear independent eigenvectors of this type:

$$\boldsymbol{\eta}^{(2)} := \begin{pmatrix} -1 \\ 1 \\ 0 \\ \vdots \\ 0 \end{pmatrix} , \ \boldsymbol{\eta}^{(3)} := \begin{pmatrix} -1 \\ 0 \\ 1 \\ 0 \\ \vdots \\ 0 \end{pmatrix} , \dots , \boldsymbol{\eta}^{(n)} := \begin{pmatrix} -1 \\ 0 \\ \vdots \\ 0 \\ 1 \end{pmatrix} . \tag{C.38}$$

All these vectors $\boldsymbol{\eta}^{(i)}$ with $i = 1, ..., n$ are orthogonal to $\boldsymbol{\eta}^{(1)}$. Therefore, by guessing we found a basis of n eigenvectors. Hence, we can calculate the determinant of the matrix M:

$$\det M = (A-B)^{(n-1)}[A + (n-1)B] = (A-B)^n + nB(A-B)^n \ . \tag{C.39}$$

C.3 Hessian Matrix

The Hessian (4.82) is very symmetric in our case. Because of the permutability of the derivatives and the symmetric matrix $\sigma_{ab} = \sigma_{ba}$, we see that

$$H_{ab,cd} = H_{ba,cd} = H_{cd,ba} = ... \ . \tag{C.40}$$

In a straightforward calculation using (4.40) and (4.60) we get the explicit result

$$\begin{aligned} H_{ab,cd} = \quad & -\frac{1}{4\beta}\Big[G_{ac}G_{bd} + G_{ad}G_{bc}\Big] + \frac{\kappa}{4\beta}\sum_e \Big[G_{ec}G_{ae}G_{bd} + G_{ec}G_{ad}G_{be} + G_{ed}G_{ad}G_{bc} \\ & + G_{ed}G_{ac}G_{be}\Big] - \frac{1}{2}\sum_{e,f} f_\xi\Big[q(e,f)\Big]\Big[G_{ec}G_{ae}G_{bd} + G_{ec}G_{ad}G_{be} + G_{ed}G_{ad}G_{bc} \\ & + G_{ed}G_{ac}G_{be} - G_{ec}G_{af}G_{bd} - G_{ec}G_{ad}G_{bf} - G_{fd}G_{ae}G_{bc} - G_{df}G_{ac}G_{be}\Big] \\ & + \sum_{e,f} f_{\xi\xi}\Big[q(e,f)\Big]\Big[G_{ae}G_{be}G_{ce}G_{de} + G_{af}G_{bf}G_{ce}G_{de} + G_{ae}G_{bf}G_{ce}G_{df} \\ & + G_{af}G_{be}G_{ce}G_{df} - G_{ae}G_{bf}G_{ce}G_{de} - G_{af}G_{be}G_{ce}G_{de} - G_{ae}G_{be}G_{ce}G_{df} \\ & - G_{af}G_{bf}G_{ce}G_{df}\Big] \end{aligned} \tag{C.41}$$

As seen, e.g., in expression (C.41) we have to deal with functions of the type $f[q(e,f)]$. In the RSA, those functions have the form $f(a+b\,\delta_{ij})$, with constants a and b. We will restrict ourselves to functions that can be expanded into a Taylor series. To handle these functions, we will employ a little mathematical trick which will be introduced now.

C.4 Functions of Kronecker symbols

At first, one expands the function f in a Taylor series:

$$f(a + b\,\delta_{ij}) = f(a) + f'(a)\,b\,\delta_{ij} + \frac{1}{2}f''(a)\,b^2\,\delta_{ij}^2 + ... \ . \tag{C.42}$$

It is useful to notice that

$$\delta_{ij}^n = \delta_{ij} \quad \text{for} \quad n \in \mathbb{N} \; . \tag{C.43}$$

Using (C.43), we can now write the series (C.42) as

$$f(a + b\,\delta_{ij}) = f(a) + \delta_{ij}\,[f(a+b) - f(a)] \; . \tag{C.44}$$

In a general order of the free energy expansion, the quantity q_{ii} may appear in the argument of a function. In the replica-symmetric ansatz, it is computed to

$$q_{ii} = \frac{2A}{\beta}\,(1 - \delta_{a_i b_i}) \; . \tag{C.45}$$

Applying the trick (C.44), these expressions simplify to

$$f(q_{ii}) = f\,(2A/\beta) + \delta_{a_i b_i}\,[f(0) - f\,(2A/\beta)] \; . \tag{C.46}$$

List of Figures

Bibliography

[1] P. W. Anderson, *Absence of Diffusion in Certain Random Lattices*, Phys. Rev. **109** (1958) 1493.

[2] H. Kleinert, *Gauge Fields in Condensed Matter, Vol. II: Stresses and Defects: Disorder Fields and Applications to Superfluid Phase Transition and Crystal Melting*, World Scientific, Singapore, 1989.

[3] P. Horak, J.-Y. Courtois, G. Grynberg, *Atom Cooling and Trapping by Disorder*, Phys. Rev. A **58** (2000) 1953.

[4] B. Klünder, *Superfluide Eigenschaften ungeordneter Bosonen*, Diploma Thesis, Universität Duisburg-Essen, 2007,
`http://users.physik.fu-berlin.de/~pelster/Theses/kluender.pdf`.

[5] M. Timmer, *Ultrakalte Atomgase in Zufallspotentialen*, Diploma Thesis, Universität Duisburg-Essen, 2006,
`http://users.physik.fu-berlin.de/~pelster/Theses/timmer.pdf`.

[6] Y. C. Zhang, *Diffusion in a Random Potential: Hopping as a Dynamical Consequence of Localization*, Phys. Rev. Lett. **56** (1986) 2113.

[7] W. Ebeling, A. Engel, B. Esser, R. Feistel, *Diffusion and Reaction in Random Media and Models of Evolution Processes*, J. Stat. Phys. **37** (1984) 369.

[8] J. P. Gleeson, *Passive Motion in Dynamical Disorder as a Model for Stock Market prices*, Physica A **351** (2005) 523.

[9] D. Sherrington, S. Kirkpatrick, *Solvable Model of a Spin Glass*, Phys. Rev. Lett. **53** (1975) 1792.

[10] G. Parisi, *Field Theory, Disorder and Simulations*, World Scientific, Singapore, 1992.

[11] V. Dotsenko, *An Introduction to the Theory of Spin Glasses and Neural Networks*, World Scientific, Singapore, 1994.

[12] H. Kleinert, *Path Integrals in Quantum Mechanics, Statistics, Polymer Physics, and Financial Markets*, 4th Edition, World Scientific, Singapore, 2006.

[13] P. D. Gujrati, *Breakdown of Replica Analyticity in the One-Dimensional Axis Model*, Phys. Rev. B **32** (1985) 3319.

[14] H. Kleinert, *Gauge Fields in Condensed Matter, Vol. I: Superflow and Vortex Lines*, World Scientific, Singapore, 1989.

[15] G. Parisi, *The Order Parameter for Spin Glasses: a Function on the Interval 0-1*, J. Phys. A **13** (1980) 1101.

[16] M. Mezard, G. Parisi, M. A. Virasoro, *Spin Glass Theory and Beyond*, World Scientific, Singapore, 1986.

[17] J. L. de Almeida, D. J. Thouless, *Stability of the Sherrington-Kirkpatrick Solution of a Spin Glass Model*, J. Phys. A. **11** (1978) 983.

[18] A. Kirman, J.-B. Zimmermann (Eds.), *Economics with Heterogenous Interacting Agents*, Springer, Berlin, 2001.

[19] A. Engel, *Replica Symmetry Breaking in Zero Dimension*, Nucl. Phys. B **410** (1993) 617.

[20] Y. Y. Goldschmidt, *Quantum Fluctuations and Glassy Behavior: The Case of a Quantum Particle in a Random Potential*, Phys. Rev. E **53** (1996) 343.

[21] B. Roling, S. Murugavel, A. Heuer, L. Luhning, R. Friedrich, S. Röthel, *Field-Dependent Ion Transport in Disordered Solid Electrolytes*, Phys. Chem. Chem. Phys. **10** (2008) 4211.

[22] J. Shiferaw, Y. Y. Goldschmidt, *Localization of a Polymer in Random Media: Relation to the Localization of a Quantum Particle*, Phys. Rev. E **63** (2001) 051803.

[23] J. Dietel, H. Kleinert, *Phase Diagram of Vortices in high-*$\mathrm{T_c}$ *Superconductors from Lattice Defect Model with Pinning*, Phys. Rev. B **75** (2007) 144513.

[24] J. Dietel, H. Kleinert, *Phase Diagram of Vortices in High-*T_c *Superconductors with a Melting Line in the Deep* H_{c2} *Region*, accepted by Phys. Rev. B (2008) arXiv:0807.2757.

[25] T. Giamarchi, P. L. Doussal, *Elastic Theory of Pinned Flux Lattices*, Phys. Lett. **72** (1994) 1530.

[26] T. Giamarchi, P. L. Doussal, *Elastic Theory of Pinned Flux Lattices in the Presence of Weak Disorder*, Phys. Rev. B **52** (1995) 1242.

[27] R. Brown, *A brief Account of Microscopical Observations made in the Months of June, July, and August, 1827, on the Particles contained in the Pollen of Plants; and on the general Existence of active Molecules in Organic and Inorganic Bodies*, Philos. Mag. N. S. **4** (1828) 161.

[28] R. Brown, *Additional Remarks on Active Molecules*, Philos. Mag. N. S. **6** (1829) 166.

[29] A. Einstein, *Über die von der molekularkinetischen Theorie der Wärme geforderte Bewegung von in ruhenden Flüssigkeiten suspendierten Teilchen*, Ann. Phys. **17** (1905) 549.

[30] A. Einstein, *Eine neue Bestimmung der Molekühldimensionen*, Ann. Phys. **19** (1906) 289.

[31] M. von Smoluchowski, *Zur kinetischen Theorie der Brownschen Molekularbewegung und der Suspensionen*, Ann. Phys. **21** (1906) 756.

[32] L. Bachelier, *Théorie de la spéculation*, Ann. Sci. É. N. S. **3** (1900) 21.

[33] P. Langevin, *Sur la théorie du mouvement brownien*, C. R. Acad. Sci. **146** (1908) 530.

[34] J. Dreger, *Untersuchung des Starkkopplungsverhalten der Fokker-Planck-Gleichung mit anharmonischer Drift*, Diploma Thesis, Freie Universität Berlin, 2002, `http://users.physik.fu-berlin.de/~pelster/Theses/dreger.pdf`.

[35] H. Haken, *Synergetics: An Introduction*, 2nd Edition, Springer, Berlin, 1978.

[36] H. Risken, *The Fokker-Planck Equation: Methods of Solution and Applications*, 2nd Edition, Springer, Berlin, 1989.

[37] A. D. Fokker, *Die mittlere Energie elektrischer Dipole im Strahlungsfeld*, Ann. Sci. É. N. S. **43** (1914) 810.

[38] M. Planck, *Über einen Satz der statistichen Dynamik und eine Erweiterung in der Quantumtheorie*, Sitzungberichte der Preussischen Akadademie der Wissenschaften (1917) 324.

[39] A. N. Kolmogorov, *Über die analytischen Methoden in der Wahrscheinlichkeitsrechnung*, Math. Ann. **104** (1931) 415.

[40] H. Kleinert, A. Pelster, M. V. Putz, *Variational Perturbation Theory for Markov Processes*, Phys. Rev. E. **65** (2002) 0066128.

[41] J. Dreger, A. Pelster, B. Hamprecht, *Variational Perturbation Theory for Fokker-Planck Equation with Nonlinear Drift*, Eur. Phys. B **45** (2005) 355.

[42] A. Pelster, *Bose-Einstein-Kondensation*, Lecture Notes, Universität Duisburg-Essen, 2004, `http://www.theo-phys.uni-essen.de/tp/ags/pelster_dir/SS04/skript.pdf`.

[43] J. Majda, P. Kramer, *Simplified Models for Turbulent Diffusion: Theory, Numerical Modelling, and Physical Phenomena*, Phys. Rep. **314** (1999) 237.

[44] P. Kramer, O. Kurbanmuradov, K. K. Sabelfeld, *Comparative Analysis of Multiscale Gaussian Random Field Simulation Algorithms*, J. Comput. Phys. **226** (2007) 897.

[45] W. Kürzinger, *Variationsstörungstheorie an der quantenmechanischen Zustandssumme*, Diploma Thesis, Freie Universität Berlin, 1998, `http://www.physik.fu-berlin.de/~pelster/Theses/kuerzinger.ps`.

[46] P. M. Stevenson, *Optimized Perturbation Theory*, Phys. Rev. D **23** (1981) 2916.

[47] S. Brandt, *Beyond Effective Potential Via Variational Perturbation Theory*, 2004, `http://www.physik.fu-berlin.de/~pelster/Theses/brandt.ps`.

[48] H. Kleinert, A. Pelster, B. Kastening, M. Bachmann, *Recursive Graphical Construction of Feynman Diagrams and Their Multiplicities in ϕ^4- and ϕ^2 A-Theory*, Phys. Rev. E **62** (2000) 1537.

[49] T. Fließbach, *Allgemeine Relativitätstheorie*, 3rd Edition, Spektrum, Heidelberg, 1998.

[50] R. P. Feynman, H. Kleinert, *Effective Classical Partition Functions*, Phys. Rev. A **34** (1986) 5080.

[51] H. Kleinert, W. Kürzinger, A. Pelster, *Effective Classical Potential to Higher Orders Via Smearing*, J. Phys. A **31** (1998) 8307.

[52] J. L. de Almeida, D. J. Thouless, J. M. Kosterlitz, *Stability and Susceptibility in Parisi's Solution of a Spin Glass Model*, J. Phys. C. **13** (1980) 3271.

[53] A. Engel, C. van den Broeck, *Statistical Mechanics of Learning*, Cambridge University Press, Cambridge, 2001.

[54] M. Mézard, G. Parisi, *Replica Field Theory for Random Manifolds*, J. Phys. I **1** (1991) 809.

[55] K. J. Wiese, *Vorlesung: Ungeordnete Systeme*, Lecture Notes, Universität Duisburg-Essen, 2002,
`http://www.phys.ens.fr/~wiese/vorlesung/disorder.ps`.

[56] D. M. Carlucci, C. De Dominicis, T. Temesvari, *Stability of the Mézard-Parisi Solution for Random Manifolds*, J. Phys. I **6** (1996) 1031.

[57] W. Press, B. Flannery, S. Teukolsky, W. Vetterling, *Numerical Recipes*, Cambridge University Press, Cambridge, 1986.

[58] W. Janke, H. Kleinert, *Convergent Strong-Coupling Expansions from Divergent Weak-Coupling Perturbation Theory* , Phys. Rev. Lett. **75** (1995) 2787.

[59] W. Janke, H. Kleinert, *Scaling property of variational perturbation expansion for general anharmonic oscillator with x^p-potential*, Phys. Lett. A **199** (1995) 287.

[60] A. de Martino, M. Marsili, *Replica Symmetry Breaking in the Minority Game*, J. Phys. A **34** (2001) 2525.

[61] A. de Martino, M. Marsili, *Statistical Mechanics of Socio-Economic Systems with Heterogeneous Agents*, J. Phys. A **39** (2006) R465.

[62] M. Matthies, H. Malchow, J. Kriz (Eds.), *Integrative Systems Approaches to Natural and Social Dynamics - System Sciences 2000*, Springer, Berlin, 2001.

[63] W. Ebeling, F. Schweitzer, *Self-Organization, Active Brownian Dynamics, and Biological Applications*, Nova Acta Leopoldina NF **88** (2003) 169.

[64] J. A. Freund, T. Pöschel (Eds.), *Stochastic Processes in Physics, Chemistry and Biology*, Springer, Berlin, 2000.

[65] `http://www.gnu.org/software/gsl/`.

[66] `http://users.physik.fu-berlin.de/~duettman/freieEnergie.cpp`.

[67] `http://users.physik.fu-berlin.de/~duettman/disorder.cpp`.

Acknowledgements

This Diploma thesis could not have been possible without the help of quite a few people. I want to reserve the last page of this work to acknowledge their support.

First of all I want to thank Prof. Dr. Dr. h.c. Hagen Kleinert for giving me the opportunity to work on my Diploma thesis in his group. Whenever approached he took the time for a discussion. He provided a great deal of help understanding the subtleties of variational perturbation theory. I would never have imagined how certain side notes could save that much time.

I am also truly indebted to Priv.-Doz. Dr. Axel Pelster. I have always been impressed with his seemingly endless enthusiasm about physics. Apart from providing hints to solve all kind of expressions, several corrections of this thesis and many useful tips concerning LaTeX, it was important to him that I learned to approach problems in a systematic and efficient way. I am very thankful for that.

Likewise, I want to acknowledge the support of Dr. Jürgen Dietel. He always had some tea bags in reserve and, moreover, helped me to understand Parisi's replica-symmetry breaking method. Also, his rigorous critique of all my obtained results helped to iron out all possible mistakes.

Furthermore, I am very thankful for the pleasant working atmosphere guaranteed by Walja Korolevski, Matthias Ohliger, Konstantin Glaum, Tobias Graß, Ednilson Santos, Victor Bezerra and Aristeu Lima. It was good hanging out with you guys!

Last but not least, I want to thank my parents for their financial support and, more important, the encouragement they have given me throughout the years.

Erklärung:

Ich versichere, dass ich diese Arbeit selbständig verfasst und keine anderen als die angegebenen Quellen und Hilfsmittel benutzt habe.

Berlin, 6. Januar 2009 .....